(12) INTERNATIONAL APPLICATION PUBLISHED UNDER THE PATENT COOPERATION TREATY (PCT)

(19) World Intellectual Property Organization
International Bureau

(43) International Publication Date
30 May 2014 (30.05.2014)

WIPO | PCT

(10) International Publication Number
WO 2014/081851 Al

(51) International Patent Classification:
G01N 33/68 (2006.01) *G01N 33/48* (2006.01)
G01N 33/53 (2006.01)

(21) International Application Number:
PCT/US20 13/07 1042

(22) International Filing Date:
20 November 2013 (20.1 1.2013)

(25) Filing Language: English

(26) Publication Language: English

(30) Priority Data:
61/728,692 20 November 2012 (20. 11.2012) US

(71) Applicant: **WASHINGTON UNIVERSITY** [US/US]; One Brookings Drive, St. Louis, Missouri 63 130 (US).

(72) Inventors; and
(71) Applicants : **BATEMAN, Randall** [US/US]; One Brookings Drive, St. Louis, Missouri 63 130 (US). **PATTERSON, Bruce W.** [US/US]; One Brookings Drive, St. Louis, Missouri 63 130 (US). **ELBERT, Donald L.** [US/US]; One Brookings Drive, St. Louis, Missouri 63130 (US).

(74) Agents: **RILEY-VARGAS, Rebecca** et al; Polsinelli PC, Mark Twain Plaza III, 105 West Vandalia, Suite 400, Edwardsville, IL 62025 (US).

(81) Designated States *(unless otherwise indicated, for every kind of national protection available):* AE, AG, AL, AM, AO, AT, AU, AZ, BA, BB, BG, BH, BN, BR, BW, BY, BZ, CA, CH, CL, CN, CO, CR, CU, CZ, DE, DK, DM, DO, DZ, EC, EE, EG, ES, FI, GB, GD, GE, GH, GM, GT, HN, HR, HU, ID, IL, IN, IR, IS, JP, KE, KG, KN, KP, KR, KZ, LA, LC, LK, LR, LS, LT, LU, LY, MA, MD, ME, MG, MK, MN, MW, MX, MY, MZ, NA, NG, NI, NO, NZ, OM, PA, PE, PG, PH, PL, PT, QA, RO, RS, RU, RW, SA, SC, SD, SE, SG, SK, SL, SM, ST, SV, SY, TH, TJ, TM, TN, TR, TT, TZ, UA, UG, US, UZ, VC, VN, ZA, ZM, ZW.

(84) Designated States *(unless otherwise indicated, for every kind of regional protection available):* ARIPO (BW, GH, GM, KE, LR, LS, MW, MZ, NA, RW, SD, SL, SZ, TZ, UG, ZM, ZW), Eurasian (AM, AZ, BY, KG, KZ, RU, TJ, TM), European (AL, AT, BE, BG, CH, CY, CZ, DE, DK, EE, ES, FI, FR, GB, GR, HR, HU, IE, IS, IT, LT, LU, LV, MC, MK, MT, NL, NO, PL, PT, RO, RS, SE, SI, SK, SM, TR), OAPI (BF, BJ, CF, CG, CI, CM, GA, GN, GQ, GW, KM, ML, MR, NE, SN, TD, TG).

Published:

— *with international search report (Art. 21(3))*

— *with sequence listing part of description (Rule 5.2(a))*

WO 2014/081851 A1

(54) **Title:** METHODS OF DIAGNOSING AMYLOID PATHOLOGIES USING ANALYSIS OF AMYLOID-BETA ENRICHMENT KINETICS

(57) **Abstract:** A method of diagnosing an amyloid pathology in the central nervous system of a patient using measurements of enrichment kinetics of at least one amyloid-β isoform is provided. In addition, a model to predict enrichment kinetics of at least one amyloid-β isoform, methods of calibrating the model, and methods of using the model to diagnosing an amyloid pathology in the central nervous system of a patient are provided.

METHODS OF DIAGNOSING AMYLOID PATHOLOGIES USING ANALYSIS OF AMYLOID-BETA ENRICHMENT KINETICS

GOVERNMENTAL RIGHTS IN THE INVENTION

[0001] This invention was made with government support under 5P01 AG026276-S1 awarded by the National Institute on Aging, and R-01 - NS065667 awarded by the National Institutes of Health. The government has certain rights in the invention.

REFERENCE TO RELATED APPLICATIONS

[0002] This application claims priority to U.S. Provisional Patent Application No. 61/728,692 filed on November 20, 201 2, and entitled "METHODS OF DIAGNOSING AMYLOID PATHOLOGIES USING ANALYSIS OF AMYLOID-BETA ENRICHMENT KINETICS", which is hereby incorporated herein by reference in its entirety.

FIELD OF THE INVENTION

[0003] This disclosure generally relates to methods of diagnosing an amyloid pathology in the central nervous system of a patient using measurements of enrichment kinetics of at least one amyloid- β isoform. In addition, this disclosure relates to methods of developing and using a mathematical model to predict enrichment kinetics of at least one amyloid- β isoform and to diagnose an amyloid pathology in the central nervous system of a patient using the model.

BACKGROUND OF THE INVENTION

[0004] Alzheimer's Disease (AD) is the most common cause of dementia and is an increasing public health problem. AD, like other central nervous system (CNS) degenerative diseases, is characterized by disturbances in protein production, accumulation, and clearance. In AD, dysregulation in the metabolism of the protein, amyloid-beta (Aβ), is indicated by a massive buildup of this protein in the brains of those with the disease. Because of the severity and

increasing prevalence of this disease in the population, it is urgent that better treatments be developed.

[0005] The pathogenic causes of Alzheimer's disease are not fully understood, partly due to the difficulty in demonstrating the steps that lead to dementia in humans. Although rare, autosomal dominant AD (ADAD) can be predicted with near 100% certainty in individuals with specific mutations in presenilin 1 (PSE/V1), presenilin 2 *(PSEN2),* or the amyloid precursor protein (APP). Recent findings suggest that a series of ADAD pathophysiological changes occur in the brain decades before clinical dementia manifests. However, the mechanisms by which these mutations lead to AD pathophysiology are not well understood.

[0006] The amyloid hypothesis predicts that AD is caused by increased production or decreased clearance of Aβ in the brain, resulting in amyloidosis (the deposition of amyloid proteins in an organ or tissue) and AD's pathologic hallmark of amyloid plaques, which are principally composed of Aβ42. An APP mutation which reduces Aβ production is associated with a strong protective effect against AD, while duplication of APP or mutations which are thought to increase Aβ or Aβ42 cause dominantly inherited AD. Aβ is cleaved from the c-terminal fragment of APP (C99) by PSE/V1 and *PSEN2,* the enzymatic components of gamma-secretase. In cell culture and in plasma, *PSEN* mutations have been associated with increased Aβ42:Aβ40 ratio, which is hypothesized to increase the risk of amyloidosis. However, others have found that neither the Aβ42:Aβ40 ratio nor Aβ42 levels are increased *in vitro.* Further, findings of paradoxically reduced cerebrospinal fluid (CSF) Aβ42 concentrations in ADAD patients do not appear to directly support the predicted increased Aβ42 production as an etiologic mechanism in dominantly inherited AD.

[0007] Sporadic AD may be characterized by decreased Aβ clearance measured by stable isotope labeling kinetics (SILK). Both sporadic AD and ADAD are associated with lower CSF Aβ42 concentrations and Aβ42:Aβ40 ratios. However, *PSEN* ADAD mutations are hypothesized to cause increased

Aβ42 production, although direct evidence for increased production of Aβ42 in humans has not been reported.

[0008] A need exists, therefore, for a method for modeling the *in vivo* kinetics of Aβ. In particular, a method is needed for modeling the *in vivo* fractional synthesis rate and clearance rate of proteins associated with a neurodegenerative disease, e.g., the metabolism of Aβ in AD. Such a model may serve as a useful tool in research directed to the characterization and treatment of the underlying processes of AD.

SUMMARY OF THE INVENTION

[0009] The present disclosure generally relates to systems and methods of modeling and calibrating models for the metabolism and trafficking of CNS biomolecules in a patient.

[001 0] In one aspect, a method of calibrating a compartmental model for the steady-state kinetics of a biomolecule includes obtaining data values for a level of a labeled moiety in a patient as a function of time. A fraction of the biomolecule is the labeled moiety. The method includes modeling a metabolic pathway of the biomolecule with a compartmental model based on the obtained data values for the labeled moiety, plotting a result of the compartmental model, and comparing a plot of the result to another plot of measured data values. If the plot of the model results matches the other plot of measured data values then the model is sufficiently calibrated. Conversely, if the plot of the result does not match the other plot of the measured data values, then at least one rate constant of the compartmental model is modified. The metabolic pathway of the biomolecule is remodeled using the at least one modified rate constant. The remodeled result of the compartmental model is plotted and compared to the other plot of the measured data values. The actions of comparing and modifying at least one rate constant are repeated, as necessary, to produce a plot the matches the plot of measured data values.

[001 1] In various other aspects, the method may be performed on one or more computing devices. The computing devices may be distributed

across a network or stand-alone devices. In one aspect, the computing device may be used to permit a user to modify and compare plots simultaneously, and in near real time.

[001 2] In a second aspect, a method for detecting amyloid pathology in the central nervous system of a patient provided that includes: i) determining one or more kinetic parameters of Aβ42 and at least one other Aβ peptide, (ii) comparing the Aβ42 kinetic parameter and the same kinetic parameter for a second Aβ measurement, and (iii) determining whether a subject has amyloid pathology based on a difference between the two kinetic parameters. The kinetic parameter may be selected from the group consisting of fractional synthesis rate, peak time, peak enrichment, initial downturn monoexponential slope, terminal monoexponential slope, and a combination thereof. Two or more kinetic parameters may be determined, three or more kinetic parameters may determined, four or more kinetic parameters may be determined, or at least five kinetic parameters may be determined. The kinetic parameter may be fractional synthesis rate and the Aβ42 fractional synthesis rate may be faster than the fractional synthesis rate for the second Aβ measurement, the kinetic parameter may be peak time and the Aβ42 peak time may be earlier than the peak time for the second Aβ measurement, the kinetic parameter may be peak enrichment and the Aβ42 peak enrichment may be lower than the peak enrichment for the second Aβ measurement, the kinetic parameter may be initial downturn monoexponential slope and the initial Aβ42 slope may be faster than the initial slope for the second Aβ measurement, or the kinetic parameter may be terminal monoexponential slope and the terminal Aβ42 slope may be slower than the terminal slope for the second Aβ measurement. The one or more kinetic parameters may be determined by stable isotope labeling kinetics. A labeled amino acid may be administered to the subject hourly for a time period selected from the group consisting of 6 to 12 hours, 6 to 9 hours, and 9 to 12 hours. The amount of labeled peptide and the amount of unlabeled peptide may be detected by a means selected from the group consisting of mass spectrometry, tandem mass spectrometry, and a combination thereof. The one or more kinetic

parameters may be determined using a mathematical model for the enrichment kinetics of Aβ. The method may further include calculating the isotopic enrichment of Aβ42 compared to the second Aβ measurement at a single timepoint after administration of the labeled amino acid to the patient. The second Aβ measurement may be selected from the group consisting of an Aβ peptide other than Aβ42 and total Aβ. The Aβ peptide other than Aβ42 may be Aβ38 or Aβ40. The method may further include (i) calculating the ratio between the Aβ42 kinetic parameter and the same kinetic parameter for the second Aβ measurement, and (ii), comparing the ratio calculated in (i) to a threshold value, wherein a value lower than the threshold indicates the patient has amyloid plaques.

[001 3] In a third aspect, a method to diagnose an amyloid pathology in a patient is provided. The method includes (i) creating a mathematical model for the steady-state kinetics of Aβ including a set of model parameters (ii) calculating ten times k_{ex42} and adding that to the FTR ratio, and (iii) comparing the value from (ii) to a threshold value, wherein a value lower than the threshold value indicates a subject has Alzheimer's Disease. The set of model parameters includes: k_{ex42}, a rate constant for an irreversible loss for Aβ42, and a rate constant for an irreversible loss for Aβ40. k_{ex42} describes the rate of entry of Aβ42 into the exchange compartment and the FTR ratio is the ratio of the rate constants for irreversible loss for Aβ42 versus Aβ40. The amyloid pathology may be selected from the group consisting of amyloid plaques, altered Aβ kinetics, and Alzheimer's Disease.

[0014] In a fourth aspect, a method of calibrating a model to estimate a time course of enrichment kinetics of at least one Aβ isoform is provided. The method includes: a) obtaining data values for an amount of a labeled moiety introduced into a patient as a function of time, wherein a fraction of the at least one Aβ isoforms includes the labeled moiety; b) modeling a metabolic pathway of the at least one Aβ isoform with the model based on the obtained data values to calculate a set of model parameters and an estimated time course of enrichment kinetics of the at least one amyloid; and c) comparing the estimated time course

of enrichment kinetics of the at least one Aβ isoform to a measured time course of enrichment kinetics of the at least one Aβ isoform obtained from the patient. If the estimated time course of enrichment kinetics matches the measured time course of enrichment kinetics, the model determines that the compartmental model is calibrated. If the estimated time course of enrichment kinetics does not match the measured time course of enrichment kinetics the model may modify at least one of the set of model parameters and remodel metabolic pathway of the Aβ peptide using the modified model parameters to calculate a new estimated time course of enrichment of the at least one amyloid; these steps may be repeated until the compartmental model is calibrated.

[001 5] In a fifth aspect, an amyloid kinetics modeling system for estimating a time course of enrichment kinetics of at least one Aβ isoform is provided. The system may include: a) at least one processor; and b) a CRM containing an amyloid kinetics application including a plurality of modules executable on the at least one processor. The plurality of modules may include: i) a plasma module to represent infusion of a labeled moiety into the plasma of a patient and to represent transport of the labeled moiety across the blood brain barrier (BBB) of the patient; ii) a brain tissue module to represent incorporation of the labeled moiety into APP and formation of C99; iii) an amyloid kinetics module to represent cleavage of the C99 to form at least one Aβ isoform and subsequent kinetics of the at least one Aβ isoform within the brain of the patient; iv) a CSF module to represent transport of the at least one Aβ isoform into the CSF of the patient; v) a model tuning module to iteratively adjust a set of model parameters defining a dynamic response of the model to an input time history of plasma leucine enrichment into the plasma module in order to optimize a match between predicted enrichment kinetics and measured enrichment kinetics of the at least one Aβ isoform in the patient; and vi) a GUI module to generate one or more forms used to receive inputs to the system and to deliver output from the system. The plasma module includes a plasma amino acid compartment including a plasma concentration of at least one amino acid, wherein the plasma concentration of the at least one amino acid may be determined using an input

including a time history of an infusion of a labeled amino acid into a patient. The brain tissue module includes: a) an APP compartment including a total amount of APP; b) an APP incorporation rate including a rate of incorporation of the at least one amino acid from the plasma amino acid compartment into an APP molecule in the APP compartment; c) a C99 compartment including a total amount of C99 c-terminal fragments; d) a C99 formation rate including a rate of formation of the C99 c-terminal fragments in the C99 compartment from the APP molecules; and e) a C99 clearance rate including a rate of disappearance of the C99 c-terminal fragments from the C99 compartment. The amyloid kinetics module includes: a) a soluble Aβ42 isoform compartment including an amount of a soluble Aβ42 isoform; b) an Aβ42 isoform formation rate including a rate of formation of soluble Aβ42 isoform from the C99 c-terminal fragments; c) an Aβ42 isoform clearance rate including a rate of disappearance of Aβ42 isoforms from the soluble Aβ compartment; d) an Aβ42 incorporation rate including a rate of transformation of the soluble Aβ42 isoform to an incorporated Aβ42 isoform; and e) a recycled Aβ42 compartment including a total amount of incorporated Aβ42 isoform. The CSF module includes a) a CSF Aβ42 compartment including a total amount of CSF Aβ42 isoforms; b) a CSF Aβ42 transfer rate including a rate of transfer of soluble Aβ42 isoform from the soluble Aβ42 compartment to the CSF Aβ42 compartment; and c) a CSF Aβ42 clearance rate including a rate of disappearance of CSF Aβ42 from the CSF Aβ42 pool. The amyloid kinetics module may further include: a) a soluble comparison Aβ isoform compartment including an amount of a soluble comparison Aβ isoform; b) a comparison Aβ isoform formation rate including a rate of formation of soluble comparison Aβ isoform from the C99 c-terminal fragments; and c) a comparison Aβ isoform clearance rate including a rate of disappearance of soluble comparison Aβ isoforms from the soluble comparison Aβ isoform compartment. The CSF module may further include: a) a CSF comparison Aβ isoform compartment including a total amount of CSF comparison Aβ isoforms; b) a CSF comparison Aβ isoform transfer rate including a rate of transfer of soluble comparison Aβ isoform from the soluble comparison Aβ isoform compartment to the CSF comparison Aβ

isoform compartment; and c) a CSF comparison Aβ isoform clearance rate including a rate of disappearance of CSF comparison Aβ isoform from the CSF comparison Aβ isoform compartment. The comparison Aβ isoform may be chosen from Aβ38 and Aβ40.

[001 6] In a sixth aspect, a system for estimating the kinetics of amyloid-beta (Aβ) in the CNS of a patient is disclosed that includes: at least one processor; and a CNS Aβ kinetic model application including a plurality of modules executable using the at least one processor. The modules may include: a) a plasma amino acid module to estimate a plasma amino acid compartment including a plasma concentration of at least one amino acid; b) an APP incorporation module to estimate an APP incorporation rate including a rate of incorporation of the at least one amino acid from the plasma amino acid compartment into an APP molecule in an APP compartment; c) an APP module to estimate the APP compartment including a total amount of APP molecules; d) a C99 formation module to estimate a C99 formation rate including a rate of formation of a C99 c-terminal fragment in a C99 compartment from the APP molecules; e) a C99 clearance module to estimate a C99 clearance rate including a rate of disappearance of the C99 c-terminal fragment from the C99 compartment; e) a C99 module to estimate the C99 compartment including a total amount of the C99 c-terminal fragments; f) a free Aβ formation module to estimate at least one free Aβ isoform formation rate, each free Aβ isoform formation rate including a rate of formation of a free Aβ isoform in a free Aβ compartment from the C99 c-terminal fragments; g) a free Aβ clearance module to estimate at least one free Aβ isoform clearance rate, each free Aβ isoform clearance rate including a rate of disappearance of one of the free Aβ isoforms from the free Aβ compartment; h) a free Aβ module to estimate the free Aβ compartment including the total amount of all free Aβ isoforms; i) a free Aβ recycling module to estimate at least one free Aβ incorporation rate, each free Aβ incorporation rate including a rate of transformation of a free Aβ isoform to an incorporated Aβ isoform in a recycled Aβ compartment, and at least one Aβ recycling rate, each Aβ recycling rate including a rate of recycling an

incorporated Aβ isoform in the recycled Aβ compartment back into a free Aβ isoform in the free Aβ compartment; j) a CSF Aβ transfer module to estimate at least one CSF Aβ transfer rate, each Aβ transfer rate including a rate of transfer of one free Aβ isoform from the free Aβ compartment to a CSF Aβ compartment; k) a CSF Aβ clearance module to estimate at least one CSF Aβ clearance rate, each CSF Aβ clearance rate including a rate of disappearance of one CSF Aβ isoform from the CSF Aβ compartment; and l) a CSF Aβ module to estimate the CSF Aβ compartment including the total amount of CSF Aβ isoforms. The Aβ isoforms may be chosen from Aβ38, Aβ40, and Aβ42. At least a portion of the plasma amino acid compartment may include a plasma concentration of at least one labeled amino acid. At least a portion of the APP compartment may include an amount of enriched APP molecules incorporating the at least one labeled amino acid. At least a portion of the C99 compartment may further include an amount of enriched C99 c-terminal fragments formed from the amount of enriched APP molecules. At least a portion of the Aβ isoforms may further include an amount of enriched Aβ isoforms formed from the amount of enriched C99 c-terminal fragments. The CSF Aβ transfer module may further estimate at least one CSF Aβ delay, each CSF Aβ delay including a delay in the transfer of one free Aβ isoform from the free Aβ compartment to the CSF Aβ compartment. The at least one CSF Aβ transfer rate may be represented by a fluid flow of ISF within the brain.

[001 7] In a seventh aspect, a method of using a model of amyloid β (Aβ) isoform enrichment kinetics is provided that includes: a) obtaining from a patient measured Aβ enrichment kinetics data including a time course of concentration of a labeled moiety infused into the patient, a measured time course of Aβ42 enrichment kinetics in the CSF of the patient, and a measured time course of at least one other comparison Aβ isoform enrichment kinetics in the patient; b) inputting the measured Aβ enrichment kinetics data into the model, wherein the model represents enrichment kinetics of Aβ42 and the at least one other comparison Aβ isoform; c) obtaining a set of model parameters from the model; d) calculating a model index including a mathematical combination of at

least two model parameters from the model; e) comparing the model index to a pre-selected threshold range; and f) identifying a disease state of the patient if the model index falls outside of the threshold range. The disease state may be identified as Alzheimer's if the model index falls outside of the threshold range. The severity of the disease state may be identified by comparing the model index to a pre-selected correlation of the disease state with the model index. The correlation of the disease state may be a correlation of the model index with PIB imaging values obtained from a population of patients with a range of disease states. The measured Aβ enrichment kinetics data from a patient may be obtained by the SILK method. The labeled moiety may be labeled leucine. The at least one other comparison Aβ isoform may be chosen from Aβ38 and Aβ40. The model parameters may be chosen from: concentration of Aβ isoforms, rates of transfer, rates of irreversible loss, rates of exchange, rates of delay, and combinations thereof. The model index may be calculated using a rate of irreversible loss of Aβ42 and a rate of transfer of Aβ42. The model parameters may be obtained by iteratively varying the model parameters until a best fit of the estimated Aβ enrichment kinetics to the measured Aβ enrichment kinetics is obtained.

[001 8] In an eighth aspect, an amyloid kinetics modeling system for estimating a time course of enrichment kinetics of at least one Aβ isoform is provided that includes: a) at least one processor; and b) a CRM containing an amyloid kinetics application including a plurality of modules executable on the at least one processor. The plurality of modules may include: i) a plasma module to represent infusion of a labeled moiety into the plasma of a patient and to represent transport of the labeled moiety across the blood brain barrier (BBB) of the patient; ii) a brain tissue module to represent incorporation of the labeled moiety into APP and formation of C99; iii) an amyloid kinetics module to represent cleavage of the C99 to form at least one Aβ isoform and subsequent kinetics of the at least one Aβ isoform within the brain of the patient; iv) a CSF module to represent transport of the at least one Aβ isoform into the CSF of the patient; v) a blood enrichment module to represent transport of the at least one

Aβ isoform into the blood of the patient; v) a model tuning module to iteratively adjust a set of model parameters defining a dynamic response of the model to an input time history of plasma leucine enrichment into the plasma module in order to optimize a match between predicted enrichment kinetics and measured enrichment kinetics of the at least one Aβ isoform in the patient; and vi) a GUI module to generate one or more forms used to receive inputs to the system and to deliver output from the system. The plasma module includes a plasma amino acid compartment including a plasma concentration of at least one amino acid, wherein the plasma concentration of the at least one amino acid may be determined using an input including a time history of an infusion of a labeled amino acid into a patient. The brain tissue module includes: a) an APP compartment including a total amount of APP; b) an APP incorporation rate including a rate of incorporation of the at least one amino acid from the plasma amino acid compartment into an APP molecule in the APP compartment; c) a C99 compartment including a total amount of C99 c-terminal fragments; d) a C99 formation rate including a rate of formation of the C99 c-terminal fragments in the C99 compartment from the APP molecules; and e) a C99 clearance rate including a rate of disappearance of the C99 c-terminal fragments from the C99 compartment. The amyloid kinetics module includes: a) a soluble Aβ42 isoform compartment including an amount of a soluble Aβ42 isoform; b) an Aβ42 isoform formation rate including a rate of formation of soluble Aβ42 isoform from the C99 c-terminal fragments; c) an Aβ42 isoform clearance rate including a rate of disappearance of Aβ42 isoforms from the soluble Aβ compartment; d) an Aβ42 incorporation rate including a rate of transformation of the soluble Aβ42 isoform to an incorporated Aβ42 isoform; and e) a recycled Aβ42 compartment including a total amount of incorporated Aβ42 isoform. The CSF module includes: a) a CSF Aβ42 compartment including a total amount of CSF Aβ42 isoforms; b) a CSF Aβ42 transfer rate including a rate of transfer of soluble Aβ42 isoform from the soluble Aβ42 compartment to the CSF Aβ42 compartment; and c) a CSF Aβ42 clearance rate including a rate of disappearance of CSF Aβ42 from the CSF Aβ42 pool. The amyloid kinetics module may further include: a) a soluble

comparison Aβ isoform compartment including an amount of a soluble comparison Aβ isoform; b) a comparison Aβ isoform formation rate including a rate of formation of soluble comparison Aβ isoform from the C99 c-terminal fragments; and c) a comparison Aβ isoform clearance rate including a rate of disappearance of soluble comparison Aβ isoforms from the soluble comparison Aβ isoform compartment. The CSF module may further include: a) a CSF comparison Aβ isoform compartment including a total amount of CSF comparison Aβ isoforms; b) a CSF comparison Aβ isoform transfer rate including a rate of transfer of soluble comparison Aβ isoform from the soluble comparison Aβ isoform compartment to the CSF comparison Aβ isoform compartment; and c) a CSF comparison Aβ isoform clearance rate including a rate of disappearance of CSF comparison Aβ isoform from the CSF comparison Aβ isoform compartment. The blood enrichment module includes: a) a blood Aβ42 compartment including a total amount of blood Aβ42 isoforms; b) a blood Aβ42 transfer rate including a rate of transfer of soluble Aβ42 isoform from the soluble Aβ42 compartment to the blood Aβ42 compartment; and c) a blood Aβ42 clearance rate including a rate of disappearance of blood Aβ42 from the blood Aβ42 pool. The comparison Aβ isoform may be chosen from Aβ38 and Aβ40.

[001 9] In a ninth aspect, an amyloid kinetics modeling system for estimating a time course of enrichment kinetics of at least one Aβ isoform is provided that may include: a) at least one processor; and b) a CRM containing an amyloid kinetics application including a plurality of modules executable on the at least one processor. The plurality of modules may include: i) a plasma module to represent infusion of a labeled moiety into the plasma of a patient and to represent transport of the labeled moiety across the blood brain barrier (BBB) of the patient; ii) a brain tissue module to represent incorporation of the labeled moiety into APP and formation of C99; iii) an amyloid kinetics module to represent cleavage of the C99 to form at least one Aβ isoform and subsequent kinetics of the at least one Aβ isoform within the brain of the patient; v) a blood enrichment module to represent transport of the at least one Aβ isoform into the blood of the patient; v) a model tuning module to iteratively adjust a set of model

parameters defining a dynamic response of the model to an input time history of plasma leucine enrichment into the plasma module in order to optimize a match between predicted enrichment kinetics and measured enrichment kinetics of the at least one Aβ isoform in the patient; and vi) a GUI module to generate one or more forms used to receive inputs to the system and to deliver output from the system. The plasma module includes a plasma amino acid compartment including a plasma concentration of at least one amino acid, wherein the plasma concentration of the at least one amino acid may be determined using an input including a time history of an infusion of a labeled amino acid into a patient. The brain tissue module includes: a) an APP compartment including a total amount of APP; b) an APP incorporation rate including a rate of incorporation of the at least one amino acid from the plasma amino acid compartment into an APP molecule in the APP compartment; c) a C99 compartment including a total amount of C99 c-terminal fragments; d) a C99 formation rate including a rate of formation of the C99 c-terminal fragments in the C99 compartment from the APP molecules; and e) a C99 clearance rate including a rate of disappearance of the C99 c-terminal fragments from the C99 compartment. The amyloid kinetics module includes: a) a soluble Aβ42 isoform compartment including an amount of a soluble Aβ42 isoform; b) an Aβ42 isoform formation rate including a rate of formation of soluble Aβ42 isoform from the C99 c-terminal fragments; c) an Aβ42 isoform clearance rate including a rate of disappearance of Aβ42 isoforms from the soluble Aβ compartment; d) an Aβ42 incorporation rate including a rate of transformation of the soluble Aβ42 isoform to an incorporated Aβ42 isoform; and e) a recycled Aβ42 compartment including a total amount of incorporated Aβ42 isoform. The amyloid kinetics module may further include: a) a soluble comparison Aβ isoform compartment including an amount of a soluble comparison Aβ isoform; b) a comparison Aβ isoform formation rate including a rate of formation of soluble comparison Aβ isoform from the C99 c-terminal fragments; and c) a comparison Aβ isoform clearance rate including a rate of disappearance of soluble comparison Aβ isoforms from the soluble comparison Aβ isoform compartment. The blood enrichment module includes: a) a blood Aβ42 compartment including a

total amount of blood Aβ42 isoforms; b) a blood Aβ42 transfer rate including a rate of transfer of soluble Aβ42 isoform from the soluble Aβ42 compartment to the blood Aβ42 compartment; and c) a blood Aβ42 clearance rate including a rate of disappearance of blood Aβ42 from the blood Aβ42 pool. The comparison Aβ isoform may be chosen from Aβ38 and Aβ40.

BRIEF DESCRIPTION OF THE DRAWINGS

[0020] **FIG. 1** is a schematic diagram illustrating the processing of amyloid precursor protein (APP) [SEQ. ID. NO. 1] into amyloid-β (Aβ) within a cell.

[0021] **FIG. 2** is a schematic diagram illustrating the processing of Aβ and paths the Aβ isoforms may take *in vivo.*

[0022] **FIG. 3** is a simplified diagram illustrating the overall architecture of a compartment model for the metabolism and trafficking of Aβ.

[0023] **FIG. 4** is a detailed diagram illustrating the detailed architecture of a compartment model for the metabolism and trafficking of Aβ with measured Aβ concentrations at the CSF.

[0024] **FIG. 5** is a graph summarizing a time course of plasma leucine enrichment normalized to the enrichment plateau during and after labeled leucine infusion.

[0025] **FIGS. 6A - 6B** illustrate an average Aβ isotropic kinetic time course profile in CSF of non-mutation carriers as an isotropic enrichment ratio **(FIG. 6A)** and as enrichments normalized to plasma leucine plateau enrichments with a model fit line **(FIG. 6B). FIGS. 6C - 6D** illustrate an average Aβ isotropic kinetic time course profile in CSF of PIB- mutation carriers as an isotropic enrichment ratio **(FIG. 6C)** and as enrichments normalized to plasma leucine plateau enrichments with a model fit line **(FIG. 6D). FIGS. 6E - 6F** illustrate an average Aβ isotropic kinetic time course profile in CSF of PIB+ mutation carriers as an isotropic enrichment ratio **(FIG. 6E)** and as enrichments normalized to plasma leucine plateau enrichments with a model fit line **(FIG. 6F).**

[0026] **FIG. 7** is a block diagram illustrating a computing environment for calibrating and executing a compartment model according to one embodiment.

[0027] **FIG. 8** is a block diagram illustrating a computing device for calibrating and executing a compartment model according to one embodiment.

[0028] **FIG. 9** is a block diagram illustrating a data source that may be used when calibrating and executing a compartment model according to one embodiment.

[0029] **FIG. 10** is a block diagram illustrating a computing device for calibrating and executing a compartment model according to one embodiment. **FIG. 11** is a flowchart illustrating one method of calibrating a compartmental model according to one embodiment.

[0030] **FIG. 12** is a diagram illustrating a modified architecture of a compartment model for the metabolism and trafficking of Aβ in one aspect.

[0031] **FIG. 13** is a diagram illustrating flow of Aβ42 from the ventricles to the brain surface/CSF.

[0032] **FIGS. 14A - 14B** are graphs summarizing the pressure **(FIG. 14A)** and velocity of flow **(FIG. 14B)** from the ventricles to the brain surface/CSF. **FIG. 15** is a flowchart illustrating a method of using the kinetic model to identify a patient's disease state.

[0033] **FIG. 16** is a block diagram illustrating the modules of an amyloid kinetics modeling system in an aspect.

[0034] **FIG. 17** is a schematic diagram illustrating the nodes of a flow model in one aspect.

[0035] **FIG. 18** is a schematic diagram illustrating a detailed architecture of a single node of a flow model in one aspect.

[0036] **FIG. 19** depicts two graphs showing a monoexponential slope fit to the descending enrichment on the back end of the kinetic tracer curve for Aβ42. **FIG. 19A** illustrates that the entire back end of the peak is monoexponential to the end of the time course (36 h). In contrast, **FIG. 19B** illustrates that there is evidence of a 2nd, slower exponential tail to the peak; in

these cases, an initial rapid slope that visually excludes the slower tail is selected. The graphs show the natural log of enrichment vs. time; the monoexponential slope FCR is the negative of the slope.

[0037] **FIG. 20** depicts three graphs showing that a comparison of isotopic enrichments around the midpoint on the back end of the kinetic tracer curve is able to discriminate the PIB groups highly significantly. **FIG. 20A** shows the ratio of Aβ42 percent labeled / Aβ40 percent labeled at 23 hours graphed on the y-axis and PIB staining graphed on the x-axis. A threshold ratio of 0.9 is indicated by the dashed line. **FIG. 20B** shows the average of the ratio of Aβ42 percent labeled / Aβ40 percent labeled at 23 hours and 24 hours graphed on the y-axis and PIB staining graphed on the x-axis. A threshold ratio of 0.9 is indicated by the dashed line. **FIG. 20C** shows the calculated values of ten times k_{ex42} added to ratio of the rate constants for irreversible loss for Aβ42 versus Aβ40 (10x k_{ex42} + FTR ratio) plotted as a function of PIB staining. A threshold ratio of 1.75 is indicated by the dashed line. MC+ = patients with PSEN1 or PSEN2 mutations that were PIB positive by PET; MC- = patients with PSEN1 or PSEN2 mutations that were PIB negative by PET; NC = non-carrier mutation carrier sibling controls.

[0038] **FIG. 21** is a detailed diagram illustrating the detailed architecture of a compartment model for the metabolism and trafficking of Aβ with measured Aβ concentrations at the blood.

[0039] Corresponding reference characters and labels indicate corresponding elements among the views of the drawings. The headings used in the figures should not be interpreted to limit the scope of the claims.

DETAILED DESCRIPTION

[0040] Provided herein are methods for modeling the *in vivo* kinetics and metabolism of a CNS biomolecule, in particular one or more amyloid-β (Aβ) isoforms. As used herein, the term "CNS biomolecule" refers to a biomolecule synthesized in the central nervous system (CNS). A skilled artisan will appreciate that while a biomolecule may be synthesized in the CNS, the biomolecule may

be transported to other compartments of the body, such that the biomolecule may be detected in the CNS, peripheral nervous system, or outside the nervous system (e.g. in the blood). The kinetic model may be developed and/or calibrated utilizing measured data from patients including, but not limited to the blood and/or the cerebrospinal fluid (CSF) of the patients. Blood, as defined herein, may refer to whole blood, plasma, serum, and any other blood fraction known in the art. This disclosure further provides methods for developing a model by determining and predicting steady state metabolic kinetic parameters. In addition, this disclosure additionally provides methods for modeling *in vivo* metabolism of one or more Aβ isoforms to determine concentrations of the Aβ isoforms at various states, fractional turnover rates of the one or more Aβ isoforms, and production rates of the one or more Aβ isoforms. Also provided are methods for using the model to identify a patient's disease state and predict aspects of Aβ isoform enrichment kinetics and/or concentrations within a patient. In particular, this disclosure relates to methods of modeling Aβ turnover kinetics in a kinetic model. In an aspect, the kinetic model may be a steady state compartmental model, a flow model, or any combination thereof without limitation. In an aspect, the kinetic model may be used to model the metabolism of any CNS biomolecule.

[0041] The method of developing the model may include, but is not limited to, measuring a concentration of a labeled moiety introduced into a patient over a period of time. The labeled moiety may be incorporated into an Aβ precursor within the patient. The method may further include measuring concentrations in a biological sample of the Aβ isoforms incorporating the labeled moiety in the patient, and incorporating the measured data into known or hypothesized relationships and/or metabolic processes. In an aspect, the model may predict the measured values. The model may be developed by calibrating the predicted values against measured values and adjusting a set of model parameters to provide a best fit of the predicted enrichment kinetics of the one or more Aβ isoforms in the CNS to the measured kinetics from the patient. In an aspect, the model may output model parameters specific for each patient.

[0042] The concentrations of the one or more Aβ precursors and/or one or more Aβ isoforms and associated metabolic processes in the brain may be represented within the model. In one aspect, this representation within the model may include a compartment, a rate constant, flow equation, and/or any other mathematical representation known in the art without limitation. In an aspect, the concentration in a compartment may be calculated by multiplying the concentration in the previous compartment by a transfer rate constant between the two compartments minus any irreversible loss. Different aspects of the model may be differentiated by different numbers of compartments or types of compartments, the order of the compartments, the equations governing the trafficking and flow of Aβ isoforms, the Aβ isoform being modeled, or any other aspect for modeling the metabolism of a CNS biomolecule.

[0043] In another aspect, the kinetic model may represent the movement of soluble Aβ isoforms within the brain as a flow from the ventricles to the brain surface and into the CSF and/or blood. In an aspect, the movement of an Aβ isoform in the brain interstitial fluid (ISF) may be represented by at least one fluid flow equation. In another aspect, the flow of Aβ isoforms may be represented as a transfer between nodes distributed spatially between the point where the Aβ isoform may enter the ISF and the surface of the brain.

[0044] In an aspect, the concentration of a labeled moiety and measured concentrations of labeled Aβ isoforms in the CSF and/or blood may be used to develop a model of the metabolism of the labeled Aβ and to determine the rate constants associated with each compartment or flow equation. In addition, the model may be used to calculate predicted concentrations of the Aβ isoforms in the CSF, in the brain, in the blood, or at any other location in a patient. Non-limiting examples of how the model of *in vivo* Aβ metabolism may be used include identifying the disease state of a patient, fitting a curve of measured data acquired from a patient, predicting the metabolism, processing, and/or concentration of Aβ and its isoforms in a patient, identifying sensitive pathway components to help design drugs or understand a CNS disease, and

investigating changes in the kinetics of the isoforms that may be induced by investigational drugs.

[0045] Detailed descriptions of various aspects of the methods of modeling the *in vivo* metabolism of Aβ are provided herein below.

I. Methods of developing a model of the *in vivo* metabolism of Aβ

[0046] In various aspects, a method to develop a model to represent the synthesis of one or more Aβ isoforms in the central nervous system *in vivo* and to predict the turnover and production rates of the one or more Aβ isoforms in one or more patients is provided. Data from patients, including time course amounts of a labeled moiety and the concentration of at least one Aβ isoform, may be used in the development of the model.

(a) Degenerative diseases

[0047] In various aspects, the model may be used to predict the turnover and production rates of at least one Aβ isoform in a patient. In an aspect, the model may be used to predict the effects of the dysregulation of Aβ isoform turnover and production rates in a subject with Aβ amyloidosis. The term "Aβ amyloidosis' refers to Aβ deposition in a subject that may result from differential metabolism (e.g. increased production, reduced clearance, or both). Aβ amyloidosis is clinically defined as evidence of Aβ deposition in the brain either by amyloid imaging (e.g. PiB PET) or by decreased cerebrospinal fluid (CSF) Aβ42 or Aβ42/40 ratio. See, for example, Klunk W E et al. *Ann Neurol* 55(3) 2004, and Fagan AM et al. *Ann Neurol* 59(3) 2006, each hereby incorporated by reference in its entirety. Subjects with Aβ amyloidosis are also at an increased risk of developing a disease associated with Aβ amyloidosis. Diseases associated with Aβ amyloidosis include, but are not limited to, Alzheimer's Disease (AD), cerebral amyloid angiopathy, Lewy body dementia, and inclusion body myositis. Non-limiting examples of symptoms associated with Aβ amyloidosis may include impaired cognitive function, altered behavior,

abnormal language function, emotional dysregulation, seizures, dementia, and impaired nervous system structure or function.

[0048] In another aspect, the model may be used to predict the effects of the dysregulation of Aβ isoform turnover and production rates resulting from a degenerative disease in a patient. Any degenerative disease characterized by the dysregulation in the turnover and production rate of any CNS biomolecule including, but not limited to at least one Aβ isoform may be predicted using the model without limitation. By way of non-limiting example, Alzheimer's Disease (AD) is a debilitating disease characterized by accumulation of amyloid plaques in the central nervous system resulting from increased production, decreased clearance, or a combination of increased production and decreased clearance of Aβ protein. While AD is an exemplary disease that may be diagnosed or monitored by various aspects of this disclosure, this disclosure is not limited to AD. It is envisioned that the method may be used in modeling the kinetics, diagnosis, and assessment of treatment efficacy of several neurological and neurodegenerative diseases, disorders, or processes including, but not limited to, AD, Parkinson's Disease, stroke, frontal temporal dementias (FTDs), Huntington's Disease, progressive supranuclear palsy (PSP), corticobasal degeneration (CBD), aging-related disorders and dementias, Multiple Sclerosis, Prion Diseases (e.g. Creutzfeldt-Jakob Disease, bovine spongiform encephalopathy or Mad Cow Disease, and scrapie), Lewy Body Disease, and Amyotrophic Lateral Sclerosis (ALS or Lou Gehrig's Disease). It is also envisioned that the method of modeling *in vivo* kinetics of a CNS disease may be used to study the normal physiology, metabolism, and function of the CNS.

[0049] The *in vivo* metabolism of at least one Aβ isoform or other CNS biomolecule may be modeled in any human patient without limitation. In one aspect, the human patient may be of an advanced age including, but not limited to, human patients older than about 85. Alternatively, the *in vivo* metabolism of CNS biomolecules may be modeled in other mammalian patients without limitation. In another aspect, the patient may be a companion animal such as a dog or cat. In another alternative aspect, the patient may be a livestock animal

such as a cow, pig, horse, sheep or goat. In yet another alternative embodiment, the patient may be a zoo animal. In another aspect, the patient may be a research animal such as a non-human primate or a rodent.

(b) Overview of Aβ *metabolism and labeling*

[0050] In various aspects, the architecture of the model may be developed using any known or hypothesized pathways and/or mechanisms of Aβ biometabolism without limitation.

[0051] Without being limited to any particular theory, amino acids, including labeled amino acids, may be incorporated into amyloid precursor protein (APP) in neural cells. Amyloid precursor protein (APP) is a transmembrane protein expressed in many cells and may be concentrated in neurons and neuronal synapses. APP may be processed by α-, β-, and/or γ-secretases, creating peptides of varying length including, but not limited to, Aβ. C99 forms the c-terminal fragment of APP and is cleaved by the action of β-secretase. Aβ is a peptide of 36-43 amino acids located within the membrane-spanning domain of APP. Aβ is typically formed by the cleavage of APP by the β- and γ-secretases in succession or by the cleavage of C99 by γ-secretase. γ-secretase includes enzymatic components *PSEN1* and *PSEN2.* Varying isoforms of Aβ (e.g. Aβ38, Aβ40, Aβ42) may be produced through further processing and cleavage in the endoplasmic reticulum, the trans-Golgi network, or other areas of post-processing. **FIG. 1** depicts a schematic illustrating the processing of APP into Aβ within a cell and indicates the locations where the secretases cleave APP. The amino acid sequence of Aβ (SEQ ID NO: 1) is shown at the bottom.

[0052] Because APP and C99 are cell-associated proteins, these proteins are not considered soluble and are not transported within the brain via flow mechanisms. However, after cleavage by γ-secretase, Aβ peptides can flow within the brain's interstitial fluid (ISF). The Aβ peptides may be degraded within the brain, taken up in reversible higher order structures (e.g. micelles), taken up irreversibly into plaques, transported across the blood-brain barrier to the blood stream, and/or transported out of the brain as the ISF merges with the CSF, as

illustrated in **FIG. 2.** There may be some recycling of the higher order structures and the plaques with the soluble Aβ isoform monomers, whereas degradation and exiting the blood brain barrier may irreversibly remove at least a portion of the soluble Aβ isoform monomers from the brain. ISF in the brain may be derived from the brain capillaries and from the ventricles. Without being limited to any particular theory, the pressure in the ventricles is typically higher than the pressure in the CSF, thereby inducing an outward flow of fluid from the ventricles to the surface of the brain and to the CSF.

[0053] To track the formation and kinetics of Aβ *in vivo,* newly formed APP may be labeled by incorporation of a labeled moiety during protein production. The labeled APP may then be cleaved into labeled Aβ isoforms. In an aspect, the labeled moiety may be an amino acid with a stable isotope of carbon, nitrogen, or any other isotope that may be incorporated into amino acids during protein production. Because leucine is more easily capable of crossing the blood brain barrier compared to other amino acids, leucine may be better-suited for use with CNS biomolecules and Aβ. Referring back to **FIG. 1,** labeled leucines (L) within Aβ are indicated in black.

(c) CNS Biomolecule

[0054] The method for developing a model may include representing the metabolism of any biomolecule derived from the CNS *in vivo* including, but not limited to, at least one Aβ isoform. The CNS biomolecule may include, but is not limited to, a protein, a lipid, a nucleic acid, a carbohydrate, or any CNS biomolecule known in the art. Any CNS biomolecule may be represented, so long as the CNS biomolecule may be labeled during *in vivo* synthesis and a sample may be collected from which their metabolism may be measured. In an aspect, the CNS biomolecule is a protein synthesized in the CNS. Non-limiting examples of suitable proteins to be modeled include: amyloid-β (Aβ), Aβ isoforms and other variants, soluble amyloid precursor protein (APP), apolipoprotein E (isoforms 2, 3, or 4), apolipoprotein J (also called clusterin), Tau (another protein associated with AD), glial fibrillary acidic protein, alpha-2 macroglobulin, synuclein, S100B,

Myelin Basic Protein (implicated in multiple sclerosis), prions, interleukins, TDP-43, superoxide dismutase-1 , huntingtin, and tumor necrosis factor (TNF). Additional CNS biomolecules that may be targeted include products of, or proteins or peptides that interact with, GABAergic neurons, noradrenergic neurons, histaminergic neurons, seratonergic neurons, dopaminergic neurons, cholinergic neurons, and glutaminergic neurons.

[0055] The method may model the metabolism of APP in one aspect. In an additional aspect, the CNS biomolecule whose *in vivo* metabolism is modeled may be amyloid-beta (Aβ) protein. In another aspect, isoforms of Aβ (e.g., Aβ40, Aβ42, Aβ38 and/or others) may be modeled. In a further aspect, digestion products of Aβ (e.g., $A\beta_{6\text{-}16}$, $A\beta_{17\text{-}2\beta)}$ may be modeled. In an aspect, the model may represent the metabolism of more than one CNS biomolecule at a time. In one aspect, the CNS biomolecule may include, but is not limited to, C99, APP, Aβ38, Aβ40, Aβ42, and any other Aβ isoform.

(d) Labeled moiety

[0056] In an aspect, the plasma concentration of a labeled moiety may be input into the model. In one aspect, the labeled moiety plasma concentration may be used to develop the model and determine the model parameters.

[0057] When the method is employed to model the metabolism of a protein, the labeled moiety may be an amino acid. Those of skill in the art will appreciate that at least several amino acids may be used to provide the label of a CNS biomolecule. Generally, the choice of amino acid is based on a variety of factors such as: (1) the amino acid generally is present in at least one residue of the protein or peptide of interest; (2) the amino acid is generally able to quickly reach the site of protein synthesis and rapidly equilibrate across the blood-brain barrier; (3) the amino acid ideally may be an essential amino acid (not produced by the body), so that a higher percent of labeling may be achieved; (4) the amino acid label generally does not influence the metabolism of the protein of interest (e.g., very large doses of leucine may affect muscle metabolism); and (5) the

relatively wide availability of the desired amino acid (i.e., some amino acids are much more expensive or harder to manufacture than others).

[0058] In an aspect, the amino acid leucine may be used to label proteins that are synthesized in the CNS. Non-essential amino acids may also be used; however, measurements may be less accurate. In one aspect, $^{13}C_6$-phenylalanine, which contains six ^{13}C atoms, may be used to label a neurally derived protein. In an aspect, $^{13}C_6$-leucine may be used to label a neurally derived protein. In an exemplary aspect, $^{13}C_6$-leucine may be used to label amyloid-β.

[0059] There are numerous commercial sources of labeled amino acids, containing both non-radioactive isotopes and radioactive isotopes. Generally, the labeled amino acids may be produced either biologically or synthetically. Biologically produced amino acids may be obtained from an organism (e.g., kelp/seaweed) grown in an enriched mixture of ^{13}C, ^{15}N, or another isotope that is incorporated into amino acids as the organism produces proteins. The amino acids are then separated and purified. Alternatively, amino acids may be made using any known synthetic chemical processes.
The labeled moiety may be administered to a patient using any one of at least several methods known in the art. Non-limiting examples of suitable methods of administration include intravenous, intra-arterial, subcutaneous, intraperitoneal, intramuscular, and oral administration. In one aspect, the labeled moiety is administered to the patient using intravenous infusion.

[0060] The labeled moiety may be administered slowly over a period of time or as a large single dose depending upon the type of analysis chosen (e.g., steady state or bolus). To achieve steady-state levels of the labeled CNS biomolecule, the labeling time generally should be of sufficient duration so that the labeled CNS biomolecule may be reliably quantified. The labeling time sufficient for reliable quantification of steady state levels of a labeled Aβ in a blood sample is typically less than required time for reliable quantification of steady state levels of Aβ in a CSF sample. See for example, US 7,892,845 and US 13/669,497, each hereby incorporated by reference in its entirety. This

duration may be selected to be sufficient to result in saturation of the biochemical pathways associated with the synthesis of the CNS biomolecule. In one aspect, the duration may be sufficient to result in the saturation of the biochemical pathways associated with the synthesis and kinetics of at least one Aβ isoform in the brain of a patient, including, but not limited to: APP synthesis, cleavage of C99 and the at least one Aβ isoform, the transport of the at least one Aβ isoform to the CSF, and the transport of the at least one Aβ isoform to the blood. In another aspect, the saturation of the biochemical pathways may be indicated by the detection of stabilized levels of the at least one Aβ isoform in the CSF and/or blood as measured in a patient.

[0061] In an aspect, the labeled moiety is administered intravenously for an amount of time that is less than the half-life of Aβ in blood or CSF. In other aspect, the labeled moiety is administered intravenously for an amount of time that is greater than the half-life of Aβ in blood or CSF. For example, the labeled moiety may be administered intravenously over a duration of minutes to hours, including, but not limited to, for at least 10 minutes, at least 20 minutes, at least 30 minutes, at least 1.0 hour, at least 1.5 hours, at least 2.0 hours, at least 2.5 hours, at least 3.0 hours, at least 3.5 hours, at least 4.0 hours, at least 4.5 hours, at least 5.0 hours, at least 5.5 hours, at least 6.0 hours, at least 6.5 hours, at least 7.0 hours, at least 7.5 hours, at least 8.0 hours, at least 8.5 hours, at least 9.0 hours, at least 9.5 hours, at least 10.0 hours, at least 10.5 hours, 1 at least 1.0 hours, at least 11.5 hours, or at least 12 hours. In another aspect, the labeled moiety may be administered intravenously over a period ranging from about 6 hours to about 18 hours. In another aspect, the labeled moiety may be administered intravenously over a period of about 9 hours. In another aspect, the labeled moiety may be administered intravenously over a period of about 3 hours. In yet another aspect, a labeled moiety is administered orally as multiple doses. The multiple doses may be administered sequentially or an amount of time may elapse between each dose. The amount of time between each dose may be a few seconds, a few minutes, or a few hours. In each of the above embodiments, the labeled moiety can be labeled leucine, labeled phenylalanine,

or any other labeled amino acid that is capable of crossing the blood-brain barrier.

[0062] Those of skill in the art will appreciate that the amount (or dose) of the labeled moiety can and will vary. Generally, the amount is dependent on (and estimated by) the following factors. (1) The type of analysis desired. For example, to achieve a steady state of about 15% labeled leucine in plasma requires about 2 mg/kg/hr over 9 hr after an initial bolus of about 3 mg/kg over 10 min. In contrast, if no steady state is required, a bolus of labeled leucine (e.g., about 400mg to about 800mg of labeled leucine) may be given. (2) The Aβ variant under analysis. For example, if the Aβ variant is being produced rapidly, then less labeling time may be needed and less label may be needed - perhaps as little as 100mg or less as a bolus. And (3) the sensitivity of the technology to detect label. For example, as the sensitivity of label detection increases, the amount of label that is needed may decrease.

[0063] In another aspect, a labeled moiety is administered orally as a single bolus. In another aspect, a labeled moiety is administered intravenously as a single bolus. In still another aspect, a labeled moiety is administered intravenously as an infusion for about 1 hour. All three methods of administration (oral bolus, IV bolus, and IV infusion) work equally well in terms of providing a reliable measure of amyloid beta metabolism. An intravenous bolus of a labeled moiety and an oral bolus of labeled moiety are easier to administer than an intravenous infusion, and also results in maximal levels of free label at an earlier time point (e.g. about 5 to about 10 minutes, and about 30 to about 60 minutes, respectively, for labeled leucine). In each of the above embodiments, the labeled moiety can be labeled leucine, labeled phenylalanine, or any other labeled amino acid that is capable of crossing the blood brain barrier.

(e) Biological sample

[0064] The method of developing the model may include obtaining a biological sample from a patient so that the *in vivo* metabolism of the labeled CNS biomolecule may be determined. Information from a patient's biological

sample may be used as an input in the method of developing and/or calibrating a model of *in vivo* metabolism of a CNS biomolecule.

[0065] Suitable biological samples include, but are not limited to, cerebral spinal fluid (CSF), blood plasma, blood serum, urine, saliva, perspiration, and tears. In one aspect, biological samples may be taken from the CSF. In an alternate aspect, biological samples may be collected from the urine. In another aspect, biological samples may be collected from the blood.

[0066] Cerebrospinal fluid may be obtained by lumbar puncture with or without an indwelling CSF catheter (a catheter is preferred if multiple collections are made over time). Blood may be collected by veni-puncture with or without an intravenous catheter. Urine may be collected by simple urine collection or more accurately with a catheter. Saliva and tears may be collected by direct collection using standard good manufacturing practice (GMP) methods.

[0067] In general, when the CNS biomolecule is a protein, the method of developing and/or calibrating the model may include obtaining a first biological sample to be taken from the patient prior to administration of the labeled moiety to provide a baseline for the patient. After administration of the labeled amino acid or protein, one or more samples generally may be taken from the patient. As will be appreciated by those of skill in the art, the number of samples and when they may be taken generally depend upon a number of factors such as: the type of analysis, type of administration, the protein of interest, the rate of metabolism, the type of detection, etc.

[0068] In general, samples obtained during the labeling phase may be used to determine the rate of synthesis of the Aβ variant, and samples taken during the clearance phase may be used to determine the clearance rate of the Aβ variant. Labeled Aβ increases during labeling and then decreases after the labeling has stopped. In one aspect, the CNS biomolecule may be a protein including, but not limited to at least one Aβ isoform and one or more samples of CSF may be taken hourly for 36 hours. Alternatively, the samples may be taken every other hour or even less frequently. Typically, biological samples obtained during the first 12 hours of sampling (i.e., 12 hrs after the start of labeling (IV

bolus or infusion) may be used to determine the rate of synthesis of the protein, and biological samples taken during the final 12 hours of sampling (i.e., 24-36 hrs after the initial infusion of labeled moieties) may be used to determine the clearance rate of the protein. In another aspect, a single sample may be taken after labeling for a period of time, such as 12 hours, to estimate the synthesis rate, but this may be less accurate than multiple samples. In another aspect, the CNS biomolecule may be a protein including, but not limited to at least one Aβ isoform and one or more samples of blood may be taken hourly for 24 hours. Alternatively, the samples may be taken every other hour or even less frequently. Typically, blood samples obtained during the first 4 hours of sampling (i.e., about 1 minute to about 4 hrs after administration of an IV or oral bolus, about 10 minutes to about 4 hrs after administration of an IV or oral bolus, about 30 minutes to about 4 hrs after administration of an IV or oral bolus, about 1 minute to about 3 hrs after administration of an IV or oral bolus, about 10 minutes to about 3 hrs after administration of an IV or oral bolus, or about 30 minutes to about 3 hrs after administration of an IV or oral bolus) may be used to determine the rate of synthesis of the protein, and blood samples taken during the final 20 hours after administration of an IV or oral bolus (i.e., about 4 hours to about 12 hours after administration of an IV or oral bolus, about 12 hours to about 24 hours after administration of an IV or oral bolus, about 18 hours to about 24 hours after administration of an IV or oral bolus, or about 4 hours to about 24 hours after administration of an IV or oral bolus) may be used to determine the clearance rate of the protein. In another aspect, a single sample may be taken after administration of an IV or oral bolus, such as at about 3 hours, to estimate the synthesis rate, but this may be less accurate than multiple samples. In yet a further aspect, samples may be taken from an hour to days or even weeks apart depending upon the protein's synthesis and clearance rate.

(f) Developing a model

[0069] The method of developing a kinetic model may include developing a model that may fit experimental findings in a manner consistent with

known molecular biology and physiologic structures. In an aspect, the kinetic model may be a comprehensive steady state compartmental model that uses tracer kinetics to determine the rate constants within the model. In another aspect, the model may account for the time course of at least one Aβ isoform *in vivo.* In yet another aspect, the model may mathematically represent the one-dimensional flow of soluble Aβ isoforms in the brain from the ventricles to the CSF and/or blood. In this aspect, the flow may be due to the pressure difference between the ventricles and the brain surface.

[0070] **FIG. 16** is a block diagram of an amyloid kinetics modeling system **1600** in one aspect. The amyloid kinetics modeling system **1600** may include one or more processors **1602** and a computer-readable medium (CRM) **1604** containing an amyloid kinetics application **1606.** The amyloid kinetics application **1606** includes a plurality of modules executable on the one or more processors **1602.**

[0071] The plasma module **1608** represents the infusion of the labeled moiety into the plasma of a patient and the transport of the labeled moiety across the blood brain barrier (BBB). The brain tissue module **1610** represents the incorporation of the labeled moiety into APP and the formation of C99. The amyloid kinetics module **1612** represents the cleavage of the C99 to form at least one Aβ isoform and the subsequent kinetics of the at least one Aβ isoform within the brain including, but not limited to, recycling, fractional turnover, incorporation into plaques, transport across the blood brain barrier (BBB), and breakdown of the at least one Aβ isoform. The CSF module **1614** represents transport of the at least one Aβ isoform into the CSF. The model tuning module **1616** may iteratively adjust a set of parameters defining the dynamic response of the model to the input time history of plasma leucine enrichment into the plasma module **1608** in order to optimize the match between the predicted CSF enrichment kinetics and the measured CSF enrichment kinetics of the at least one Aβ isoform in the patient.

[0072] In an aspect, the amyloid kinetics application **1606** may further include a blood enrichment module (not shown). The blood enrichment module

represents transport of the at least one Aβ isoform into the blood. In an additional aspect, the amyloid kinetics application **1606** may include the blood enrichment module in the place of the CSF module **1614.**

[0073] The GUI module **1618** may generate one or more forms to receive inputs to the system **1600** such as the time history of plasma leucine enrichment and the measured CSF enrichment kinetics of the at least one Aβ isoform in the patient. The GUI module **1618** may further receive additional user inputs such as defined ranges for parameters defining the dynamic response of the model and other values used to specify the operation of the system **1600.** The GUI module **1618** may also generate one or more forms used to display outputs of the application **1606** including, but not limited to graphs of the predicted CSF enrichment kinetics of the at least one Aβ isoform, listings of model parameters, predictions of a disease state of a patient, and any other relevant output.

[0074] Any method of modeling may be used to implement any one or more of the modules **1608 - 1614** without limitation. Non-limiting examples of suitable modeling methods include compartmental models, flow models, mathematical equations, fluid dynamic flow equations, diffusion equations, any other suitable modeling method known in the art. In one aspect, the modules **1608 - 1614** may be implemented using compartmental models. In another aspect, the modules **1608 - 1614** may be implemented using a combination of compartmental models and flow models.

(i) Compartmental Model

[0075] **FIG. 3** is a schematic diagram showing the overall architecture of a model **10** of Aβ kinetics using a compartmental model in an aspect. **FIG. 4** is a diagram of the full architecture of a model **20** of Aβ kinetics using a compartmental model in another aspect. In this other aspect, the model **20** may include a series of interconnected compartments with first order rate constants that describe the transfer of labeled species between compartments. The compartments may represent different forms of Aβ or different locations of Aβ

isoforms along a metabolic pathway. **FIG. 21** is a schematic diagram showing the overall architecture of an additional model 50 of Aβ kinetics using a compartmental model in an aspect

[0076] The kinetic model may account for the full time course of Aβ38, Aβ40, and Aβ42 enrichments and CSF concentrations in one aspect. In an aspect, the model may describe fundamental processes that affect Aβ kinetics including, but not limited to: production, reversible exchange, and irreversible loss, and may account for the effect of the kinetics of these processes on CSF concentrations of Aβ.

[0077] The model may be implemented on any software or device without limitation. In an aspect, modeling may be performed using SAAM II software (Resource for Kinetic Analysis, University of Washington, Seattle). In various aspects, the number, order, and location of compartments may vary. In various other aspects, the interconnections between the various compartments may vary. In various additional aspects, functions other than first-order rate constants may be used to represent the movement of a quantity from one compartment to another. Non-limiting examples of suitable functions include linear functions, exponential functions, differential equations, logarithmic equations, and any other known kinetic and/or rate equation known in the art. The functions may be constant with respect to other variables within the model, or the functions may include other variables generated within the model. For example, the rate of synthesis of an Aβ isoform may be influenced by the concentration of soluble Aβ isoform already produced in an aspect.

[0078] The kinetic model may include a compartment for the concentration of a labeled moiety. In one aspect, the kinetic model may include a compartment for labeled plasma leucine. In another aspect, the kinetic model may include at least one compartment for APP. In other aspects, the kinetic model may include compartments for iAPP and mAPP. In yet another aspect, the kinetic model may include a compartment for C99. The kinetic model may include parallel arms for different CNS biomolecules or Aβ isoforms. In an aspect, the kinetic model may include three parallel arms with corresponding

compartments, one for each Aβ isoform (Aβ42, Aβ40, Aβ38), as illustrated in **FIG. 4.** In another aspect, the kinetic model may include a reversible exchange compartment for at least one Aβ isoform. In one aspect, the kinetic model may include a reversible exchange compartment for Aβ42. In other aspects, the kinetic model may include at least one delay compartment for the transport of the Aβ isoforms from the brain to the CSF. The compartments may be connected by rate constants for the rate of transfer from one compartment to the next. In yet another aspect, the model may account for irreversible loss of C99 and each soluble Aβ isoform that may not be recovered in the CSF.

[0079] The method of developing the kinetic model may include acquiring data from various patients to input into the development of the model. In one aspect, the enrichment of the labeled moiety and labeled Aβ isoform peptides may be measured at frequent time intervals (indicated by solid triangles in **FIGS. 3, 4,** and **21).** In an aspect, the labeled moiety may be plasma $^{13}C_6$-leucine. In another aspect, the measured values for each patient may be used to optimize the parameters of the model for each patient. The model parameter values may be averaged for each patient type or disease state including, but not limited to non-carriers/normal controls (NC), mutation carriers (MC) PIB-, mutation carriers PIB+, and other neurological disease states.

[0080] Referring to **FIG. 4,** the model may include, but is not limited to, compartments for plasma leucine, APP, C99, Aβ38, Aβ40, Aβ42, CSF/delay, recycling, and any other compartment that may be necessary to model the metabolism of Aβ. In an aspect, a "forcing function" may be used to describe the time course of plasma $^{13}C_6$-leucine enrichment using a linear interpolation of $^{13}C_6$-leucine enrichment between measured plasma samples. Each Aβ isoform may be optimally described by a single turning over compartment coupled with a long time delay that may include one or more sub-compartments. In an aspect, delay compartments representing APP and C99 peptides may be placed in front of the compartments that represent the brain "soluble" Aβ peptides. Without being limited to any particular theory, these delay compartments may be added because *in vivo* tracer studies in mice indicated that APP and C99 have relatively

long half-lives (about 3 hours) that should contribute to the overall time delay before labeled Aβ is detected at the lumbar sampling site. Other compartments may be placed after the "soluble" Aβ compartments to represent perfusion of labeled peptides through brain tissue, flow within the ISF, and heterogeneous CSF fluid transport processes. Since preliminary modeling indicates that a single time delay process could be identified within the data, the turnover rates APP, C99, and each of the three CSF delay compartments may be set to a single adjustable parameter that affects the overall time delay in an aspect.

[0081] The kinetic model may take into consideration that some of the C99 and soluble Aβ peptides may be metabolized to fates other than Aβ peptides that appear at the CSF sampling site in an aspect. Without being limited to any particular theory, the physiologic nature of these other losses for soluble Aβ peptides may be unknown at this time, but the model may include all processes that remove soluble peptides irreversibly, e.g. deposition into plaques, cellular uptake, proteolytic degradation, and/or transfer into the blood. In an aspect, the model may include an irreversible loss of each soluble Aβ isoform that was not recovered in CSF.

[0082] In an aspect, a reversible exchange compartment in exchange with the "soluble" Aβ peptide may be added to the model to optimally fit the sigmoid shape of the CSF Aβ enrichment time courses after the peak enrichment. The reversible exchange may represent possible recycling of Aβ isoforms to and/or from plaques, the exchange of labeled Aβ for unlabeled Aβ, the recycling of higher order Aβ structures, or any other reversible exchange of Aβ. In one aspect, a reversible exchange compartment may be included for Aβ42. In an aspect, the exchange process may only be added for an isoform if it improves the Akaike Information Criteria (AIC) of the fit as provided by SAAM II software.

[0083] In another aspect, a scaling factor (SF) may be applied to each of the Aβ isoform enrichments after the kinetic model has first been developed if it improves the AIC. Without being limited to any particular theory, the SF may account for small amounts of isotopic dilution between plasma leucine and the

biosynthetic precursor pool (generally less than about 5%) or to correct for minor calibration errors (generally less than about 10%) in the measurement of isotope enrichments of plasma leucine and/or Aβ peptides.

One principle parameter obtained with the model is the fractional turnover rate (pools/h) of the "soluble" Aβ peptides, i.e. the sum of the fractional rate of loss of these compartments to CSF and other losses from the system. Based on the calibrated kinetic parameters that describe the shape and magnitude of the CSF Aβ enrichment time course, the model may determine the rate constant (pools/h) for production of each Aβ peptide isoform from their common C99 precursor to accurately project the measured baseline CSF Aβ peptide concentrations. The model may project the steady state masses (ng) within and the flux rates (ng/h) between all compartments for each Aβ isoform.

[0084] The rate constants for transfer between compartments in the model may be calibrated for each patient by utilizing the labeled moiety time course and the measured time course of the Aβ isoforms in the biological sample. The model parameters to be calibrated may include, but are not limited to, transfer rate constants for APP, C99, Aβ38, Aβ40, and Aβ42; irreversible loss rate constants for C99, Aβ38, Aβ40, Aβ42, and CSF; exchange rate constants for Aβ38, Aβ40, and Aβ42; return rate constants; delay rate constants; and scaling factors. In another aspect, a database, similar to the data source shown and described below with reference to **FIG. 9**, and containing one or more optimal rate constants may be created. In one aspect, the calibrated rate constants may be obtained by developing an optimal model for each patient with a disease state. The database may also include values for all other necessary model parameters for a particular CNS biomolecule or Aβ isoforms for both the normal and various disease states. In an aspect, the model parameters and database may be used to calculate a model index and threshold respectively, as described herein below. As such, the values within the database may be used to identify a patient's disease state or predict and/or calibrate the kinetic model of desired CNS biomolecules in future patients, as discussed herein below.

[0085] Referring to **FIG. 21**, at least a fraction of Aβ isoforms in the brain may be transferred to the blood stream, generally across the blood brain barrier (BBB) in another aspect. In this other aspect, clearance from the brain, represented by V_{38}, V_{40} and V_{42}, may include degradation and transfer to the CSF, while $vBBB_{38}$, $vBBB_{40}$ and $vBBB_{42}$ represent clearance to the blood or plasma of Aβ 38, Aβ 40 and Aβ 42, respectively. The blood/plasma mathematical model **50** may be fit to isotope enrichment data of Aβ isoforms collected from blood/plasma using the same methodology by which the CSF mathematical model is used to fit isotope enrichment data of Aβ isotopes collected from the CSF.

[0086] In an aspect, the model may include a representation of transfers of at least a fraction of the Aβ isoforms in the brain to the CSF. In an aspect, the model may include a representation of transfers of at least a fraction of the Aβ isoforms in the brain to the blood. In an additional aspect, the model may include a representation of transfers of at least a fraction of the Aβ isoforms in the brain to the CSF as well as a representation of transfers of at least an additional fraction of the Aβ isoforms in the brain to the blood.

[0087] In various aspects, the architecture of the model may be developed using the data measured from various patients as described above. The results of alternative model architectures that may vary in the number, order, location, and/or interconnections between compartments may be compared using a figure of merit, and the model architecture associated with the most favorable figure of merit may be selected. Non-limiting examples of suitable figures of merit include Akaike information criterion, Bayesian information criterion, Deviance information criterion, Focused information criterion, Hannan-Quinn information criterion, and any other suitable figure of merit known in the art.

[0088] Those skilled in the art will recognize that the order of the compartments in a linear model does not affect the fit of the data or the values of the determined parameters. Those skilled in the art will also recognize that some distinct rate constants in these mathematical models may be set to the same

value in some cases where the individual parameters are unidentifiable or poorly identified by the data. The impact of these small changes to the structure of the model on the values of the rate constants may typically be minimal.

(\l) *Flow Model*

[0089] In an aspect, the kinetic model may be a flow model. **FIG. 12** is a diagram of the architecture of a model of Aβ kinetics using a flow model in one aspect. In an aspect, the flow model may include any compartments or transfer rates from the compartmental model described above. In another aspect, the flow model may be used in combination with the compartmental model.

[0090] The kinetic model may account for one-dimensional flow of Aβ isoforms in the ISF of the brain from the ventricles to the brain surface and into the CSF through a pressure differential as illustrated in **FIGS. 13** and **14A.** In an aspect, a continuity equation and momentum balance of ISF in the brain may be used to model the flow of the Aβ isoforms in the flow model. In another aspect, the steady state flow of Aβ within the brain may be calculated. In an additional aspect, the flow of Aβ may be described by the equations in Example 4 herein below. Implementation of a full 3D flow model may be developed using 3D structural MRI data in another additional aspect.

[0091] In an aspect, Illustrated in **FIG. 17,** the kinetic model may include nodes to represent the movement of the Aβ isoforms from the brain ventricles to the surface of the brain. Each node may be situated at a distance *x* from the ventricle *(x=0)* to the surface of the brain or CSF (x=1) associated with a local region of ISF. The ISF may move through each local region at a velocity prescribed by a computed velocity profile, summarized in one aspect in **FIG. 14B.** Within each local region, illustrated in **FIG. 18,** Aβ may be removed by exchange or irreversible loss and Aβ may be added by synthesis by the tissues in contact with the ISF in the immobile portion within that node. In one aspect, the kinetic model may include about 100 nodes for each Aβ isoform. The flow model may be represented by a plasma leucine compartment that is then divided into each node, as illustrated in **FIG. 18.**

[0092] Each node may be divided into an immobile and mobile portion, with the immobile portion remaining at that location in the brain and the mobile portion moving toward the surface of the brain at a velocity that may be derived from the computed velocity summarized in **FIG. 14B.** Referring back to **FIG. 18,** the immobile portion may include the compartments and transfer rates for Leucine, APP, iAPP, mAPP, C99, or any Aβ isoform in an exchange compartment. The mobile portion may include concentrations, irreversible loss, and flow rates for at least one soluble Aβ isoform.

[0093] The irreversible loss of each Aβ isoform may occur simultaneously with the flow of the Aβ isoform in the ISF. The movement of an Aβ isoform at any node or position within the ISF may be described in terms of flow and reaction. The reactions may be defined by the production of the Aβ isoform from C99, the degradation of the Aβ isoform (irreversible loss), and the exchange of the Aβ isoform with immobile forms of the Aβ isoform. In an aspect, each Aβ isoform may be tracked spatially in one dimension and the addition and removal of the Aβ isoform may be accounted for at each *x* location.

[0094] In another aspect, the flow may be incorporated into a compartment or rate constant within the compartmental model. The kinetic model may account for three-dimensional flow of Aβ in one aspect.

II. Methods for modeling the *in vivo* metabolism of Aβ

[0095] In various aspects, the methods for modeling the *in vivo* metabolism of at least one CNS biomolecule may be performed on one or more processing systems having one or more processors. In an aspect, the CNS molecule may be Aβ or an Aβ isoform. In one aspect, an Aβ modeling calibration system provides one or more graphical user interfaces that enable users to selectively calibrate a modeling system to identify, track, and estimate amounts or levels of a particular Aβ isoform or labeled protein segments at various time points in the metabolic pathway of Aβ. The Aβ modeling calibration system may be used to refine and calibrate a kinetic model for estimating amounts of Aβ lost to: degradation, formation of higher order structures and insoluble plaques, or Aβ

otherwise transported to the blood or CSF. The Aβ modeling calibration system may therefore be used to calibrate a model for determining or predicting the fractional turnover rate of the "soluble" Aβ peptides (pools/h). In particular, by comparing model-derived data with known data values stored in memory, in a database, or in any other data storage medium, the system **100** may be used to calibrate the kinetic parameters, also stored in memory, for predicting various rate constants for the metabolism of Aβ peptides based on the measured baseline CSF Aβ peptide concentrations. As previously described, the CNS Aβ modeling calibration system **100** may be used to calibrate the optimal rate constants for the transfer between the various compartments in the kinetic models **10, 20,** and **50** by comparing measured labeled moiety concentrations and the measured concentrations of the Aβ isoforms in a biological sample. Moreover, the system **100** may determine or predict the steady state masses (ng) within and the flux rates (ng/h) between the compartments of the model, as shown in **FIGS. 3, 4,** and **20** for each Aβ isoform.

[0096] Other aspects of the Aβ modeling calibration system enable users to interact with one or more graphical user interfaces to view and calibrate the optimized rate constant values, predicted fractional turnover rates, or in some embodiments, the kinetic model itself. The Aβ modeling calibration system **100** enables a user to select and manually or automatically adjust or modify one or more input values or rate constant values of the kinetic model.

[0097] **FIG.** 7 is a block diagram of an exemplary computing environment **30** that includes an Aβ modeling calibration system (MCS) **100** in accordance with aspects of the disclosure. The MCS **100** includes a computing device **102** that includes an Aβ modeling application (MCA) **104** and a data source **106.** The MCS **100** may be located on a single computing device **102.** Alternately, the MCS **100** may be distributed across computing devices or located on a computing device configured as a server that communicates with one or more client computing devices (client) **108** via a communication network **110.** Although the data source **106** is shown as being located on, at, or within the computing device **102,** it is contemplated that the data source **106** can be located

remotely from the computing device **102** in one or more other computing devices of the computing environment **30.** For example, the data source **106** can be located on, at, or within a database of another computing device or system having at least one processor and volatile and/or non-volatile memory.

[0098] As shown in **FIGS. 7, 8, and 10** the computing device **102** is a computer or processing device that includes one or more processors 112 and memory **114** to execute the MCA **104** to identify, determine, calibrate, and /or predict various values and constants of the kinetic model **20.** The computing device **102** may also include a display device **116,** such as a computer monitor, for displaying data and/or graphical user interfaces (GUIs) generated by a GUI module **300** of the MCA **104,** as shown in **FIG. 10.** The computing device **102** may also include an input device **120,** such as a keyboard or a pointing device (e.g., a mouse, trackball, pen, or touch screen) to enter data into or otherwise interact with various graphical user interfaces.

[0099] Each processing device **102** or **108** may also include a stand-alone or distributed version of the MCA application **104,** to generate one or more graphical user interface(s) **120** on the display **114.** The graphical user interface **120** enables a user of the processing devices **102** or **108** to view actual experimental data, predicted data, and other data manually input using the input device **116** or otherwise stored in the data source **106.** The graphical user interface **120** also enables a user of the processing devices **102** or **108** to view and modify the stored data as well as any determined or predicted data values. According to another aspect, the graphical user interface **120** enables a user of the MCS system **100** to interact with various data entry forms to enter authentication data or other data, including but not limited to usernames, passwords or other user data, to access any restricted functionality of the MCS **100.**

[0100] According to one aspect, the computing device **102** includes a computer readable medium ("CRM") **122** configured with the MCA **104.** The CRM **122** includes instructions or modules that are executable by the processor(s) **112.** The CRM **122** may include volatile media, nonvolatile media, removable

media, non-removable media, and/or another available medium that can be accessed by the computing device **122.** By way of example and not limitation, the CRM **122** comprises computer storage media and communication media. Computer storage media includes nontransient memory, volatile media, nonvolatile media, removable media, and/or non-removable media implemented in a method or technology for storage of information, such as computer readable instructions, data structures, program modules, or other data. Communication media may embody computer readable instructions, data structures, program modules, or other data and include an information delivery media or system The data source **106** may be a database or other general repository of data including, but not limited to, MCS user data, patient data, model data, or any other data. The data source **106** or database may include memory and one or more processors or processing systems to receive, process, query, and transmit communications or requests to store and/or retrieve such data. In another aspect, the database may be a database server.

[01 0 1] Similarly, the local or client computing device **108** may be a processing device similar to the processing device **102,** one or more servers, personal computers, mobile computers, and other computing devices. In various aspects, the local computing devices **108** include one or more processors and volatile and/or non-volatile memory and may be configured to communicate over the communication network **112** via wireless and/or wireline communications.

[01 02] The computing device **102** may be configured to receive data and/or communications from and/or transmit data and/or communications to a client **108** or other computing device, including a remote data source through the communication network **112.** The communication network **112** can be can be the Internet, an intranet, and/or another wired and/or wireless communication network. In one aspect, the computing device **102,** the client **108,** and/or the data source **106** communicate data in packets, messages, or other communications using a protocol, such as a Hypertext Transfer Protocol (HTTP) or a Wireless Application Protocol (WAP). Other examples of communication protocols exist.

[0103] **FIG. 9** depicts an exemplary embodiment of a data source **106** according to one aspect of the MCS **100.** The data source **106** can be a local database or can be another server (not shown) that communicates with the computing device **102** via the communication network **212.** According to one aspect, the data source **106** stores patient data **200,** measured data values **202,** predicted or determined data values **204,** other related data **206,** and MCS user data **208.** Although the MCS **100** is depicted as including a single data source **106,** it is contemplated that the MCS **100** may include multiple data sources in other aspects.

[0104] **FIG. 10** depicts the computing device **102** with an exemplary embodiment of the MCA **104.** As shown, the MCA **104** includes a number of modules **300-310** for performing a variety of functions, as explained more fully below. In various aspects, the functionality attributed to each module **300-310** may be performed by one or more other modules or a single module may perform some or all of the described functions.

III. Methods of using the model of in vivo metabolism of Aβ

[0105] The present disclosure provides methods of using a model of the *in vivo* metabolism of a CNS biomolecule or Aβ. The model may be used to calculate metabolic parameters, such as the synthesis and clearance rates within the CNS, in one aspect. In an aspect, the kinetic model may be used to identify the disease state of a patient by comparing an index calculated from model parameters to a pre-selected threshold. In another aspect, the kinetic model may be used to predict the metabolism and/or concentration of Aβ or its various isoforms in a patient *in vivo.* In an aspect, the model may be used to create a curve fit for each Aβ isoform time course in a patient. In yet another aspect, the model may be used to identify sensitive pathway components to help design drugs or understand a CNS disease. In even another aspect, the model may be used to investigate changes in the kinetics of the isoforms that may be induced by investigational drugs. In one aspect, the model may be used to characterize Aβ in various patients.

(a) Identifying a patient's disease state

[01 06] **FIG. 15** is an illustration of a method of using the kinetic model to identify the disease state of a patient. The method of using the model **1500** may include obtaining Aβ enrichment kinetics data from the CSF of the patient as depicted in step **1502;** inputting the time course data from a labeled moiety, the Aβ42 enrichment kinetics in the CSF, and at least one other Aβ isoform enrichment kinetics in the CSF into the kinetic model as depicted in step **1504;** obtaining a set of model parameters from the kinetic model as depicted in step **1506;** calculating a model index comprising a mathematical calculation with at least one model parameter from the kinetic model as depicted in step **1508;** comparing the model index to a pre-selected threshold as depicted in step **1510;** and identifying the disease state of the patient as depicted in step **1512.**

[01 07] In an aspect, the kinetic model may represent enrichment kinetics of Aβ42 and at least one other Aβ isoform. In this aspect, the labeled moiety may be labeled plasma leucine. The Aβ enrichment kinetics data from a patient may be obtained by the SILK method and may include time course data for Aβ42, Aβ40, and/or Aβ38 in the CSF. In an aspect, the data input into the kinetic model may include the time course of Aβ42 in the CSF and the time course of Aβ40 in the CSF. In another aspect, the data input into the kinetic model may include the time course of Aβ42 in the CSF and the time course of Aβ38 in the CSF. In yet another aspect, the data input into the kinetic model may include the time course of Aβ42 in the CSF, the time course of Aβ40 in the CSF, and the time course of Aβ38 in the CSF. In an aspect, the time course data of labeled plasma leucine may be input into the kinetic model.

[01 08] The input of the data into the kinetic model may create a set of model parameters for that patient. The model parameters obtained from the kinetic model may include, but are not limited to, the concentration of Aβ isoforms, rates of transfer (e.g. k_{App}, k_{C99}, k_{Ab42}, k_{Ab40}, k_{Ab38}), rates of irreversible loss (e.g. v_{c99}, v_{42}, v_{40}, v_{38}), rates of exchange (e.g. k_{ex42}, k_{ret}), rates of delay (e.g. kdeiay), or any parameter that may be used in the kinetic model. The model index may be calculated using at least one model parameter. The model index may be

calculated using any mathematical operator with the at least one model parameters, including but not limited to multiplication, division, addition, subtraction, logarithm, or any other mathematical operator. In an aspect, the model index may be calculated using the model parameters for the rate of irreversible loss of Aβ42 and the rate of transfer of Aβ42. In one aspect, the model index may be calculated using the calculation shown in Eqn. (I) below:

$$(10 \times k_{Ab42}) + v_{42} \qquad \text{Eqn. (I)}$$

[0109] Other aspects describing alternative model indices are described herein below in the Examples.

[0110] A pre-selected threshold may be calculated in the same manner as the model index using the model parameters of other patients or an average of model parameters from other patients with a known disease state. The method of using the kinetic model to identify the disease state of a patient may include identifying Alzheimer's disease in the patient. In an aspect, the disease state may be identified as Alzheimer's if the model index is above a pre-selected threshold for Alzheimer's. In another aspect, the severity of the disease state may be identified by comparing the model index to a pre-selected correlation of the disease state. In one aspect, the correlation of the disease state may be identified by PIB imaging.

(b) Producing a curve fit for measured data

[0111] The kinetic model may be used to create a curve fit for each Aβ isoform time course in a patient. In an aspect, limited data from a patient may be input into the model and the model may produce a curve fit for each Aβ isoform time course from the data provided. The curve fit may be used to predict unknown metabolism of Aβ and project to a later time course.

(c) Predicting metabolism or concentration

[01 12] The kinetic model may be used to predict the metabolism and/or concentration of Aβ in a patient. In an aspect, a database of parameters, as described herein above, may be used within the model to predict the metabolism of a Aβ isoform in a patient by using the set of parameters from the database that most closely match the genotype or phenotype of the patient. In another aspect, the model may be used to predict the concentration of different Aβ isoforms at different locations within the body and/or at different time points. In another aspect, the model may be used to calculate the metabolic parameter within the model.

(d) Identifying a sensitive pathway

[01 13] The kinetic model may be used to identify sensitive pathway components to help design drugs or understand a CNS disease. In an aspect, compartments may be added or subtracted to observe the effect of the concentrations and rate constants of the Aβ isoforms. In one aspect, the addition or subtraction of compartments may indicate sensitive areas within the pathway and may indicate areas for potential drug action. In another aspect, the rate constants within the model may be increased or decreased to observe the effect of the concentrations and other rate constants of the Aβ isoforms. In one aspect, the adjustment of the rate constants may indicate sensitive areas within the pathway and may indicate areas for potential drug action.

(e) Simulating the action of a drug

[01 14] The model may be manipulated to simulate the action of a drug within the CNS. In an aspect, the model may be used to investigate changes in the kinetics of the Aβ isoforms that may be induced by investigational drugs. In one aspect, the model parameters may be adjusted to best represent the effect of a drug on a patient *in vivo.* In another aspect, the model may be used to predict CSF concentrations of at least one Aβ isoform CSF concentration.

(f) Characterizing Aβ

[01 15] The model may be used to characterize Aβ kinetics in various patients. In an aspect, the parameters in the database may be used to predict the kinetics of Aβ in other patients. In an aspect, a non-carrier patient may be modeled using the parameters in the database for a non-carrier without the need to measure the concentration of the Aβ isoforms in the CSF. In an aspect, a MC PIB- patient may be modeled using the parameters in the database for MC PIB- without the need to measure the concentration of the Aβ isoforms in the CSF. In an aspect, a MC PIB+ patient may be modeled using the parameters in the database for MC PIB+ without the need to measure the concentration of the Aβ isoforms in the CSF.

EXAMPLES

[01 16] The following examples are included to demonstrate preferred embodiments of the invention. It should be appreciated by those of skill in the art that the techniques disclosed in the examples that follow represent techniques discovered by the inventors to function well in the practice of the invention, and thus can be considered to constitute preferred modes for its practice. However, those of skill in the art should, in light of the present disclosure, appreciate that many changes can be made in the specific embodiments which are disclosed and still obtain a like or similar result without departing from the spirit and scope of the invention.

Example 1: Mutation and amyloid deposition was modeled by differential Aβ *isoform kinetics.*

[01 17] The following experiment assessed the development of a model of Aβ trafficking *in vivo* using data from SILK studies.

[01 18] The model consisted of the following structure and parameters. The rate of production of APP was governed by the product of the zero-order rate constant k_{App} and the fraction of isotope-labeled leucine. The units of 'concentrations' were ng per ml_ of CSF, thus not accounting explicitly for the

volume of the brain compartment. The APP degradation product C99 was produced at a rate governed by the product of the rate constant k_{C99} and the concentration of APP. C99 was further processed into the three Aβ peptides, Aβ38, Aβ40 and Aβ42 at rates governed by the product of the concentration of C99 and the rate constants $k_{A\beta38}$, $k_{A\beta40}$ and $k_{A\beta42}$, respectively. C99 may also be irreversibly degraded to produce other products, governed by the product of the rate constant $\dot{v}_{C99}$ and the C99 concentration. All irreversible clearance processes that occur within the brain (degradation, transport to the vasculature and deposition into plaques) may be described by product of the rate constants k_{38}, k_{40} or $\dot{v}_{42}$ multiplied by the soluble brain concentration of Aβ38, Aβ40 and Aβ42, respectively. Transport of the CSF to the lumbar space may be modeled as three CSF delay compartments with equal rate constants for entry and exit (k_{delay}). The concentration of predicted labeled Aβ peptide in the third delay compartment was compared to the total measured concentration of Aβ peptide in the CSF to compute a predicted fractional labeling. The parameters were optimized against the measured fractional labeling of the Aβ peptide.

[0119] *In vivo* SILK studies were performed in participants with ADAD mutations and sibling non-carrier controls. The Aβ kinetic parameters were compared by the presence of a *PSEN* mutation and insoluble amyloid deposition as measured by PiB-PET.

[0120] SILK studies were performed in 23 patients (11 with mutations in *PSEN1* or *PSEN2,* 12 non-mutation carrier sibling controls) using a 9-h primed constant infusion of $^{13}C_6$ leucine. Seven mutation carriers had evidence of plaques by PiB PET; the remaining mutation carriers and all non-carriers were PiB negative. Four mutation carriers were cognitively symptomatic, all other participants were cognitively normal. CSF Aβ38, Aβ40, and Aβ42 concentrations and isotopic enrichments were measured at hourly intervals over a 36 h period.

[0121] During the $^{13}C_6$-leucine infusion, plasma leucine enrichment approximated a constant plateau and then rapidly decreased after the infusion was stopped **(FIG. 5).** The $^{13}C_6$-leucine isotopic enrichments of Aβ38, Aβ40, and Aβ42 were compared between mutation carriers, with or without amyloidosis, and

non-mutation carriers to address the relationship between Aβ isoform metabolic kinetics, mutation status, and amyloid deposition (PIB+ indicates fibrillar amyloid deposition as measured by PET with Pittsburgh Compound B).

[01 22] To compare Aβ isoform kinetics, ratios of labeled Aβ isoform enrichments in the CSF were plotted so that a ratio of one indicates the same isotopic enrichment and kinetics between Aβ isoforms. The Aβ38:Aβ40 labeling ratio was approximately constant at one over time in all patient groups **(FIG. 6A),** indicating similar kinetics between Aβ38 and Aβ40. Similarly, the Aβ42:40 and Aβ42:38 labeling ratios were nearly constant at one over time in non-carriers. However, in both PIB- and PIB+ mutation carriers, the Aβ42:40 and Aβ42:38 labeling ratios were elevated during early time points and decreased in later time points **(FIG. 6A).** The Aβ isoform enrichment mismatch was more pronounced in participants with amyloid deposition (PIB+), caused by an earlier and lower Aβ42 peak with a flatter terminal tail compared to Aβ38 and Aβ40 **(FIG. 6B).** The time to reach peak ^{13}C-labeling in each Aβ isoform was measured for each patient. The Aβ38:Aβ40 peak time ratio was not different between mutation carrier and non-carrier groups (1.01 ±0.01 vs. 1.00±0.01 , respectively). In contrast, Aβ42 peaked at the same time as Aβ40 in the non-carrier group (Aβ42:Aβ40 peak time ratio = 1.01 ±0.03), whereas Aβ42 peaked significantly earlier than Aβ40 in the mutation group (peak time ratio = 0.93±0.05, p=0.01 5 mutation effect, p<0.001 for PIB score).

[01 23] A comprehensive compartmental model similar to the models described previously herein was developed to quantify steady state Aβ isoform kinetic parameters. The model incorporated the plasma leucine and Aβ enrichment time course profiles and the CSF Aβ isoform concentrations for each patient (schematic diagram in **FIG. 3). FIG. 4** is a detailed figure of the model. **FIG. 6B** shows curve fits from the model for average Aβ isoform time course profiles as enrichments normalized to plasma leucine. A reversible exchange compartment was incorporated to model the sigmoidal decay of many labeling curves, especially Aβ42 in PIB+ participants. The model included an irreversible loss of each soluble Aβ isoform that was not recovered in CSF. The rate

constants for transfer between compartments in the model were calibrated using measured values for each patient. Mean values for each parameter are summarized in **Table 1** below.

Table 1.

Parameter	Non-carriers	Mutation-carrier PIB-	Mutation-carrier PIB+
k_{APP}	1,171 ± 227	1,304 ± 602	1,291 ± 324
k_{C99}	0.666 ± 0.112	0.553 ± 0.083	0.695 ± 0.096
$k_{Aβ38}$	0.062 ± 0.010	0.055 ± 0.016	0.059 ± 0.008
$k_{Aβ40}$	0.238 ± 0.041	0.187 ± 0.023	0.247 ± 0.037
$k_{Aβ42}$	0.033 ± 0.006	0.034 ± 0.007	0.041 ± 0.006
v_{C99}	0.333 ± 0.056	0.276 ± 0.041	0.347 ± 0.048
v_{38}	0.069 ± 0.023	0.075 ± 0.027	0.054 ± 0.015
v_{40}	0.074 ± 0.023	0.082 ± 0.037	0.050 ± 0.013
v_{42}	0.064 ± 0.014	0.126 ± 0.072	0.120 ± 0.037
k_{CSF}	0.074 ± 0.023	0.082 ± 0.037	0.050 ± 0.013
k_{ex38}	0.020 ± 0.038	0.000 ± 0.000	0.000 ± 0.000
k_{ex40}	0.016 ± 0.032	0.009 ± 0.018	0.000 ± 0.000
k_{ex42}	0.010 ± 0.021	0.041 ± 0.045	0.120 ± 0.107
k_{ret}	0.1	0.1	0.1
k_{delay}	0.666 ± 0.112	0.553 ± 0.083	0.695 ± 0.096
SF_{38}	0.937 ± 0.066	0.885 ± 0.063	0.979 ± 0.092
SF_{40}	0.933 ± 0.043	0.916 ± 0.078	0.977 ± 0.130
SF_{42}	0.972 ± 0.102	0.879 ± 0.021	0.912 ± 0.151

[01 24] The results of this experiment demonstrated that biological mechanisms and patient data that account for Aβ isoform-specific differences may be used to develop a model of Aβ isoform kinetics and the model may

provide insights into the metabolic kinetics of Aβ peptides by both mutation and amyloid deposition status.

Example 2: An exchange process was required to fit Aβ kinetic curves.

[01 25] To demonstrate the ability of the model to account for exchange with unlabeled Aβ peptides, the following experiment was conducted.

[01 26] Using the model developed in Example 1, additional compartments were added to further develop the model. To optimally fit the shape and peak magnitude of Aβ isoform enrichment time courses, a compartment was required to model reversible exchange of newly synthesized labeled Aβ peptides with a pre-existing pool of unlabeled Aβ, as shown in **FIG. 3.** The exchange process was of minimal magnitude in non-mutation carriers, in which only about 10% of the flux of newly synthesized Aβ38, 40 or 42 underwent exchange **(Table 2).** The percent of Aβ38 and Aβ40 that underwent exchange was not significantly different between mutation carriers and non-carriers. However, the exchange for Aβ42 was significantly greater in carriers compared to the non-carriers (51 ±58% vs. 6±12% of flux, respectively, p=0.004 for mutation effect, p=0.001 for PIB status) **(Table 2).** The exchange process for Aβ42, combined with the faster turnover rate of Aβ42, provided an excellent fit to the entire shape of the Aβ42 enrichment time course in all groups including mutation carriers with amyloid deposition (mean R^2 for all participants of 0.994, 0.995, and 0.987 for Aβ38, Aβ40 and Aβ42, respectively).

Table 2.

	Non-carriers (n=13)	Mutation+ carriers (n=13)	p-values[b]	
Production rate, ng/h (e.g. C99 pool size x $k_{Aβ42}$)			Mutation	PIB MCBP
Aβ38	106[41]	111[50]	0.603	0.571
Aβ40	418±83	452±138	0.621	0.901
Aβ42	57[19]	67[35]	**0.038**	0.769
Aβ38:Aβ40 ratio	0.267[0.021]	0.252[0.052]	0.692	0.179
Aβ42:Aβ40 ratio	0.140±0.011	0.174±0.020	**$9x10^{-5}$**	0.312

Percentage of flux going to exchange (%)*			Mutation status	PIB status
Aβ38	9.8±16.6	0[a]	0.19	0.376
Aβ40	7.8±13.9	1.2±4.1	0.316	0.249
Aβ42	5.8±11.5	50.8±57.6	**0.004**	**0.001**
Permanent loss of soluble Aβ to all fates (fractional turnover rate, FTR) (pools/h) (e.g. $v_{42}+k_{CSF}$)			Mutation status	PIB MCBP
Aβ38	0.144±0.046	0.124±0.049	0.802	0.054
Aβ40	0.156[0.055]	0.109[0.035]	0.99	**0.024**
Aβ42	0.147[0.049]	0.198[0.086]	0.065	0.548
Aβ38:40 ratio	0.964±0.038	1.013±0.047	0.157	0.115
Aβ42:40 ratio	0.942±0.080	1.553±0.382	**0.0016**	**0.0003**
CSF concentration by IP-MS (ng/mL)			Mutation	PIB MCBP
Aβ38	2.05[0.69]	1.82[1.00]	0.296	0.105
Aβ40	7.15±1.80	7.79±1.89	0.199	0.272
Aβ42	1.01[0.39]	0.80[0.52]	0.537	**0.007**
Aβ38:Aβ40	0.272±0.014	0.256±0.053	0.803	0.068
Aβ42:Aβ40	0.149±0.013	0.121±0.042	0.72	**0.003**

[01 27] The results of this experiment demonstrated that a compartment for the exchange of labeled Aβ peptides with unlabeled peptides was necessary to model the exchange of Aβ42, particularly in mutation carrier groups.

Example 3: Higher irreversible loss of Aβ42 in amyloid deposition was assessed.

[01 28] To assess the ability of the model to account for irreversible loss, the following experiment was conducted. Using the model of Examples 1 and 2, additional compartments were added to further develop the model. The fractional turnover rate (FTR, pools/h) of soluble Aβ is the rate constant for *permanent* loss of soluble Aβ and is kinetically distinct from reversible exchange. The physiology of the system suggests that FTR includes irreversible losses to the CSF or bloodstream, degradation, and deposition into amyloid plaques, as illustrated in **FIG. 2**. The model was adjusted to include fractional turnover rates,

or rate of irreversible loss, for the various isoforms and each type of patient. The Aβ40 FTR was significantly *slower* in PIB+ compared to PIB- participants (p=0.024 for PIB effect) and trended towards significance for Aβ38 (p=0.054 for PIB effect), but neither was affected by mutation status **(Table 2).** The decreased turnover rate was thus associated with the presence of PIB-detectable amyloid plaques. In contrast, Aβ42 FTR trended towards an *increase* in mutation carriers (p=0.065 for mutation effect) independent of amyloid load **(Table 2).** The Aβ38:Aβ40 FTR ratio was not significantly different between non-carrier and mutation carrier groups, but the Aβ42:Aβ40 FTR ratio was 65% higher in mutation carriers (p<0.002 for both mutation status and PIB score) **(Table 2).** The measured concentration of CSF Aβ isoforms were compared by mutation status and PIB score **(Table 2).** The Aβ42 CSF concentration and the Aβ42:Aβ40 CSF concentration ratio were significantly reduced in association with amyloid deposition (p=0.003 for PIB score; not significant by mutation status), whereas there were no differences between groups for the CSF Aβ38, Aβ40, or Aβ38:Aβ40 concentration ratio. The results of this experiment confirmed that the model may be adapted to account for irreversible loss of each isoform.

Example 4. One-dimensional flow of Aβ in the brain was modeled.

[01 29] To assess the feasibility of using a one dimensional flow model to describe isotope labeling kinetics, the following experiments were conducted.

[01 30] A one-dimensional flow of Aβ from the brain's interstitial fluid (ISF) to the CSF, was incorporated into a model similar to the mode described in Examples 1 and 2. The model is summarized in the schematic in **FIG. 12** incorporated the following changes in structure and parameters. The APP compartment was divided into an immature APP and a mature APP compartment. The rate of production of iAPP was governed by the product of the zero-order rate constant $k_{iAP\ p}$ and the fraction of isotope-labeled leucine. The immature APP was assumed to be processed (glycosylated) to produce mature APP. The rate of production of mAPP was governed by the product of the first-order rate constant k_{mAPP} and the 'concentration' of iAPP. The APP degradation

product C99 was produced at a rate governed by the product of the rate constant k_{C99} and the concentration of mAPP.

[01 3 1] All three peptides flow with the brain interstitial fluid and any Aβ peptide that is transported to the surface of the brain without being cleared then becomes part of the CSF. Aβ42 may also enter a reversible exchange compartment, which was previously found to be more substantially exchanged than Aβ38 or Aβ40. Aβ42 within the exchange compartment is not subject to flow. The soluble Aβ42 concentration in the brain does not include the amount of Aβ42 within the exchange compartment. Transport of the CSF to the lumbar space was modeled as two delay compartments with equal rate constants for entry and exit (k_{delay}).

[01 32] A length from ventricle to brain surface was taken as 3 cm or 7 cm. The 7 cm value had been adopted in a previous model of ISF flow, but the 3 cm was considered more realistic. The one-dimensional flow model is further summarized in **FIG. 13.** The one-dimensional flow model was integrated with the compartmental model shown in FIG. 12 to model *in vivo* Aβ labeling kinetics.

[01 33] **FIG. 13** illustrates the brain, represented by the box, with the ventricles on the left and the brain surface on the right. C99 was represented as being bound to the brain, uniformly distributed within the brain compartment, along the one-dimensional distance from the ventricle, x. C99 was not subject to ISF flow. Each location has a source of C99 that produces Aβ. Upon enzymatic cleavage of the C99, the Aβ peptides are released and transported along with the flowing ISF. The Aβ released from each location joins in the ISF flow. The Aβ peptides may be cleared and/or degraded in the flow (decreasing concentrations are depicted as narrowing lines in **FIG. 13),** and any Aβ peptide that reaches the surface of the brain at x=1 then becomes part of the CSF.

[01 34] To develop the one-dimensional flow model from the ventricle to the surface of the brain, the continuity equation was used as shown in Eqn. (II) and the one dimensional momentum balance was used as shown in Eqn. (III):

$$\frac{dv_x}{dx} = F_V \qquad \text{Eqn. (II)}$$

$$\rho\left(\frac{\partial v_x}{\partial t} + v_x\frac{\partial v_x}{\partial x}\right) = -\frac{\partial P_i}{\partial x} + \mu\frac{\partial^2 v_x}{\partial x^2} - \frac{\mu}{\kappa}v\chi \qquad \text{Eqn. (III)}$$

, where F_v is the rate or production of fluid by the capillaries per unit volume of fluid, v is the velocity of the fluid, and x is the normalized distance from the ventricles. Eqn. (I) expresses the change in velocity of the fluid as due solely to the introduction of new fluid from the capillaries. As more fluid is added, the velocity of the fluid must increase due to the incompressibility of water.

[01 35] The introduction of fluid from the capillaries due to higher pressure in the vasculature is assumed to follow Starling's Law, as shown in Eqn. (IV):

$$F_v = L_P(S/V)[p_{vascular} - pi - \sigma(\pi_{vascular} - \pi_i)] \qquad \text{Eqn. (IV)}$$

[01 36] A non-dimensionalized continuity equation for generality becomes:

$$\frac{d\bar{v}_x}{d\bar{x}} = \frac{L}{v_s}Lp(S/V)[P_{vascu\ lar} - Pi - \sigma(\pi_{vascu\ lar} - \pi_i)] = \bar{F}_v \qquad \text{Eqn. (V)}$$

, where L_P is the hydraulic conductivity, S/V is the surface area of the capillaries per volume of the brain, σ is the reflection coefficient, P and π are pressures, v_s is the velocity at the brain surface, and P, is represented by Eqn. (VI) below:

$$\bar{P}_i = \frac{P_i - P_{SAS}}{P_{ventricle} - P_{SAS}} \qquad \text{Eqn. (VI)}$$

[01 37] After non-dimensionalizing the momentum balance equation and ignoring higher order terms, the momentum equation reduces to Eqn. (VII) (Arifin et al, 2009, Pharma. Research, 26:2289):

$$\bar{v}_x = -\frac{d\bar{P}_i}{d\bar{x}} \qquad \text{Eqn. (VII)}$$

[01 38] Combining the dimensionless continuity and momentum equations reduces to Eqn. (VIII):

$$\bar{P}i = Ae\text{-}\wedge \quad + Be\wedge \quad + \frac{\beta}{\alpha} \qquad \text{Eqn. (VIII)}$$

, where a and β may be represented by Eqns. (IX) and (X):

$$\alpha = \frac{L}{v_s}L_P(S/V)(P_{ventricle} - P_{SAS}) \qquad \text{Eqn. (IX)}$$

$$\beta = \frac{L}{v_s}Lp(S/V)[Pvascular \sim PsAS \sim \sigma(\pi_{vascular} \sim \pi_i)] \qquad \text{Eqn. (X)}$$

[01 39] This shows that the flow is pressure driven without substantial viscous losses other than due to the porosity alone. The velocity may be calculated from the now-known pressure profile:

$$\bar{v}_x = -\frac{d}{d\bar{x}}\left(A e^{-\sqrt{\alpha}\bar{x}} + B e^{\sqrt{\alpha}\bar{x}} + \frac{\beta}{\alpha}\right) = \sqrt{\alpha}\left(Ae^{-\sqrt{\alpha}\bar{x}} - Be^{\sqrt{\alpha}\bar{x}}\right) \qquad \text{Eqn. (XI)}$$

, where A and B may be represented by Eqns. (XII) and (XIII):

$$A = 1 - B - \frac{\beta}{\alpha} \qquad \text{Eqn. (XII)}$$

$$B = \frac{\frac{\beta}{\alpha}\left(e^{-\sqrt{\alpha}}-1\right)-e^{-\sqrt{\alpha}}}{e^{\sqrt{\alpha}}-e^{-\sqrt{\alpha}}} \qquad \text{Eqn. (XIII)}$$

[01 40] Using Eqns. (VIII) and (XI), the pressure and velocity have the profiles across the brain shown in **FIG. 13. FIG. 13** illustrates pressure and fluid velocity changes from the surface of the ventricles (x = 0) to the surface of the brain (x = 1).

[01 4 1] For transport of an Aβ peptide, the mass balance is (neglecting diffusion due to the P):

$$\frac{\partial A\beta}{\partial t} + v_x \frac{\partial A\beta}{\partial x} = D_{AB}\frac{\partial^2 A\beta}{\partial x^2} + kC_{99} - \dot{V}A\beta \qquad \text{Eqn. (XIV)}$$

, where k_{C99} is the rate of creation of C99 and $\dot{V}_{A\beta}$ is the rate of irreversible loss of Aβ.

[01 42] After partially non-dimensionalizing the steady state equation, the effects of diffusion and time dependent terms may be neglected without introducing substantial error, resulting in the steady state equation below:

$$\frac{\partial A\beta}{\partial \bar{x}} = \frac{L}{v_s \bar{v}_x}\left(kC_{99} - \dot{V}A\beta\right) \qquad \text{Eqn. (XV)}$$

[01 43] The expression for velocity as a function of x calculated in Eqn. (XI) was inserted into Eqn. (XV) and integrated with a boundary condition of $A\beta(\ddot{u}) = 0$ which yielded the Aβ steady state equation below:

$$A\beta_{ss} = \frac{kC_{99}}{\dot{V}}\left(1 - e^{\left(-\frac{L}{v_s}\frac{\dot{V}}{\alpha\sqrt{AB}}\left[\tanh^{-1}\left(\frac{Be^{\sqrt{\alpha}\bar{x}}}{\sqrt{AB}}\right)-\tanh^{-1}\left(\frac{B}{\sqrt{AB}}\right)\right]\right)}\right) \qquad \text{Eqn. (XVII)}$$

[0144] The 'brain' was divided into 100 equally spaced nodes and the unsteady system of differential equations was solved numerically for iAPP, mAPP, C99 immobilized in the brain, Aβ38, Aβ40, and Aβ42 in the interstitial fluid and CSF, and Aβ42 in the exchange compartment (705 equations).

[0145] The results of this experiment demonstrated that the one-dimensional flow of Aβ in the brain may be modeled.

Example 5. The one-dimensional flow model was assessed.

[0146] To assess the model of one-dimensional flow of Aβ in the brain, the following experiment was performed. The model of Examples 1 and 4 were used to model patients that were normal controls (NC) *PSEN1* or *PSEN2* mutation carriers that were both PIB positive (MC+) and negative (MC-).

[0147] The rate of production of labeled iAPP was the product of the rate constant k_{iAPP} with the fractional labeling of leucine amino acid. This value was set to 25 h^{-1} for all patients. For the production rate constant of mAPP and C99, different values were investigated while fitting the data to one of the patients with plaques detectable by PET. In Example 2, six out of seven of the patients with plaques required exchange of Aβ42 to optimally fit the data, and many required a large amount of exchange. This is due to the characteristic shape of the curves **(FIG. 13).** The exchange process only had a substantial effect on the labeling curve if the rates of clearance of the Aβ peptides (e.g. $\dot{V}_{38}$, $\dot{V}_{40}$, or $\dot{V}_{42}$) were lower than about 0.25 h^{-1}. Turnover of Aβ peptides could only be that slow if the turnover of mAPP and C99 were relatively high. Because the data likely had little information about k_{mAPP} and k_{C99} independently, these two parameters were set equal. Systematically varying the rate constant for k_{mAPP} and k_{C99} while fitting the plaque-bearing patient led to optimal values of 1.2 h^{-1} for L = 3 cm and 1.6 h^{-1} for L = 7 cm. Ranges of other parameter values were fixed based on the findings of the previous model, and the ranges were expanded when the optimized parameter reached a prescribed limit. **Tables 3** and **4** show values for parameters used in the one-dimensional flow model.

Table 3.

	Lower Limit	Upper Limit
k_{iAPP}	25	
k_{mAPP}, k_{C99}	1.2 (L=3 cm); 1.6 (L=7 cm)	
$\dot{V}_{C99}$	0.001	1.3
$k_{A\beta38}$, $k_{A\beta40}$ and $k_{A\beta42}$	Calculated from steady state relationship	
$\dot{V}_{38}$, $\dot{V}_{40}$, or $\dot{V}_{42}$	0.01	0.3
k_{ex42}	1×10^{-8}	1
k_{delay}	0.05	2
SF_{38}, SF_{40}, SF_{42}	0.7	1.3

Table 4.

	$\dot{V}_{C99}$	$k_{A\beta38}$	$k_{A\beta40}$	$k_{A\beta42}$	$k_{A\beta42}/k_{A\beta40}$
NC	0.40 ± 0.35	0.0052 ± 0.0043	0.020 ± 0.016	0.0028 ± 0.0022	0.142 ± 0.00999
MC-	0.56 ± 0.21	0.0099 ± 0.0039	0.033 ± 0.0086	0.062 ± 0.0022*	0.185 ± 0.0167**
MC+	0.31 ± 0.13	0.0024 ± 0.00065	0.0098 ± 0.0028	0.0017 ± 0.00055	0.168 ± 0.0198**

	$\dot{V}_{38}$	$\dot{V}_{40}$	$\dot{V}_{42}$	$\dot{V}_{42}/\dot{V}_{40}$	k_{ex42}	k_{delay}
NC	0.18 ± 0.056	0.19 ± 0.058	0.18 ± 0.053	0.957 ± 0.0894	0.0084 ± 0.015	0.76 ± 0.45
MC-	0.17 ± 0.050	0.17 ± 0.053	0.22 ± 0.077	1.28 ± 0.343**	0.035 ± 0.024*	0.32 ± 0.058
MC+	0.12 ± 0.037*	0.11 ± 0.035**	0.19 ± 0.050	1.71 ± 0.293**	0.14 ± 0.10**	0.84 ± 0.39

	SF38	SF40	SF42
NC	0.85 ± 0.069	0.85 ± 0.051	0.91± 0.092
MC-	0.83 ± 0.043	0.85 ± 0.061	0.82 ± 0.016
MC+	0.91 ± 0.085	0.92 ± 0.14	0.88 ± 0.13

[0148] The ratio of the rate constant for the production of Aβ42 with respect to the rate constant for the production of Aβ40 was highly significant when comparing both the MC- and MC+ groups to the normal controls (NC). However, the MC- and MC+ groups were not different from each other.

[0149] The ratio of the rate constant for the permanent loss of Aβ42 ($\dot{V}_{42}$) with respect to the rate constant for the permanent loss of Aβ40 ($\dot{V}_{40}$) was also highly significant when comparing both the MC- and MC+ groups to the normal controls. Although it was expected that only the MC+ group should show increased loss of Aβ42 relative to Aβ40, it is possible that some patients in the MC- group were beginning to deposit plaques, but these were not yet detectable by PIB. This is supported by the significant increase in the exchange rate

constant in the MC- group (p = 0.1 9), although the mean was nearly four-fold smaller than in the MC+ group. The rate constant for permanent loss was 33% higher in the MC+ compared the MC- group, and this difference trended towards significance (p = 0.057). Interestingly, the increased $\dot{V}_{42}/\dot{V}_{40}$ ratio in the MC+ group seemed to be due to a significant decrease in $\dot{V}_{40}$ rather than an increase in $\dot{V}_{42}$. This result is in agreement with the findings of the purely compartmental model of the data in Examples 1 and 2. However, in this model, the rate constant for the clearance of Aβ38 ($\dot{V}_{38}$) is also significantly lower in the MC+ group. This may represent a general decrease in clearance of from the brain in the presence of plaques, perhaps due to changes in the physiology of the brain.

[01 50] Compared to the model in Examples 1 and 2, the AIC was lower in the Example 2 model in 13/23 patients, and was lower in the current model in 10/23 patients. However, the AIC were quite similar, with the sum of AIC over all the patients of -25,81 8.2 for the previous model and -25,729.7 for the current model.

[01 5 1] In the current model, only exchange of Aβ42 is allowed, and this parameter is allowed to vary in all patients. In the Example 2 model, patients were allowed to exchange Aβ peptides only if it improved the AIC. The current model treats the exchange rate constant as a continuous variable, this facilitates comparison of this parameter with other measures of Alzheimer's disease. In particular, the correlation between the exchange rate constant and the PIB score is presented. The correlation coefficient of r = 0.851 indicates high correlation between the two measures. In contrast, the correlation coefficient between the predicted brain pool size of Aβ42 and the exchange rate constant was r = -0.441 . This indicates some relationship between these variables.

[01 52] The results of this experiment demonstrate that the model may represent one-dimensional flow of Aβ in the brain.

Example 6: Method of Calibrating a differential Aβ isoform kinetics model

[01 53] In one embodiment, the computing device **102** or client **108** executes the MCA **104** in response to a modeling request from the user. The user identifies one or more patients for whom Aβ modeling will be calibrated using the input device **120** and one or more GUI's generated by the GUI module **300.**

[01 54] A GUI module **300** receives data from the various other modules **302-310,** the input device **120,** and/or the data source **106** and generates one or more displays on the display device **116.** The displays generated by the GUI module may include input forms, charts, graphs, displays, tables, and other data for viewing by the user of the MCS **100.**

[01 55] In response, the patient data module **302** generates a request to retrieve patient data. In one embodiment, the request is transmitted to the data source **106** to retrieve patient data. The patient data may include biographical data as well as medical data for the identified patient. The patient data may also identify a diseased state of a patient. The patient data may further include baseline data values related to one or more component levels within the patient's blood, CSF, or other baseline data of interest. Alternately, if the MCA **104** is being executed contemporaneously with a new patient, the request for patient data may be transmitted to the GUI module **302,** where one or more GUI's and data entry fields are generated for display on the display device **116** for the user to input baseline values, which are received at the patient data module **302.**

[01 56] Once baseline values for the patient have been established, the MCA **104** determines a plasma leucine enrichment value for the patient. The plasma leucine enrichment value is calculated by referencing known data enrichment values as a function of time, as shown in **FIG. 5** and comparing the known data to the patient data obtained at the patient data module **302.**

[01 57] As previously described, a time-dependent delay compartment of the model is used to represent the uptake of the labeled plasma leucine by APP and the subsequent formation of the Aβ isoforms by cleaving C99 peptides. As such, the MCA **104** includes an Aβ isoforms module **304** that determines the

level of each Aβ isoform after cleavage, which incorporates the labeled leucine. The Aβ isoforms module 304 determines the amounts or values for each labeled isoform as well as each isoform's respective enrichment levels by first multiplying the determined plasma labeled leucine level by an uncalibrated APP constant ($\mathbf{k_{App}}$), as identified in Table 1, to obtain an uncalibrated level of enriched C99 peptides. The exemplary uncalibrated APP constant is retrieved from a table of mean data values stored in the data source **106.** Similarly, the Aβ isoforms module **304** determines an exemplary level for each Aβ isoform entering the CSF by multiplying the calibrated level of enriched C99 peptides by a mean transfer rate values for each respective isoform cleaved from C99 peptides. This determination also accounts for a certain level of the C99 peptides that are lost and not converted to the Aβ isoforms by using an exemplary irreversible loss C99 constant (V_{c99}).

[01 58] In one embodiment, the Aβ isoforms module **304** may also be used to calibrate and quantify the state-state kinetics of isoforms. For example, the model may be used to model the kinetics of the Aβ38, Aβ40, and Aβ42 isoforms.

[01 59] In one aspect, the Aβ isoforms module **304** may be used to determine if an exchange compartment is necessary to model the kinetics of the "soluble" peptides. The module **304** optimizes the model by creating the exchange compartment in response to a determination that the added exchange process improves the Akaike Information Criteria (AIC) for a curve fit. For example, data from exemplary modeling performed using SAAM II software may be stored in the data source **106.** In particular, the user or the MCA 104 may automatically incorporate one or more exchange compartments into the exemplary model to calibrate and improve the correspondence between the sigmoid shapes of the enriched Aβ-isoforms within the CSF with respect to time as compared to data in the data source **106.**

[01 60] When exchange compartments are used, the Aβ isoforms module **304** multiplies the previously calculated isoform levels by an exemplary exchange rate (K_{ex}) and an exemplary return rate (K_{ret}). The exchange

compartments and rate factors K_{ex} and K_{ret} are used to represent the possible recycling of Aβ isoforms to and/or from amyloid plaques, the exchange of labeled Aβ for unlabeled Aβ, the recycle of higher order Aβ structures, and other as of yet unknown losses and gains to the levels of the respective isoforms. In addition, the Aβ isoforms module **304** may multiply the calculated isoform levels by one or more scaling factors to account for small amounts of isotopic dilution between plasma leucine and the biosynthetic precursor pool (generally < 5%) or to correct for minor calibration errors (generally <10%) in the measurement of isotope enrichments of plasma leucine and/or Aβ peptides.

[01 6 1] The CSF isoform module **306** receives data related to the levels of each respective isoform within the CSF. In one aspect, the CSF isoform module **306** receives data regarding the measured or calculated isoform levels after cleavage from the C99 peptide, and/or levels calculated from one or more optional exchange compartments. In addition, the CSF isoform module **306** may be used to predict the levels of each isoform within the CSF as a function of time by multiplying the received data by an exemplary delay factor **(K_{de} i_{ay}).** As shown in the kinetic model **20, K_{de} i_{ay}** may be used to represent the perfusion of labeled peptides through various brain tissue and heterogeneous CSF fluid transport processes.

[01 62] The results module **308** processes data transmitted from the data source **106** and/or one or more other modules **300-306,** and **310** to generate a display of results generated by the kinetic model **20.** In one example, the results module **308** may generate a chart or other graphical representation of data values, while the GUI module **302** generates a display of the representation.

[01 63] The calibration module **310** allows the user to modify one or more of the rate constants or other constants used in the kinetic model **20.** In one aspect, the calibration module **310** in conjunction with the GUI module **300** and/or the results module **308** generates one or more GUIs that a user may interact with to modify the parameters of the model, the data values generated by the model, and/or the graphical representation of the data values. By way of example and not limitation, the calibration module **310** may receive data input

into a GUI using the input device **120** to modify a constant value of the kinetic model **20.** This input data may be used to modify one or more graphical representations generated by the results module **308.** As such, the user may vary the data values generated by the kinetic model **20,** which contemporaneously varies the graphical representation of the data in order to calibrate the model data values to the measured data value.

[01 64] **FIG. 11** is a flowchart illustrating a method **400** of calibrating the kinetic models **10, 20,** or **50,** shown in **FIGS. 3, 4,** and **21** according to one embodiment. At **402,** leucine enrichment and labeled isoform level data values, as previously described, are collected and plotted for one or more patients. Alternately, previously collected or plotted data may be retrieved from a data source. At **404,** the compartment model is executed using known or measured leucine enrichment data and rate constants stored in the data source. At **406,** plots of the model results are generated and, at **408,** the generated plots are compared to the plots previously retrieved or created at **402.**

[01 65] A determination regarding the fit or closeness of fit between the plots of measured data and the plots generated by the model is made at **410.** If the model-generated plots are determined to sufficiently fit the plots of measured data, the model may be deemed calibrated and used as a tool in other investigations at **412.** Conversely, if the model-generated plot does not fit the plots of measured data, then one or more of the rate constant values may be modified at **414** and the model may be re-executed at **416.** Similar to the comparison made at **408,** the plot generated by the model using the modified rate constant(s) is compared to the plot of the measured data from **402** at **418.** Another determination is made at **410** to determine if the "modified rate constant" plot sufficiently fits the plot of measured data. The process at **410-418** may be repeated as necessary, until the user is satisfied with the calibration of the model. In various embodiments, the same rate constant, different rate constants, or combinations thereof may be modified at **414.**

[01 66] The description above includes example systems, methods, techniques, instruction sequences, and/or computer program products that

embody techniques of the present disclosure. However, it is understood that the described disclosure may be practiced without these specific details. In the present disclosure, the methods disclosed may be implemented as sets of instructions or software readable by a device. Further, it is understood that the specific order or hierarchy of steps in the methods disclosed are instances of example approaches. Based upon design preferences, it is understood that the specific order or hierarchy of steps in the method can be rearranged while remaining within the disclosed subject matter. The accompanying method claims present elements of the various steps in a sample order, and are not necessarily meant to be limited to the specific order or hierarchy presented.

[01 67] The described disclosure may be provided as a computer program product, or software, that may include a machine-readable medium having stored thereon instructions, which may be used to program a computer system (or other electronic devices) to perform a process according to the present disclosure. A machine-readable medium includes any mechanism for storing information in a form (e.g., software, processing application) readable by a machine (e.g., a computer). The machine-readable medium may include, but is not limited to, magnetic storage medium (e.g., floppy diskette), optical storage medium (e.g., CD-ROM); magneto-optical storage medium; read only memory (ROM); random access memory (RAM); erasable programmable memory (e.g., EPROM and EEPROM); flash memory; or other types of medium suitable for storing electronic instructions.

[01 68] It is believed that the present disclosure and many of its attendant advantages will be understood by the foregoing description, and it will be apparent that various changes may be made in the form, construction and arrangement of the components without departing from the disclosed subject matter or without sacrificing all of its material advantages. The form described is merely explanatory, and it is the intention of the following claims to encompass and include such changes.

Example 7. Outcomes apparent in the raw data are independent of the type of mathematical model that might be used to describe the data.

[01 69] The kinetic tracer curves for Aβ42 are known to differ compared to other index peptides (for example, Aβ38 and Aβ40) for certain patient populations. The data reflect the involvement of plaques, as evidenced by PIB scores. A compartmental model was developed as one way of extracting kinetic parameters from the experimentally measured data. Numerous models may be used to describe the data, and it is predicted that all such models will reveal differences in Aβ42 kinetics if they provide satisfactory fits to the data. The following summarizes outcomes apparent in the raw data itself that are independent of the type of compartmental or non-compartmental model that might be used to describe the data, and demonstrates that the SILK tracer kinetic protocol reveals differences in Aβ42 kinetics that will be diagnostic of plaques.

Example 8. SILK tracer kinetic protocol reveals differences in Aβ42 kinetics that may be diagnostic of plaques.

[01 70] The kinetic tracer curve for Aβ42 and the other index peptides (e.g. Aβ38, Aβ40) was different during several different phases of the curve in the presence of plaques. **FIGS. 6A - 6F** show the major differences in the Aβ42 kinetic time course compared to Aβ38 and Aβ40. The different phases, or aspects, of the kinetic tracer curves to focus on are: (i) Initial rise, which is the front-end slope of the curve, and also described as the "fractional synthesis rate" (FSR) as calculated in the Science 201 0 paper); (ii) Peak time; (iii) Peak enrichment; (iv) Initial downturn monoexponential slope; and (v) Terminal monoexponential slope, which is the back-end slope of the curve between 24-36 hours, and is also described as the "fractional catabolic rate" FCR as calculated in the Science 201 0 paper). The particular Aβ42 features in the presence of plaques to focus on are: (i) Initial rise—Aβ42 might be faster; (ii) Peak time—Aβ42 peaks earlier; (iii) Peak enrichment —Aβ42 peaks lower; (iv) Initial downturn monoexponential slope—initial Aβ42 slope may be faster; and (v) Terminal

monoexponential slope—terminal Aβ42 slope may be slower. Each outcome is discussed in further detail below.

(i) Fractional synthesis rate (uses 6-12 h TTR slope and plasma leucine TTR enrichment)

[0171] None of the Aβ peptide (ABxx) FSRs discriminate PIB status or correlate with PIB score. The Aβ42/Aβχχ ratios are lower in PIB+ group (significant when Aβ38 or Total AB is used for normalization, but not when AB40 is used). The Aβ42/38 FSR ratio is significantly negatively correlated with PIB score, but a P value of 0.028 is not that impressive in comparison to other outcomes (see below). **FIGS. 6A - 6F** show that the Aβ42 enrichment is higher than Aβ38 or Aβ40 during the early rise. However, Aβ42 enrichment also rises out of the background a little earlier, and thus the early Aβ42 enrichment has an upward offset without a faster early slope. The 6-12 h time points were used for this FSR analysis. A different range of time points might show a significant difference. However, a practical issue to keep in mind is to balance having enough data points to adequately filter out noise in the data, against having too many points such that a linear slope is being fit to a sigmoidal rise peak. The front end of Aβ42 may not be significantly diagnostic of plaque involvement.

Table 5. Initial ratio of rise (6-12h slope FSR)

	FSR 38	FSR 40	FSR 42	FSR Total AB	42/38 ratio	42/40 ratio	42/total ratio
	pools/h	pools/h	pools/h	pools/h			
PIB- group:							
Mean	0.0453	0.0466	0.0481	0.0449	1.071	1.033	1.067
StDev	0.0114	0.0110	0.0120	0.0094	0.132	0.101	0.112
PIB+ group:							
Mean	0.0457	0.0448	0.0411	0.0437	0.910	0.939	0.947

StDev	0.0134	0.0161	0.0123	0.0119	0.152	0.152	0.154
P, 2-tailed t tests:							
PIB- vs. PIB+	.94	.76	.22	.79	**0.018**	.09	**0.048**
Correlations vs. PIB score:							
Correlation coefficient:	-0.075	-0.146	-0.341	-0.180	-0.459	-0.355	-0.358
P value:	.73	.51	.11	.41	**0.028**	.10	.09

(ii) Time to peak

[0172] None of the individual Aβ peptide peak times discriminate between PIB groups or are significantly correlated against PIB score. However, Aβ42 peaks significantly earlier than either Aβ38, Aβ40, or total AB in the PIB+, and the ratios of the peak times is very highly significantly correlated with the PIB score. Thus, the degree to which the Aβ42 peak is shifted earlier correlates with plaque involvement.

Table 6. Time to peak

	Peak Time 38	**Peak Time 40**	**Peak Time 42**	**Peak Time Total AB**	**42/38 ratio**	**42/40 ratio**	**42/total ratio**
	h	h	h	H			
PIB- group:							
Mean	17.7	17.6	17.6	17.5	0.994	1.000	1.007
StDev	1.4	1.4	1.4	1.4	0.033	0.032	0.032
PIB+ group:							
Mean	17.9	18.0	16.3	17.9	0.907	0.903	0.908
StDev	1.6	1.6	1.5	1.8	0.042	0.043	0.050
P, 2-tailed t tests:							
PIB- vs. PIB+	.76	.56	.05	.53	**2.45E-05**	**4.85E-06**	**1.13E-05**
Correlations vs. PIB score:							

Correlation coefficient:	0.131	0.178	-0.359	0.203	-0.776	-0.792	-0.794
P value:	.55	.42	.09	.35	**1.38E-05**	**6.67E-06**	**6.18E-06**

(Hi) Peak Enrichment

[0173] In these data, enrichment is measured as tracer-to-tracee ratio, but other units of enrichment could be used instead. By itself, the peak enrichment of Aβ42 discriminates between PIB+/- groups and is significantly negatively correlated with PIB score (higher PIB score = lower peak enrichment); but the P value of 0.016 on this is not strongly significant. The lower Aβ42 enrichment is much more strongly associated with plaques when it is normalized to the other index proteins, either Aβ38, 40, or total Aβ. This normalization is crucial as it controls for variability in the plasma leucine enrichment plateau between subjects that is observed with the SILK protocol.

Table 7. Peak Enrichment

	Peak Max 38	**Peak Max 40**	**Peak Max 42**	**Peak Max Total AB**	**42/38 ratio**	**42/40 ratio**	**42/total ratio**
	TTR	TTR	TTR	TTR			
PIB- group:							
Mean	0.0879	0.0896	0.0912	0.0874	1.040	1.018	1.042
StDev	0.0139	0.0137	0.0149	0.0119	0.085	0.063	0.077
PIB+ group:							
Mean	0.0842	0.0818	0.0724	0.0805	0.867	0.891	0.903
StDev	0.0152	0.0149	0.0123	0.0133	0.102	0.090	0.088
P, 2-tailed t tests:							
PIB- vs. PIB+	.56	.23	**0.0081**	.23	**3.97E-04**	**7.98E-04**	**9.61E-04**
Correlations vs. PIB score:							
Correlation coefficient:	-0.051	-0.168	-0.495	-0.193	-0.692	-0.714	-0.649
P value:	.82	.44	**0.0164**	.38	**2.51E-04**	**1.28E-04**	**8.11E-04**

(iv) Initial monoexponential slope FCR

[01 74] A monoexponential slope is fit to the descending enrichment on the back end of the time course. In most studies, the entire back end of the peak is monoexponential to the end of the time course (36 h) as shown in **FIG. 19A.** However, in many cases there is evidence of a 2nd, slower exponential tail to the peak as shown **FIG 19B;** in these cases, an initial rapid slope that visually excludes the slower tail is selected. The plots show the natural log of enrichment vs. time; the monoexponential slope FCR is the negative of the slope.

[01 75] None of the individual peptide monoexponential slopes significantly discriminate between PIB groups, although there is a trend that Aβ40 and total Aβ have slower slopes in the PIB+ group. Greater discriminatory power is achieved by looking at the correlation against PIB score, where the monoexponential slopes for Aβ38, Aβ40, and total Aβ are all significantly negatively correlated against PIB score (slower slope in relation to the degree of plaque quantity). In the formal compartmental model, this came out as a decreased fractional turnover rate (FTR) of soluble Aβ38 & Aβ40 in the brain in the presence of plaques.

[01 76] However, the Aβ42 monoexponential slope does not significantly discriminate between PIB groups nor does it correlate with PIB score. The FTR of soluble Aβ38 and Aβ40 was slowed down in the presence of plaques. This turnover is largely due to fluid perfusion through the brain, and we propose that the fluid perfusion rate is slowed down in the presence of plaques. In the compartmental model, it is assumed that the FTR of Aβ42 that is due to the fluid perfusion process would be the same as it is for Aβ38 and Aβ42. Since the initial monoexponential slope of Aβ42 is not significantly slower in the presence of plaques, but it should be if fluid perfusion was the sole process for Aβ42 turnover, we therefore concluded that some other process of irreversible loss was causing the total FTR of Aβ42 (fluid perfusion loss + extraneous loss) to be increased selectively in the PIB+ group. We take this as kinetic evidence for

removal of soluble Aβ42 from the brain fluid and deposition into plaques, which accounts for the observation that the initial monoexponential is not slower in the presence of plaques (even though the slopes of Aβ38 & Aβ40 are slower), and also provides a mechanism that reduces the concentration of AB42 relative to Aβ38 or Aβ40 that is recovered in CSF.

[01 77] The Aβ42 initial monoexponential slope also fails to discriminate between PIB groups or correlate with PIB score when it is normalized using either Aβ38, Aβ40 or total Aβ as a reference. Thus, in conclusion, the initial monoexponential slope FCR of Aβ42 is not diagnostic of plaques.

Table 8. Initial monoexponential slope FCR

	AB 38	**AB 40**	**AB 42**	**Total AB**	**42/38 ratio**	**42/40 ratio**	**42/total ratio**
	/h	/h	/h	/h			
PIB- group:							
Mean	0.0937	0.0963	0.0986	0.0948	1.051	1.024	1.040
StDev	0.0179	0.0182	0.0221	0.0181	0.098	0.107	0.102
PIB+ group:							
Mean	0.0815	0.0794	0.0896	0.0793	1.139	1.165	1.154
StDev	0.0204	0.0183	0.0175	0.0181	0.260	0.272	0.211
P, 2-tailed t tests:							
PIB- vs. PIB+	.16	.05	.35	.07	.24	.08	.09
Correlations vs. PIB score:							
Correlation coefficient:	-0.418	-0.494	-0.297	-0.480	0.288	0.363	0.371
P value:	**0.0473**	**0.0167**	.17	**0.0204**	.18	.09	.08

(v) Terminal monoexponential slope FCR

[01 78] A monoexponential slope was fit to t = 24-36 h of the time course as reported in the Science 201 0 paper; this is done without regard for whether the peak exhibits monoexponential or biexponential behavior (see natural log plots in **FIGS. 19A - 19B** for illustration).

[01 79] By itself, the terminal slope of Aβ42 very weakly discriminates between PIB groups (P = 0.0355), with PIB+ having a slower terminal tail. In the model, this is accounted for by the "exchange compartment" whereby newly synthesized (i.e., labeled) Aβ42 enters into an exchange process that returns labeled Aβ42 to the soluble pool later, which is a feature of tracer recycling that causes a flattening of the terminal tail. The terminal slopes of Aβ38 or Aβ40 do not discriminate between PIB groups. The terminal slopes of all 3 peptides, however, are significantly negatively correlated with PIB score, which results from the feature described above whereby the turnover of soluble Aβ peptides may be mostly driven by fluid transport through the brain tissue, and this transport process is retarded in the presence of plaques. The small degree of discrimination between groups for Aβ42 is lost when that slope is normalized to either the Aβ38 or Aβ40 slope. In conclusion, the terminal monoexponential slope of Aβ42 is not particularly diagnostic for plaques. There is a weak power to discriminate, but the enrichment measurements are somewhat noisy (especially as enrichments get lower toward the end of the protocol), and the slope is not all that useful.

Table 9. Terminal slope FCR (24-36h slope)

	Terminal slope FCR38	**Terminal slope FCR40**	**Terminal slope FCR42**	**42/38 ratio**	**42/40 ratio**
	pools/h	pools/h	pools/h		
PIB- group:					
Mean	0.0844	0.0851	0.0848	1.005	0.994
StDev	0.0115	0.0112	0.0150	0.104	0.085
PIB+ group:					
Mean	0.0765	0.0761	0.0689	0.902	0.908
StDev	0.0150	0.0166	0.0171	0.199	0.183
P, 2-tailed t tests:					
PIB- vs. PIB+	.18	.14	**0.0355**	.12	.13
Correlations vs. PIB score:					

Correlation coefficient:	-0.422	-0.472	-0.462	-0.1 94	-0.1 39
P value:	**0.0451**	**0.0229**	**0.0265**	.37	.53

(vi) Overall conclusions

[01 80] The peak time and peak enrichment of Aβ42 is very highly significantly associated with plaques: Aβ42 peaks earlier and lower when plaques are present. The slope on the front end and the initial and terminal monoexponential slopes on the back end are not particularly sensitive to the presence of plaques.

[01 8 1] The presence of plaques clearly alters biologic processes that distinguish the Aβ42 turnover curve from Aβ38, Aβ40, or total Aβ. The earlier and lower peak of Aβ42 in the presence of plaques (peak time and peak enrichment, respectively) causes a separation of enrichments on the back end of the curve (see time course plots). In addition to these two measurements, recent results show that a comparison of isotopic enrichments around the midpoint on the back end of the curve (-24 h) is also able to discriminate the PIB groups highly significantly. A fourth measurement that may be associated with plaques is the degree to which Aβ42 enrichment on the descending peak is different from Aβ38, Aβ40, or Total Aβ enrichment.

Example 9. Additional in vivo data using the SILK tracer kinetic protocol.

[01 82] It was hypothesized that simple measures that summarize some aspect of the SILK tracer curve of amyloid beta (Aβ) may provide diagnostic or prognostic information about patients with AD, at risk of AD, or suspected of having AD. To test the above hypothesis, discrimination between the three groups of patients was attempted based on the ratio of the percent of Aβ42 labeling to the percent of Aβ40 percent calculated during the downturn of the Aβ SILK tracer curve. *In vivo* SILK studies were performed in patients with *PSEN1* or *PSEN2* mutations that were PIB positive by PET (MC+), patients with *PSEN1* or *PSEN2* mutations that were PIB negative by PET (MC-), and non-carrier mutation carrier sibling controls (NC) as described elsewhere in U.S. Patent No.

7,892,845, which is hereby incorporated herein in its entirety. Briefly, subjects were administered isotope-labeled leucine ($^{13}C_6$-leucine) for 9 hours via intravenous infusion. CSF samples (6 mL/sample) were collected 23 hours and 24 hours after the start of the infusion of labeled amino acid. Quantitative measurements of labeled and unlabeled Aβ42 and Aβ40 were obtained by tandem mass spectrometry, and the ratio of labeled unlabeled Aβ42 and labeled:unlabeled Aβ40 was calculated for each timepoint. These ratios represent the percent labeled of each Aβ isoform at 23 hours and 24 hours post infusion.

[0183] A diagnostic threshold of 0.9 was defined in these experiments, such that a ratio of Aβ42 percent labeled / Aβ40 percent labeled below 0.9 classified a subject as AD positive and a ratio of Aβ42 percent labeled / Aβ40 percent labeled above 0.9 classified a subject as AD negative. To determine whether the ratio of Aβ42 percent labeled / Aβ40 percent labeled at 23 hrs post infusion was differentiated between the three groups of patients, the ratio obtained for each patient was graphed versus PIB staining. As can be seen in **FIG. 20A,** a threshold of 0.9 for this ratio clearly differentiates the majority of MC+ subjects from the NC subjects (6/7 MC+ subjects were below the threshold, while 11/12 NC subjects were above the threshold). Within the MC- group, 3/4 of the subjects were below the threshold. It is possible, however, that subjects in the MC- group were in the early stages of AD. Similarly, the average of the 23 hour and 24 hour labeling percentages may be compared as a ratio between Aβ42 and Aβ40. Aβ42 percent labeled / Aβ40 percent labeled at 23 hrs post infusion and 24 hrs was differentiated between the three groups of patients, the ratio obtained for each patient was graphed versus PIB staining. As can be seen in **FIG. 20B,** with this measure, 7/7 MC+ subjects are below the threshold, while 11/12 NC are above the threshold. For the MC- group, 2/4 subjects are below the threshold.

[0184] These data may be compared to a simple measure that uses the results from the full kinetic model. In this case, the parameter kex42, which describes the rate of entry of Aβ42 into the exchange compartment, is multiplied

by 10 and then added to the ratio of the rate constants for irreversible loss for Aβ42 versus Aβ40. As shown in **FIG. 20C,** a threshold of 1.75 shows that 6/7 of the MC+ subjects are above the threshold, with 12/12 of the NC subjects below the threshold. For the MC- group, 2/4 subjects are below the threshold.

[0185] These examples indicate that simple measures that summarize some aspect of the SILK tracer curve may be diagnostic of AD. This also indicates that short term collection of CSF may be sufficient to diagnose changes in Aβ42 kinetics.

[0186] Having described the invention in detail, it will be apparent that modifications and variations are possible without departing from the scope of the invention defined in the appended claims. Those of skill in the art should, however, in light of the present disclosure, appreciate that many changes could be made in the specific embodiments that are disclosed and still obtain a like or similar result without departing from the spirit and scope of the invention, therefore all matter set forth herein is to be interpreted as illustrative and not in a limiting sense.

[0187] While the present disclosure has been described with reference to various embodiments, it will be understood that these embodiments are illustrative and that the scope of the disclosure is not limited to them. Many variations, modifications, additions, and improvements are possible. More generally, embodiments in accordance with the present disclosure have been described in the context of particular implementations. Functionality may be separated or combined in blocks differently in various embodiments of the disclosure or described with different terminology. These and other variations, modifications, additions, and improvements may fall within the scope of the disclosure as defined in the claims that follow.

CLAIMS

What is claimed is:

1. A method for detecting amyloid pathology in the central nervous system of a patient, the method comprising (i) determining one or more kinetic parameters of Aβ42 and at least one other Aβ peptide, and (ii) comparing the Aβ42 kinetic parameter and the same kinetic parameter for a second Aβ measurement, and (iii) determining whether a subject has amyloid pathology based on a difference between the two kinetic parameters.

2. The method of claim 1, wherein the kinetic parameter is selected from the group consisting of fractional synthesis rate, peak time, peak enrichment, initial downturn monoexponential slope, terminal monoexponential slope, and a combination thereof.

3. The method of claim 1, wherein two or more kinetic parameters are determined.

4. The method of claim 1, wherein three or more kinetic parameters are determined.

5. The method of claim 1, wherein four or more kinetic parameters are determined.

6. The method of claim 1, wherein at least five kinetic parameters are determined.

7. The method of claim 1, wherein:

(i) the kinetic parameter is fractional synthesis rate and the Aβ42 fractional synthesis rate is faster than the fractional synthesis rate for the second Aβ measurement,

(ii) the kinetic parameter is peak time and the Aβ42 peak time is earlier than the peak time for the second Aβ measurement,

(iii) the kinetic parameter is peak enrichment and the Aβ42 peak enrichment is lower than the peak enrichment for the second Aβ measurement,

(iv) the kinetic parameter is initial downturn monoexponential slope and the initial Aβ42 slope is faster than the initial slope for the second Aβ measurement, or

(v) the kinetic parameter is terminal monoexponential slope and the terminal Aβ42 slope is slower than the terminal slope for the second Aβ measurement.

8. The method of claim 1, wherein the one or more kinetic parameters are determined by stable isotope labeling kinetics.

9. The method of claim 8, wherein a labeled amino acid is administered to the subject hourly for a time period selected from the group consisting of 6 to 12 hours, 6 to 9 hours, and 9 to 12 hours.

10. The method of claim 8, wherein the amount of labeled peptide and the amount of unlabeled peptide is detected by a means selected from the group consisting of mass spectrometry, tandem mass spectrometry, and a combination thereof.

11. The method of claim 1, wherein the one or more kinetic parameters are determined using a mathematical model for the enrichment kinetics of Aβ.

12. The method of claim 8, further comprising calculating the isotopic enrichment of Aβ42 compared to the second Aβ measurement at a single timepoint after administration of the labeled amino acid to the patient.

13. The method of claim 1 or 12, wherein the second Aβ measurement is selected from the group consisting of an Aβ peptide other than Aβ42 and total Aβ.

14. The method of claim 13, wherein the Aβ peptide other than Aβ42 is Aβ38 or Aβ40.

15. The method of claim 1, further comprising (i) calculating the ratio between the Aβ42 kinetic parameter and the same kinetic parameter for the second Aβ measurement, and (ii), comparing the ratio calculated in (i) to a threshold value, wherein a value lower than the threshold indicates the patient has amyloid plaques.

16. A method to diagnose an amyloid pathology in a patient, the method comprising (i) creating a mathematical model for the steady-state kinetics of Aβ comprising a set of model parameters, wherein the set of model parameters comprises k_{ex42}, a rate constant for an irreversible loss for Aβ42, and a rate constant for an irreversible loss for Aβ40, (ii) calculating ten times k_{ex42} and adding that to the FTR ratio, wherein k_{ex42} describes the rate of entry of Aβ42 into the exchange compartment and the FTR ratio is the ratio of the rate constants for

irreversible loss for Aβ42 versus Aβ40, and (iii) comparing the value from (ii) to a threshold value, wherein a value lower than the threshold value indicates a subject has Alzheimer's Disease.

17. The method of claim 16, wherein the amyloid pathology is selected from the group consisting of amyloid plaques, altered Aβ kinetics, and Alzheimer's Disease.

18. A method of calibrating a model to estimate a time course of enrichment kinetics of at least one Aβ isoform, the method comprising:

a) obtaining data values for an amount of a labeled moiety introduced into a patient as a function of time, wherein a fraction of the at least one Aβ isoforms comprises the labeled moiety;

b) modeling a metabolic pathway of the at least one Aβ isoform with the model based on the obtained data values to calculate a set of model parameters and an estimated time course of enrichment kinetics of the at least one amyloid; and

c) comparing the estimated time course of enrichment kinetics of the at least one Aβ isoform to a measured time course of enrichment kinetics of the at least one Aβ isoform obtained from the patient;

d) wherein, if the estimated time course of enrichment kinetics matches the measured time course of enrichment kinetics, determining that the compartmental model is calibrated;

e) wherein, if the estimated time course of enrichment kinetics does not match the measured time course of enrichment kinetics:

i) modifying at least one of the set of model parameters; and

ii) remodeling the metabolic pathway of the Aβ peptide using the modified model parameters to calculate a new estimated time course of enrichment of the at least one amyloid; and

f) repeating c)-e) until the compartmental model is calibrated.

19. An amyloid kinetics modeling system for estimating a time course of enrichment kinetics of at least one Aβ isoform, the system comprising:

a) at least one processor; and

b) a CRM containing an amyloid kinetics application comprising a plurality of modules executable on the at least one processor, the plurality of modules comprising:

i) a plasma module to represent infusion of a labeled moiety into the plasma of a patient and to represent transport of the labeled moiety across the blood brain barrier (BBB) of the patient;

ii) a brain tissue module to represent incorporation of the labeled moiety into APP and formation of C99;

iii) an amyloid kinetics module to represent cleavage of the C99 to form at least one Aβ isoform and subsequent kinetics of the at least one Aβ isoform within the brain of the patient;

iv) a CSF module to represent transport of the at least one Aβ isoform into the CSF of the patient

v) a model tuning module to iteratively adjust a set of model parameters defining a dynamic response of the model to an input time history of plasma

leucine enrichment into the plasma module in order to optimize a match between predicted enrichment kinetics and measured enrichment kinetics of the at least one Aβ isoform in the patient; and

vi) a GUI module to generate one or more forms used to receive inputs to the system and to deliver output from the system.

20. The system of claim 19, wherein the plasma module comprises a plasma amino acid compartment comprising a plasma concentration of at least one amino acid, wherein the plasma concentration of the at least one amino acid is determined using an input comprising a time history of an infusion of a labeled amino acid into a patient.

21. The system of claim 19, wherein the brain tissue module comprises:

a) an APP compartment comprising a total amount of APP;

b) an APP incorporation rate comprising a rate of incorporation of the at least one amino acid from the plasma amino acid compartment into an APP molecule in the APP compartment;

c) a C99 compartment comprising a total amount of C99 c-terminal fragments;

d) a C99 formation rate comprising a rate of formation of the C99 c-terminal fragments in the C99 compartment from the APP molecules; and

e) a C99 clearance rate comprising a rate of disappearance of the C99 c-terminal fragments from the C99 compartment.

22. The system of claim 19, wherein the amyloid kinetics module comprises:

a) a soluble Aβ42 isoform compartment comprising an amount of a soluble Aβ42 isoform;

b) an Aβ42 isoform formation rate comprising a rate of formation of soluble Aβ42 isoform from the C99 c-terminal fragments;

c) an Aβ42 isoform clearance rate comprising a rate of disappearance of Aβ42 isoforms from the soluble Aβ compartment;

d) an Aβ42 incorporation rate comprising a rate of transformation of the soluble Aβ42 isoform to an incorporated Aβ42 isoform; and

e) a recycled Aβ42 compartment comprising a total amount of incorporated Aβ42 isoform.

23. The system of claim 19, wherein the CSF module comprises

a) a CSF Aβ42 compartment comprising a total amount of CSF Aβ42 isoforms;

b) a CSF Aβ42 transfer rate comprising a rate of transfer of soluble Aβ42 isoform from the soluble Aβ42 compartment to the CSF Aβ42 compartment; and

c) a CSF Aβ42 clearance rate comprising a rate of disappearance of CSF Aβ42 from the CSF Aβ42 pool.

24. The system of claim 22, wherein the amyloid kinetics module further comprises:

a) a soluble comparison Aβ isoform compartment comprising an amount of a soluble comparison Aβ isoform;

b) a comparison Aβ isoform formation rate comprising a rate of formation of soluble comparison Aβ isoform from the C99 c-terminal fragments; and

c) a comparison Aβ isoform clearance rate comprising a rate of disappearance of soluble comparison Aβ isoforms from the soluble comparison Aβ isoform compartment.

25. The system of claim 24, wherein the comparison Aβ isoform is chosen from Aβ38 and Aβ40.

26. The system of claim 23, wherein the CSF module comprises

a) a CSF comparison Aβ isoform compartment comprising a total amount of CSF comparison Aβ isoforms;

b) a CSF comparison Aβ isoform transfer rate comprising a rate of transfer of soluble comparison Aβ isoform from the soluble comparison Aβ isoform compartment to the CSF comparison Aβ isoform compartment; and

c) a CSF comparison Aβ isoform clearance rate comprising a rate of disappearance of CSF comparison Aβ isoform from the CSF comparison Aβ isoform compartment.

27. The system of claim 26, wherein the comparison Aβ isoform is chosen from Aβ38 and Aβ40.

28. A system for estimating the kinetics of amyloid-beta (Aβ) in the CNS of a patient, the system comprising:

at least one processor; and

a CNS Aβ kinetic model application comprising a plurality of modules executable using the at least one processor, the modules comprising:

a) a plasma amino acid module to estimate a plasma amino acid compartment comprising a plasma concentration of at least one amino acid;

b) an APP incorporation module to estimate an APP incorporation rate comprising a rate of incorporation of the at least one amino acid from the plasma amino acid compartment into an APP molecule in an APP compartment;

c) an APP module to estimate the APP compartment comprising a total amount of APP molecules;

d) a C99 formation module to estimate a C99 formation rate comprising a rate of formation of a C99 c-terminal fragment in a C99 compartment from the APP molecules;

e) a C99 clearance module to estimate a C99 clearance rate comprising a rate of disappearance of the C99 c-terminal fragment from the C99 compartment;

e) a C99 module to estimate the C99 compartment comprising a total amount of the C99 c-terminal fragments;

f) a free Aβ formation module to estimate at least one free Aβ isoform formation rate, each free Aβ isoform formation rate comprising a rate of formation of a free Aβ isoform in a free Aβ compartment from the C99 c-terminal fragments;

g) a free Aβ clearance module to estimate at least one free Aβ isoform clearance rate, each free Aβ isoform clearance rate comprising a rate of disappearance of one of the free Aβ isoforms from the free Aβ compartment;

h) a free Aβ module to estimate the free Aβ compartment comprising the total amount of all free Aβ isoforms;

i) a free Aβ recycling module to estimate:

at least one free Aβ incorporation rate, each free Aβ incorporation rate comprising a rate of transformation of a free Aβ isoform to an incorporated Aβ isoform in a recycled Aβ compartment, and

at least one Aβ recycling rate, each Aβ recycling rate comprising a rate of recycling an incorporated Aβ isoform in the recycled Aβ compartment back into a free Aβ isoform in the free Aβ compartment;

j) a CSF Aβ transfer module to estimate at least one CSF Aβ transfer rate, each Aβ transfer rate comprising a rate of transfer of one free Aβ isoform from the free Aβ compartment to a CSF Aβ compartment;

k) a CSF Aβ clearance module to estimate at least one CSF Aβ clearance rate, each CSF Aβ clearance rate comprising a rate of disappearance of one CSF Aβ isoform from the CSF Aβ compartment; and

l) a CSF Aβ module to estimate the CSF Aβ compartment comprising the total amount of CSF Aβ isoforms.

29. The system of claim 28, wherein the Aβ isoforms are chosen from Aβ38, Aβ40, and Aβ42.

30. The system of claim 28, wherein:

at least a portion of the plasma amino acid compartment comprises a plasma concentration of at least one labeled amino acid;

at least a portion of the APP compartment comprises an amount of enriched APP molecules incorporating the at least one labeled amino acid;

at least a portion of the C99 compartment further comprises an amount of enriched C99 c-terminal fragments formed from the amount of enriched APP molecules; and

at least a portion of the Aβ isoforms further comprises an amount of enriched Aβ isoforms formed from the amount of enriched C99 c-terminal fragments.

31. The system of claim 28, wherein CSF Aβ transfer module further estimates at least one CSF Aβ delay, each CSF Aβ delay comprising a delay in the transfer of one free Aβ isoform from the free Aβ compartment to the CSF Aβ compartment.

32. The method of claim 28, wherein the at least one CSF Aβ transfer rate is represented by a fluid flow of ISF within the brain.

33. A method of using a model of amyloid β (Aβ) isoform enrichment kinetics, the method comprising:

obtaining from a patient measured Aβ enrichment kinetics data comprising a time course of concentration of a labeled moiety infused into the patient, a measured time course of Aβ42 enrichment kinetics in the CSF of the patient, and a measured time course of at least one other comparison Aβ isoform enrichment kinetics in the patient;

inputting the measured Aβ enrichment kinetics data into the model, wherein the model represents enrichment kinetics of Aβ42 and the at least one other comparison Aβ isoform;

obtaining a set of model parameters from the model;

calculating a model index comprising a mathematical combination of at least two model parameters from the model;

comparing the model index to a pre-selected threshold range; and

identifying a disease state of the patient if the model index falls outside of the threshold range.

34. The method of claim 33, wherein the disease state is identified as Alzheimer's if the model index falls outside of the threshold range.

35. The method of claim 33, wherein the severity of the disease state is identified by comparing the model index to a pre-selected correlation of the disease state with the model index.

36. The method of claim 35, wherein the correlation of the disease state is a correlation of the model index with PIB imaging values obtained from a population of patients with a range of disease states.

37. The method of claim 33, wherein the measured Aβ enrichment kinetics data from a patient are obtained by the SILK method.

38. The method of claim 33, wherein the labeled moiety is labeled leucine.

39. The method of claim 33, wherein the at least one other comparison Aβ isoform is chosen from Aβ38 and Aβ40.

40. The method of claim 33, wherein the model parameters are chosen from: concentration of Aβ isoforms, rates of transfer, rates of irreversible loss, rates of exchange, rates of delay, and combinations thereof.

41. The method of claim 33, wherein the model index is calculated using a rate of irreversible loss of Aβ42 and a rate of transfer of Aβ42.

42. The method of claim 33, wherein the model parameters are obtained by iteratively varying the model parameters until a best fit of the estimated Aβ enrichment kinetics to the measured Aβ enrichment kinetics is obtained.

43. An amyloid kinetics modeling system for estimating a time course of enrichment kinetics of at least one Aβ isoform, the system comprising:

a) at least one processor; and

b) a CRM containing an amyloid kinetics application comprising a plurality of modules executable on the at least one processor, the plurality of modules comprising:

i) a plasma module to represent infusion of a labeled moiety into the plasma of a patient and to represent transport of the labeled moiety across the blood brain barrier (BBB) of the patient;

ii) a brain tissue module to represent incorporation of the labeled moiety into APP and formation of C99;

iii) an amyloid kinetics module to represent cleavage of the C99 to form at least one Aβ isoform and subsequent kinetics of the at least one Aβ isoform within the brain of the patient;

iv) a CSF module to represent transport of the at least one Aβ isoform into the CSF of the patient;

v) a blood enrichment module to represent transport of the at least one Aβ isoform into the blood of the patient;

v) a model tuning module to iteratively adjust a set of model parameters defining a dynamic response of the model to an input time history of plasma leucine enrichment into the plasma module in order to optimize a match between predicted enrichment kinetics and measured enrichment kinetics of the at least one Aβ isoform in the patient; and

vi) a GUI module to generate one or more forms used to receive inputs to the system and to deliver output from the system.

44. The system of claim 43, wherein the plasma module comprises a plasma amino acid compartment comprising a plasma concentration of at least one amino acid, wherein the plasma concentration of the at least one amino acid is determined using an input comprising a time history of an infusion of a labeled amino acid into a patient.

45. The system of claim 43, wherein the brain tissue module comprises:

a) an APP compartment comprising a total amount of APP;

b) an APP incorporation rate comprising a rate of incorporation of the at least one amino acid from the plasma amino acid compartment into an APP molecule in the APP compartment;

c) a C99 compartment comprising a total amount of C99 c-terminal fragments;

d) a C99 formation rate comprising a rate of formation of the C99 c-terminal fragments in the C99 compartment from the APP molecules; and

e) a C99 clearance rate comprising a rate of disappearance of the C99 c-terminal fragments from the C99 compartment.

46. The system of claim 43, wherein the amyloid kinetics module comprises:

a) a soluble Aβ42 isoform compartment comprising an amount of a soluble Aβ42 isoform;

b) an Aβ42 isoform formation rate comprising a rate of formation of soluble Aβ42 isoform from the C99 c-terminal fragments;

c) an Aβ42 isoform clearance rate comprising a rate of disappearance of Aβ42 isoforms from the soluble Aβ compartment;

d) an Aβ42 incorporation rate comprising a rate of transformation of the soluble Aβ42 isoform to an incorporated Aβ42 isoform; and

e) a recycled Aβ42 compartment comprising a total amount of incorporated Aβ42 isoform.

47. The system of claim 43, wherein the CSF module comprises

a) a CSF Aβ42 compartment comprising a total amount of CSF Aβ42 isoforms;

b) a CSF Aβ42 transfer rate comprising a rate of transfer of soluble Aβ42 isoform from the soluble Aβ42 compartment to the CSF Aβ42 compartment; and

c) a CSF Aβ42 clearance rate comprising a rate of disappearance of CSF Aβ42 from the CSF Aβ42 pool.

48. The system of claim 46, wherein the amyloid kinetics module further comprises:

a) a soluble comparison Aβ isoform compartment comprising an amount of a soluble comparison Aβ isoform;

b) a comparison Aβ isoform formation rate comprising a rate of formation of soluble comparison Aβ isoform from the C99 c-terminal fragments; and

c) a comparison Aβ isoform clearance rate comprising a rate of disappearance of soluble comparison Aβ isoforms from the soluble comparison Aβ isoform compartment.

49. The system of claim 48, wherein the comparison Aβ isoform is chosen from Aβ38 and Aβ40.

50. The system of claim 47, wherein the CSF module comprises

a) a CSF comparison Aβ isoform compartment comprising a total amount of CSF comparison Aβ isoforms;

b) a CSF comparison Aβ isoform transfer rate comprising a rate of transfer of soluble comparison Aβ isoform from the soluble comparison Aβ isoform compartment to the CSF comparison Aβ isoform compartment; and

c) a CSF comparison Aβ isoform clearance rate comprising a rate of disappearance of CSF comparison Aβ isoform from the CSF comparison Aβ isoform compartment.

51. The system of claim 50, wherein the comparison Aβ isoform is chosen from Aβ38 and Aβ40.

52. The system of claim 43, wherein the blood enrichment module comprises

a) a blood Aβ42 compartment comprising a total amount of blood Aβ42 isoforms;

b) a blood Aβ42 transfer rate comprising a rate of transfer of soluble Aβ42 isoform from the soluble Aβ42 compartment to the blood Aβ42 compartment; and

c) a blood Aβ42 clearance rate comprising a rate of disappearance of blood Aβ42 from the blood Aβ42 pool.

53. An amyloid kinetics modeling system for estimating a time course of enrichment kinetics of at least one Aβ isoform, the system comprising:

a) at least one processor; and

b) a CRM containing an amyloid kinetics application comprising a plurality of modules executable on the at least one processor, the plurality of modules comprising:

i) a plasma module to represent infusion of a labeled moiety into the plasma of a patient and to represent transport of the labeled moiety across the blood brain barrier (BBB) of the patient;

ii) a brain tissue module to represent incorporation of the labeled moiety into APP and formation of C99;

iii) an amyloid kinetics module to represent cleavage of the C99 to form at least one Aβ isoform and subsequent kinetics of the at least one Aβ isoform within the brain of the patient;

v) a blood enrichment module to represent transport of the at least one Aβ isoform into the blood of the patient;

v) a model tuning module to iteratively adjust a set of model parameters defining a dynamic response of the model to an input time history of plasma leucine enrichment into the plasma module in order to optimize a match between predicted enrichment kinetics and measured enrichment kinetics of the at least one Aβ isoform in the patient; and

vi) a GUI module to generate one or more forms used to receive inputs to the system and to deliver output from the system.

54. The system of claim 53, wherein the plasma module comprises a plasma amino acid compartment comprising a plasma concentration of at least one amino acid, wherein the plasma concentration of the at least one amino acid is determined using an input comprising a time history of an infusion of a labeled amino acid into a patient.

55. The system of claim 53, wherein the brain tissue module comprises:

a) an APP compartment comprising a total amount of APP;

b) an APP incorporation rate comprising a rate of incorporation of the at least one amino acid from the plasma amino acid compartment into an APP molecule in the APP compartment;

c) a C99 compartment comprising a total amount of C99 c-terminal fragments;

d) a C99 formation rate comprising a rate of formation of the C99 c-terminal fragments in the C99 compartment from the APP molecules; and

e) a C99 clearance rate comprising a rate of disappearance of the C99 c-terminal fragments from the C99 compartment.

56. The system of claim 53, wherein the amyloid kinetics module comprises:

a) a soluble Aβ42 isoform compartment comprising an amount of a soluble Aβ42 isoform;

b) an Aβ42 isoform formation rate comprising a rate of formation of soluble Aβ42 isoform from the C99 c-terminal fragments;

c) an Aβ42 isoform clearance rate comprising a rate of disappearance of Aβ42 isoforms from the soluble Aβ compartment;

d) an Aβ42 incorporation rate comprising a rate of transformation of the soluble Aβ42 isoform to an incorporated Aβ42 isoform; and

e) a recycled Aβ42 compartment comprising a total amount of incorporated Aβ42 isoform.

57. The system of claim 56, wherein the amyloid kinetics module further comprises:

a) a soluble comparison Aβ isoform compartment comprising an amount of a soluble comparison Aβ isoform;

b) a comparison Aβ isoform formation rate comprising a rate of formation of soluble comparison Aβ isoform from the C99 c-terminal fragments; and

c) a comparison Aβ isoform clearance rate comprising a rate of disappearance of soluble comparison Aβ isoforms from the soluble comparison Aβ isoform compartment.

58. The system of claim 57, wherein the comparison Aβ isoform is chosen from Aβ38 and Aβ40.

59. The system of claim 53, wherein the blood enrichment module comprises

a) a blood Aβ42 compartment comprising a total amount of blood Aβ42 isoforms;

b) a blood Aβ42 transfer rate comprising a rate of transfer of soluble Aβ42 isoform from the soluble Aβ42 compartment to the blood Aβ42 compartment; and

c) a blood Aβ42 clearance rate comprising a rate of disappearance of blood Aβ42 from the blood Aβ42 pool.

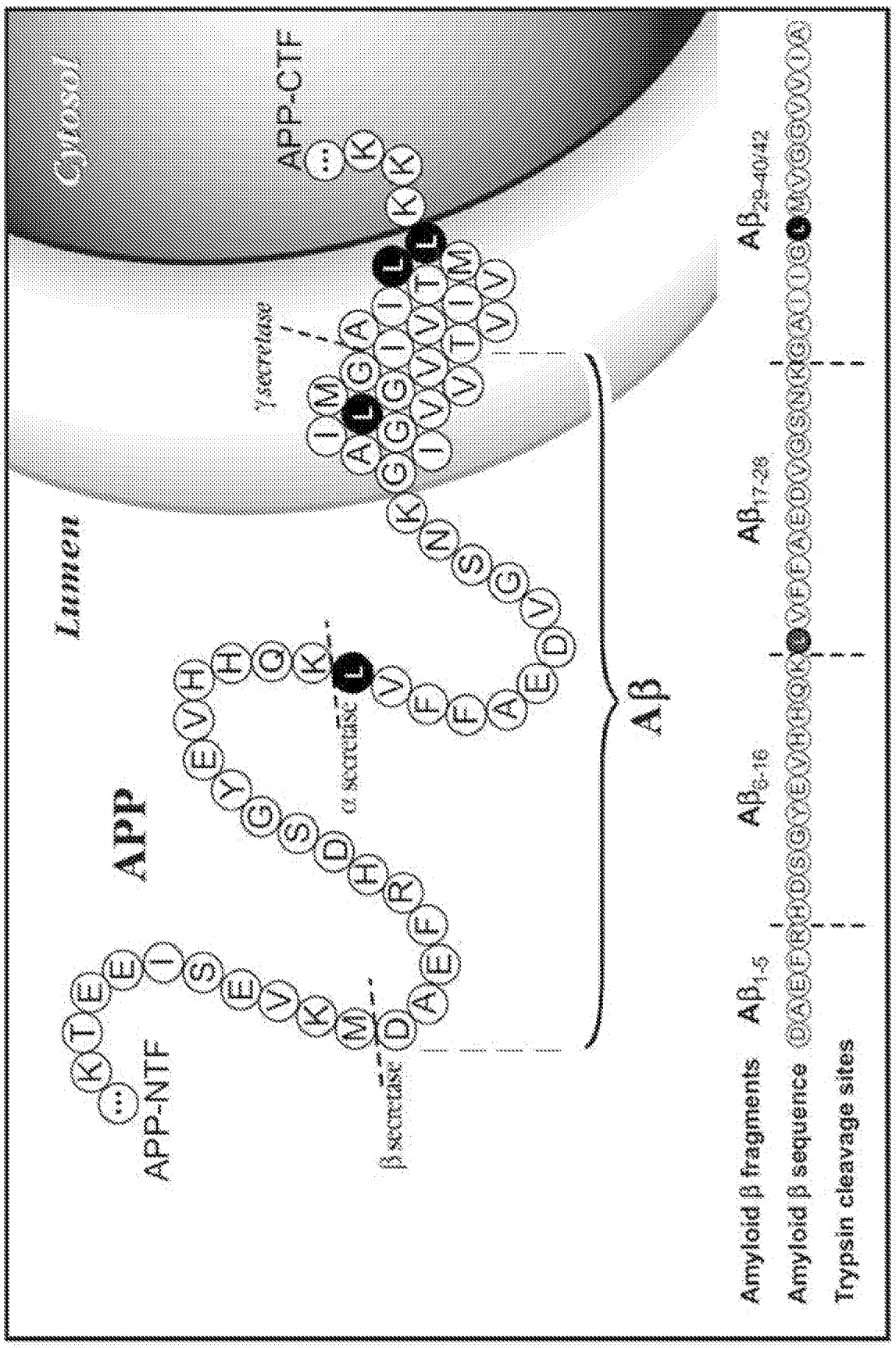
Cytosol
Lumen
APP
APP-NTF
APP-CTF
β secretase
α secretase
γ secretase
Aβ
Amyloid β fragments
Aβ1-5
Aβ6-16
Aβ17-28
Aβ29-40/42
Amyloid β sequence
Trypsin cleavage sites

FIG. 1

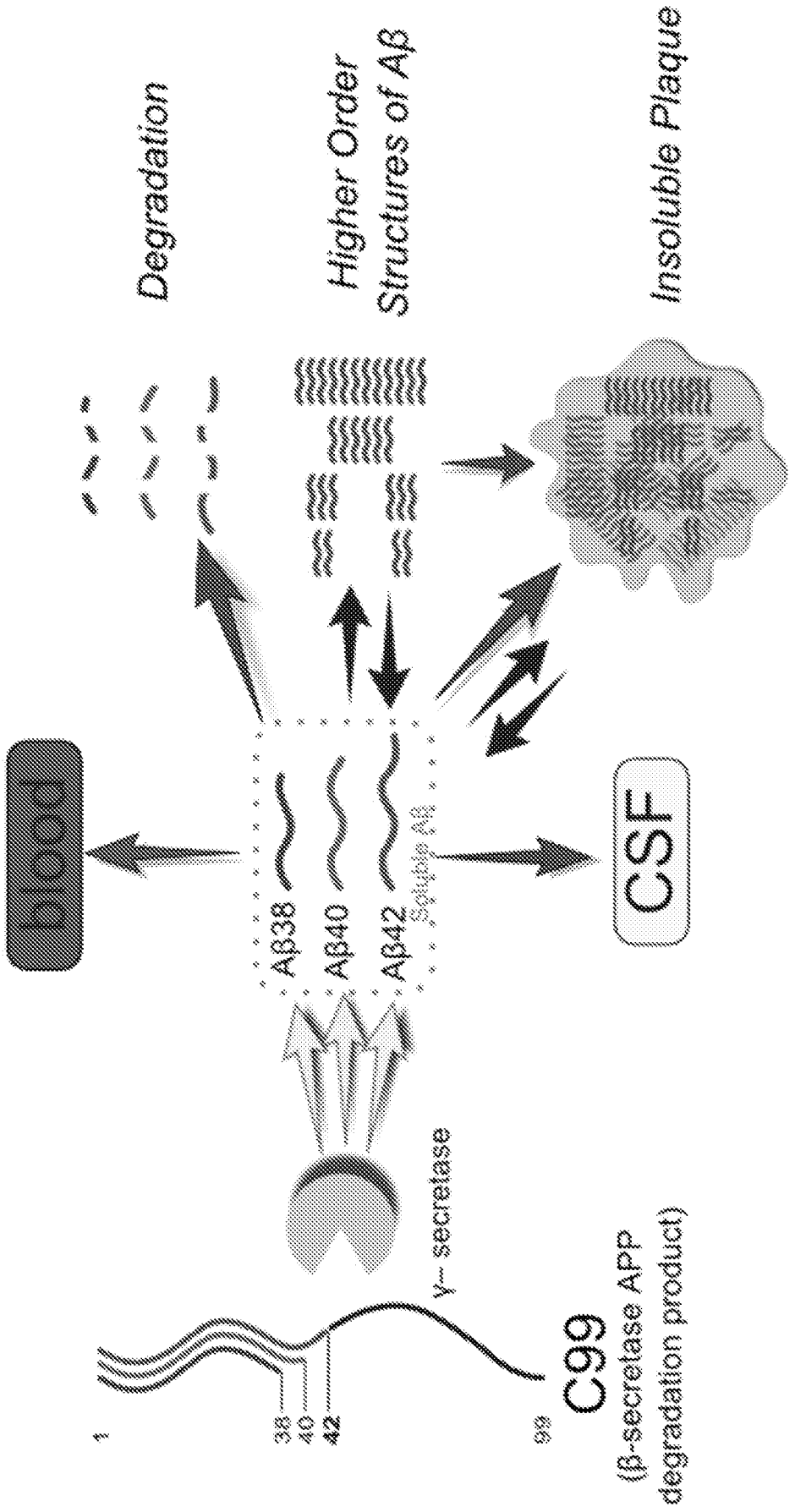
Degradation
Higher Order Structures of Aβ
Insoluble Plaque
Blood
CSF
Aβ38
Aβ40
Aβ42
Soluble Aβ
γ– secretase
C99
(β-secretase APP degradation product)
1
38
40
42
99

FIG. 2

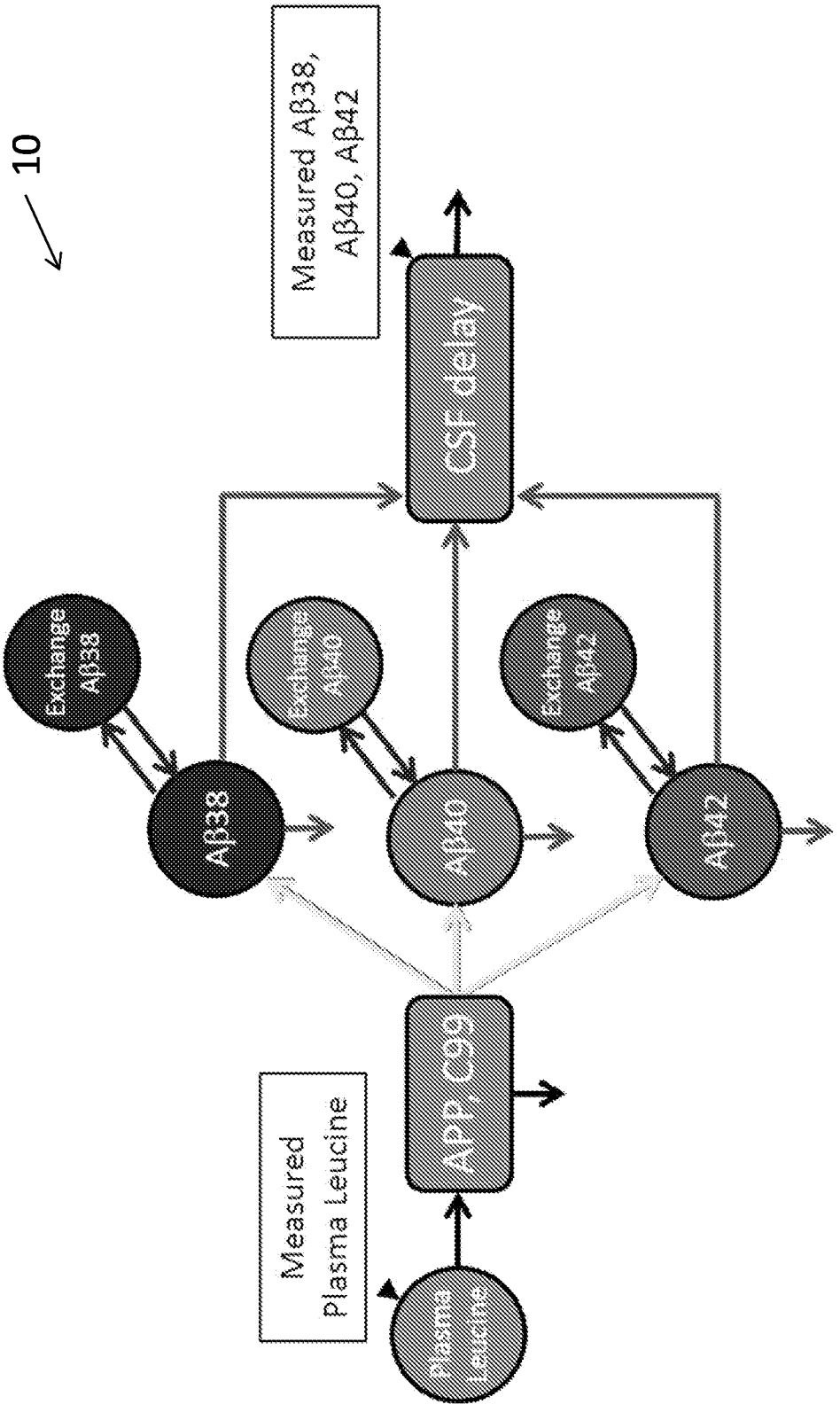
10
Measured Aβ38, Aβ40, Aβ42
CSF delay
Exchange Aβ38
Exchange Aβ40
Exchange Aβ42
Aβ38
Aβ40
Aβ42
Measured Plasma Leucine
APP, C99
Plasma Leucine

FIG. 3

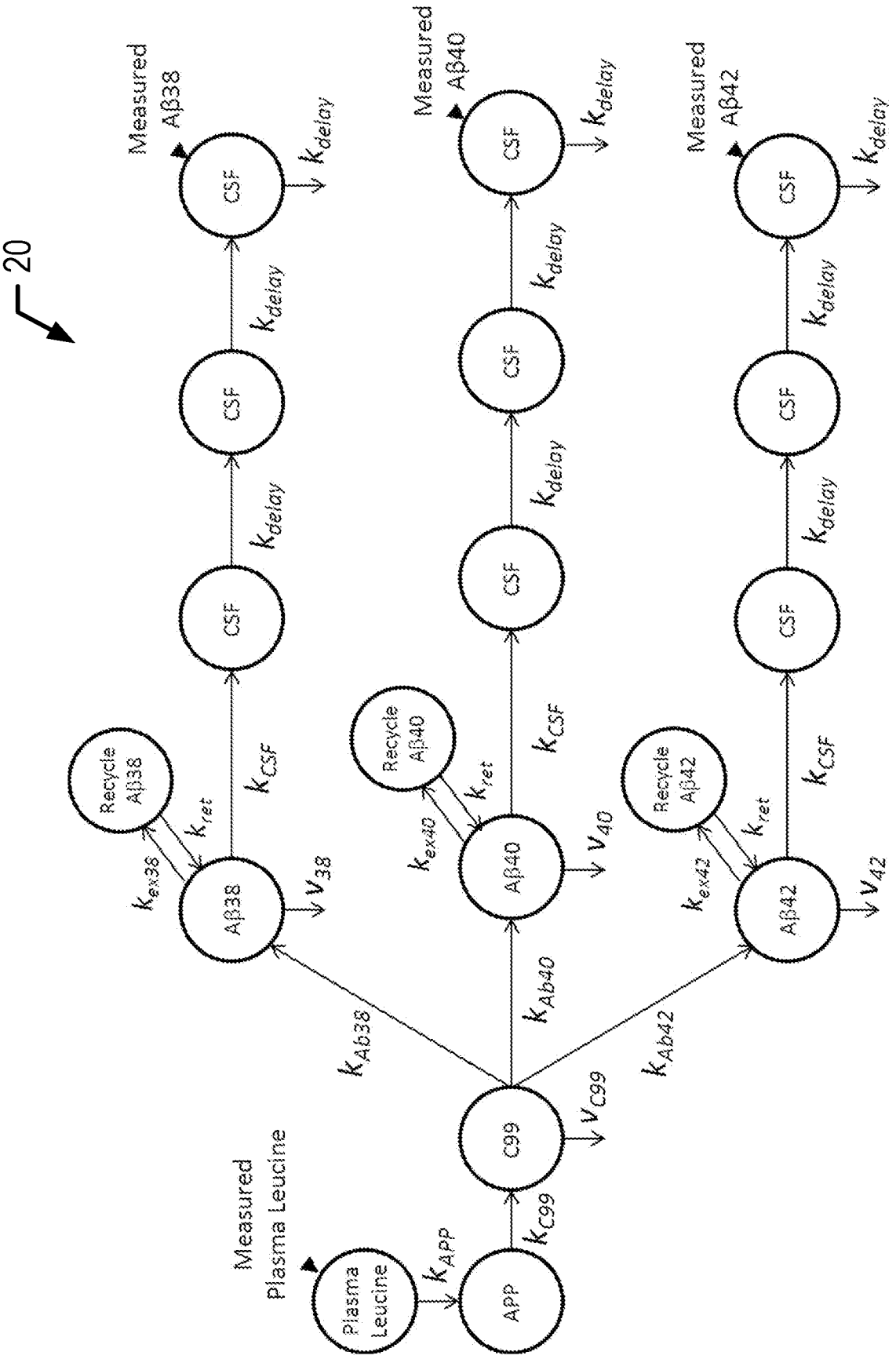
20
Measured Aβ38
Measured Aβ40
Measured Aβ42
Measured Plasma Leucine
Plasma Leucine
APP
C99
Aβ38
Aβ40
Aβ42
Recycle Aβ38
Recycle Aβ40
Recycle Aβ42
CSF
k_{APP}
k_{C99}
k_{Ab38}
k_{Ab40}
k_{Ab42}
k_{CSF}
k_{ret}
k_{ex38}
k_{ex40}
k_{ex42}
k_{delay}
v_{38}
v_{40}
v_{42}
v_{C99}

FIG. 4

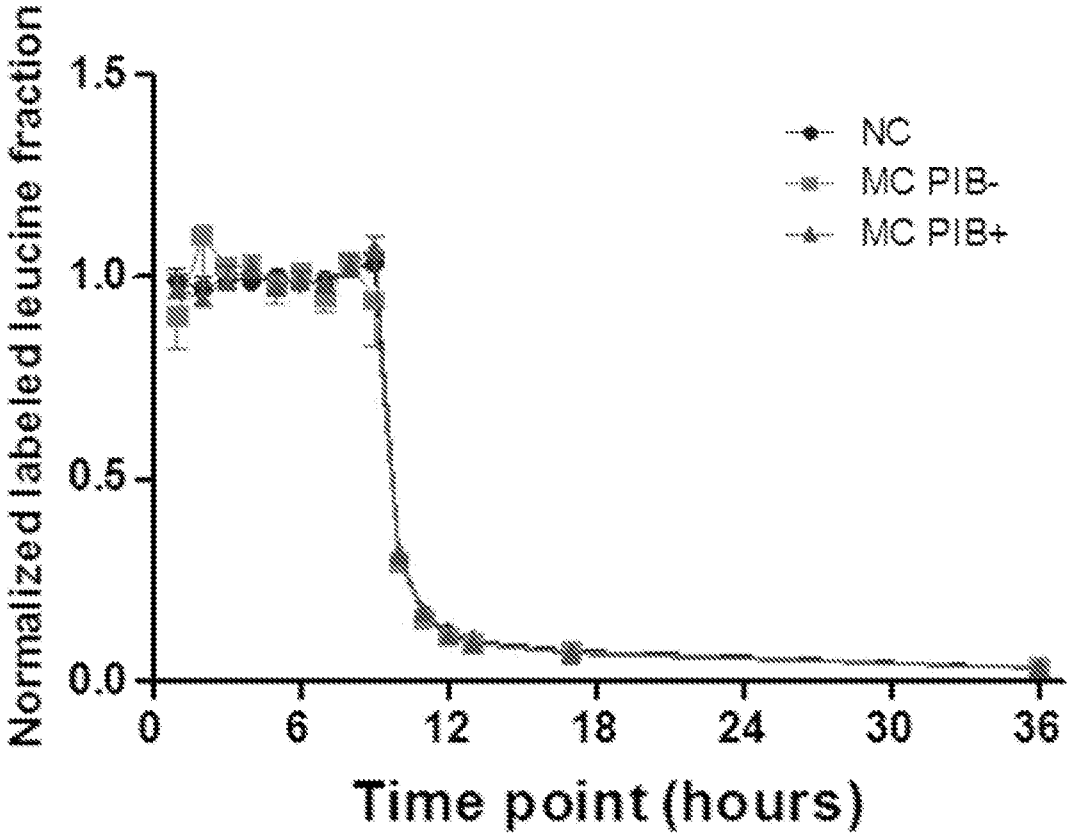
Normalized labeled leucine fraction
1.5
1.0
0.5
0.0
0
6
12
18
24
30
36
Time point (hours)
NC
MC PIB-
MC PIB+

FIG. 5

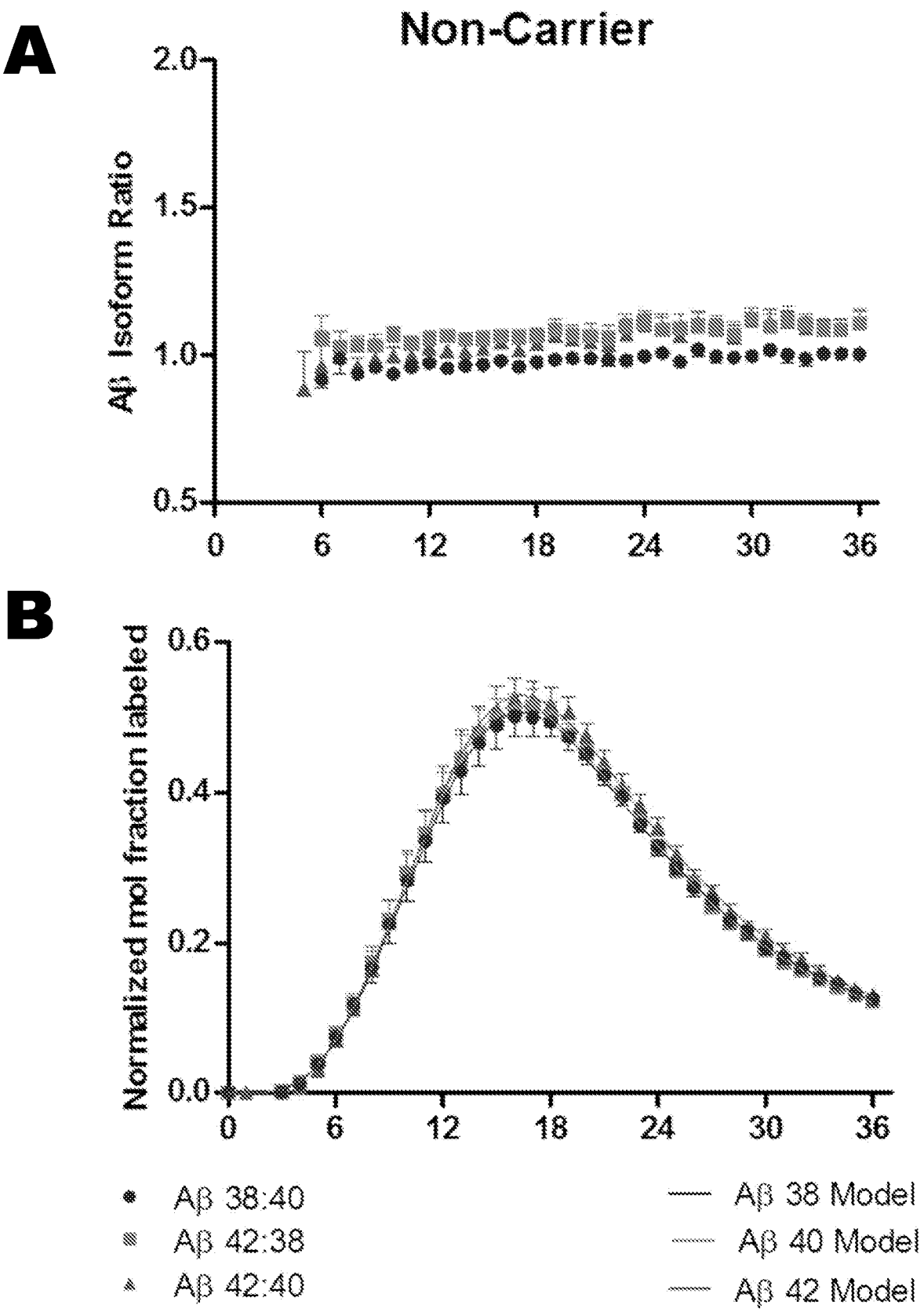
A
Non-Carrier
Aβ Isoform Ratio
2.0
1.5
1.0
0.5
0
6
12
18
24
30
36
B
Normalized mol fraction labeled
0.6
0.4
0.2
0.0
0
6
12
18
24
30
36
Aβ 38:40
Aβ 42:38
Aβ 42:40
Aβ 38 Model
Aβ 40 Model
Aβ 42 Model

FIG. 6

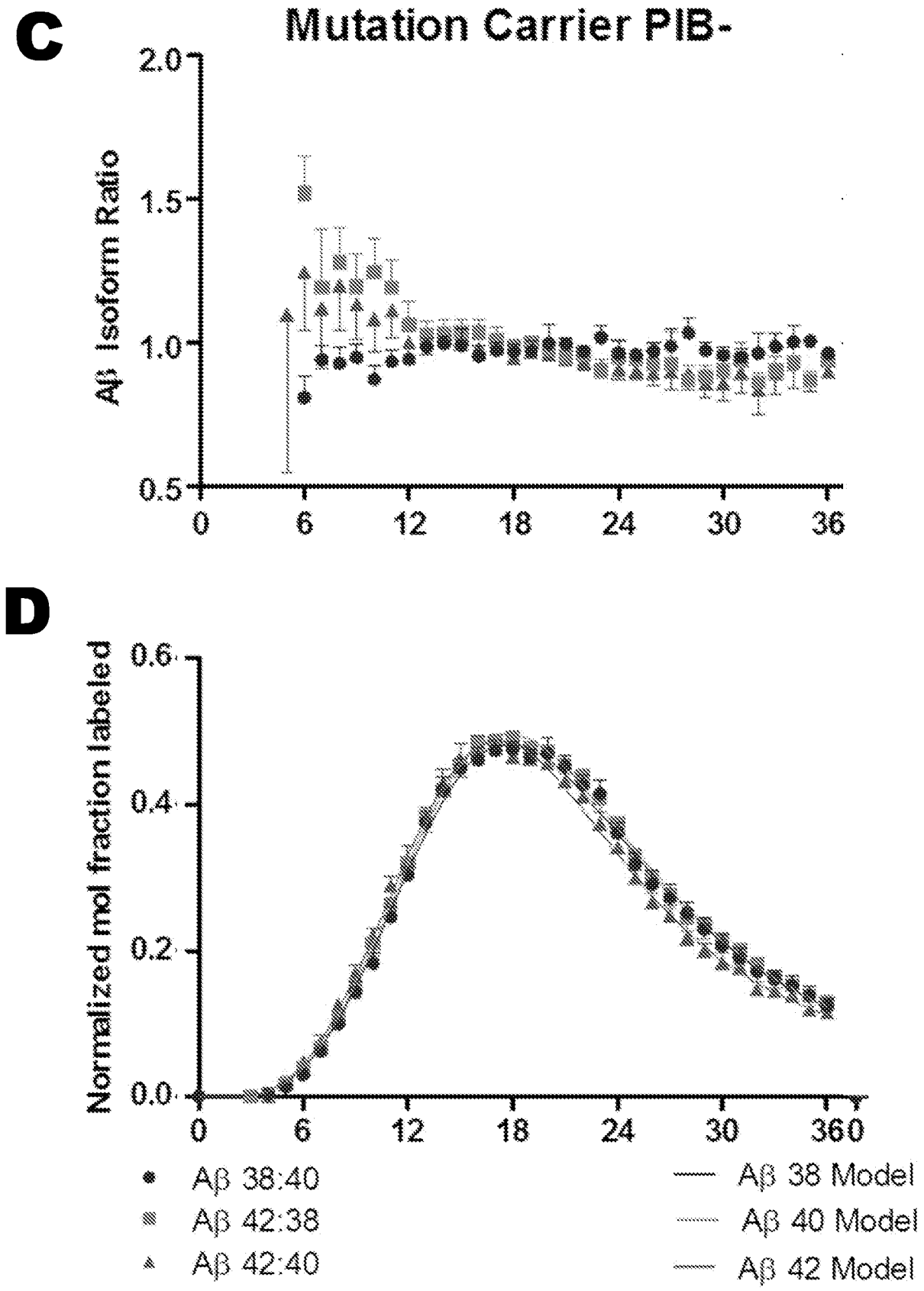
C
Mutation Carrier PIB-
Aβ Isoform Ratio
2.0
1.5
1.0
0.5
0
6
12
18
24
30
36
D
Normalized mol fraction labeled
0.6
0.4
0.2
0.0
0
6
12
18
24
30
360
Aβ 38:40
Aβ 42:38
Aβ 42:40
Aβ 38 Model
Aβ 40 Model
Aβ 42 Model

FIG. 6

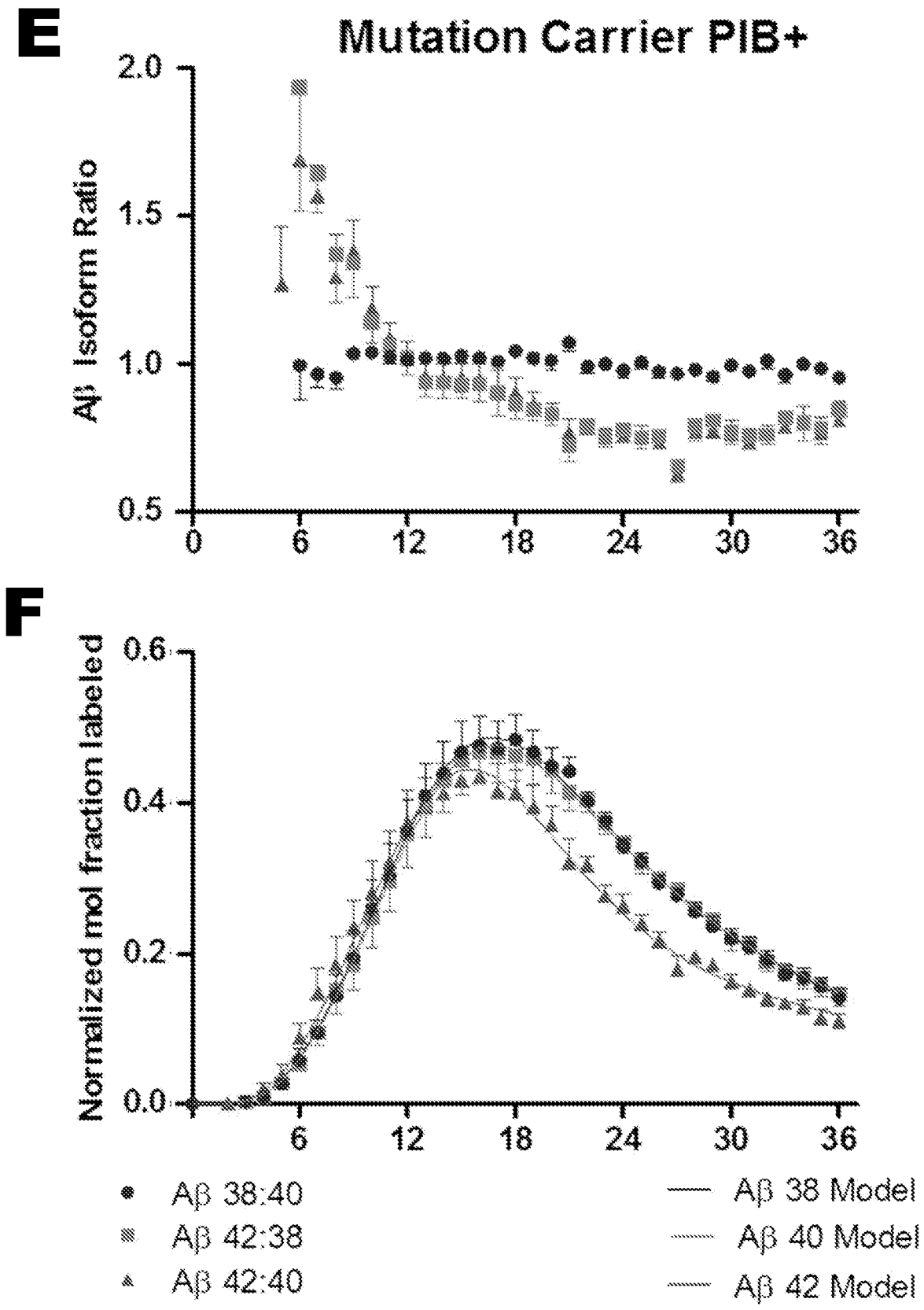
E
Mutation Carrier PIB+
Aβ Isoform Ratio
2.0
1.5
1.0
0.5
0
6
12
18
24
30
36
F
Normalized mol fraction labeled
0.6
0.4
0.2
0.0
6
12
18
24
30
36
Aβ 38:40
Aβ 42:38
Aβ 42:40
Aβ 38 Model
Aβ 40 Model
Aβ 42 Model

FIG. 6

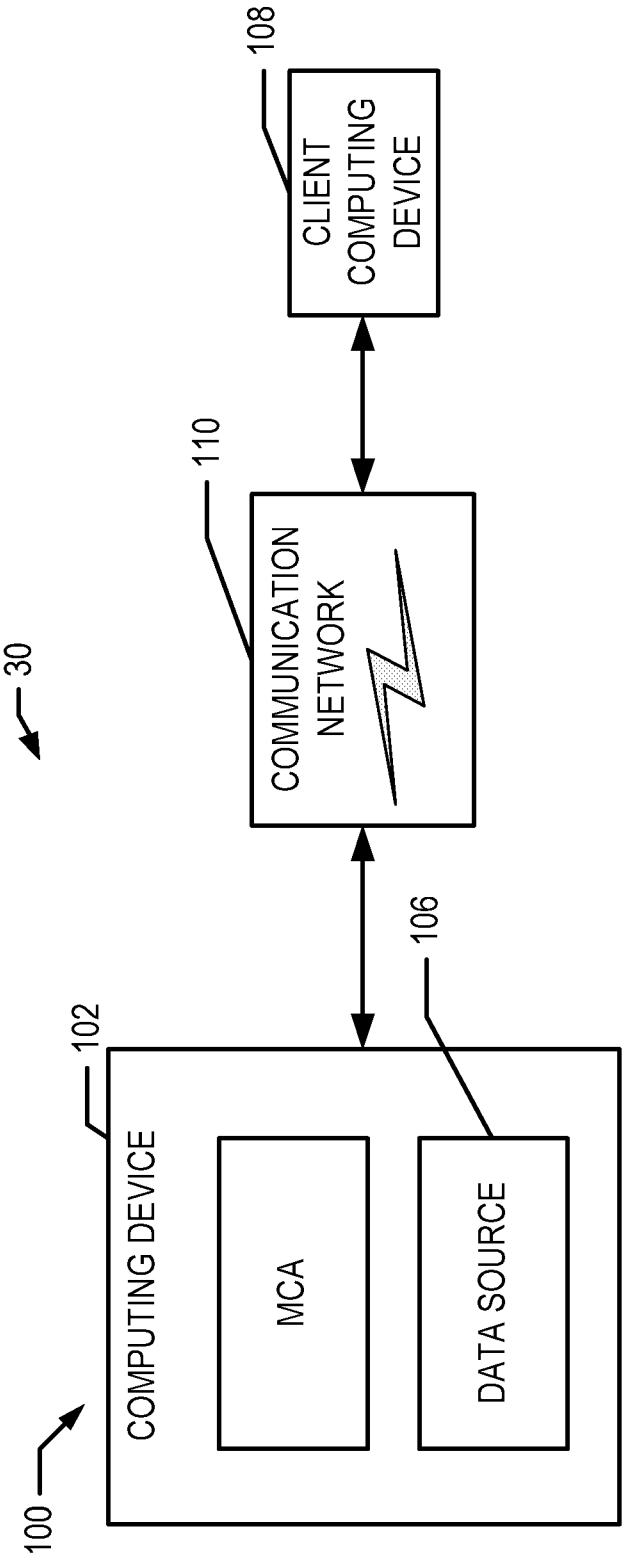
108
CLIENT COMPUTING DEVICE
110
COMMUNICATION NETWORK
30
106
102
COMPUTING DEVICE
MCA
DATA SOURCE
100

FIG. 7

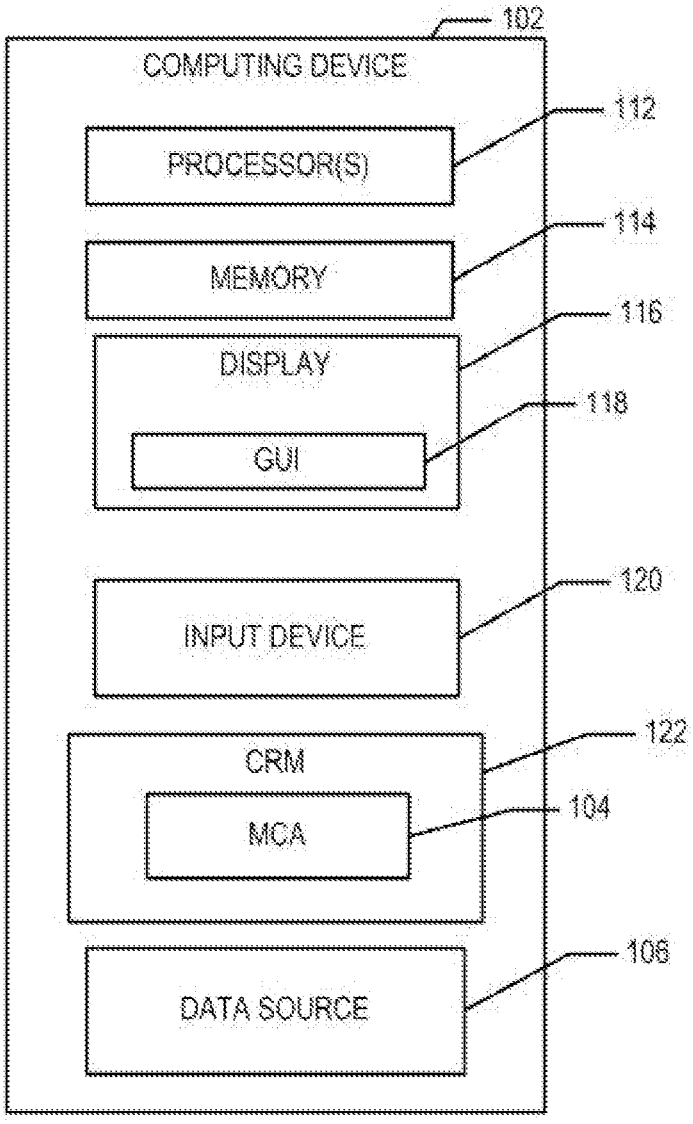
102
COMPUTING DEVICE
112
PROCESSOR(S)
114
MEMORY
116
DISPLAY
118
GUI
120
INPUT DEVICE
122
CRM
104
MCA
106
DATA SOURCE

FIG. 8

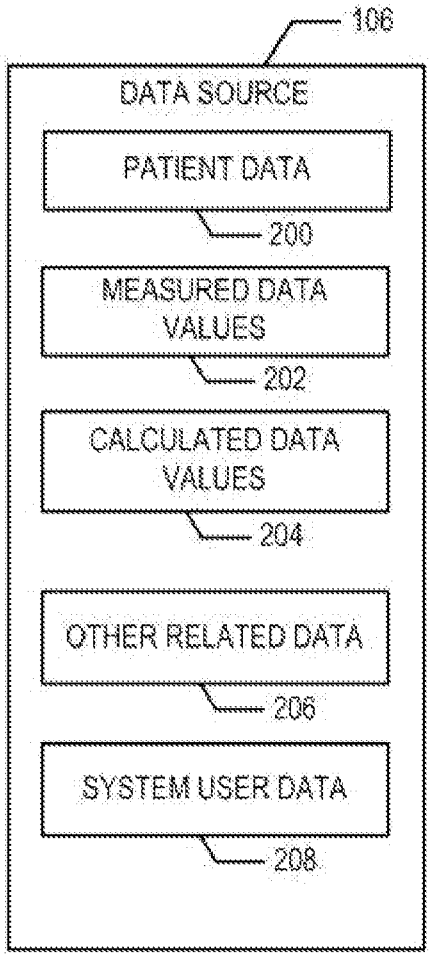
106
DATA SOURCE
PATIENT DATA
200
MEASURED DATA VALUES
202
CALCULATED DATA VALUES
204
OTHER RELATED DATA
206
SYSTEM USER DATA
208

FIG. 9

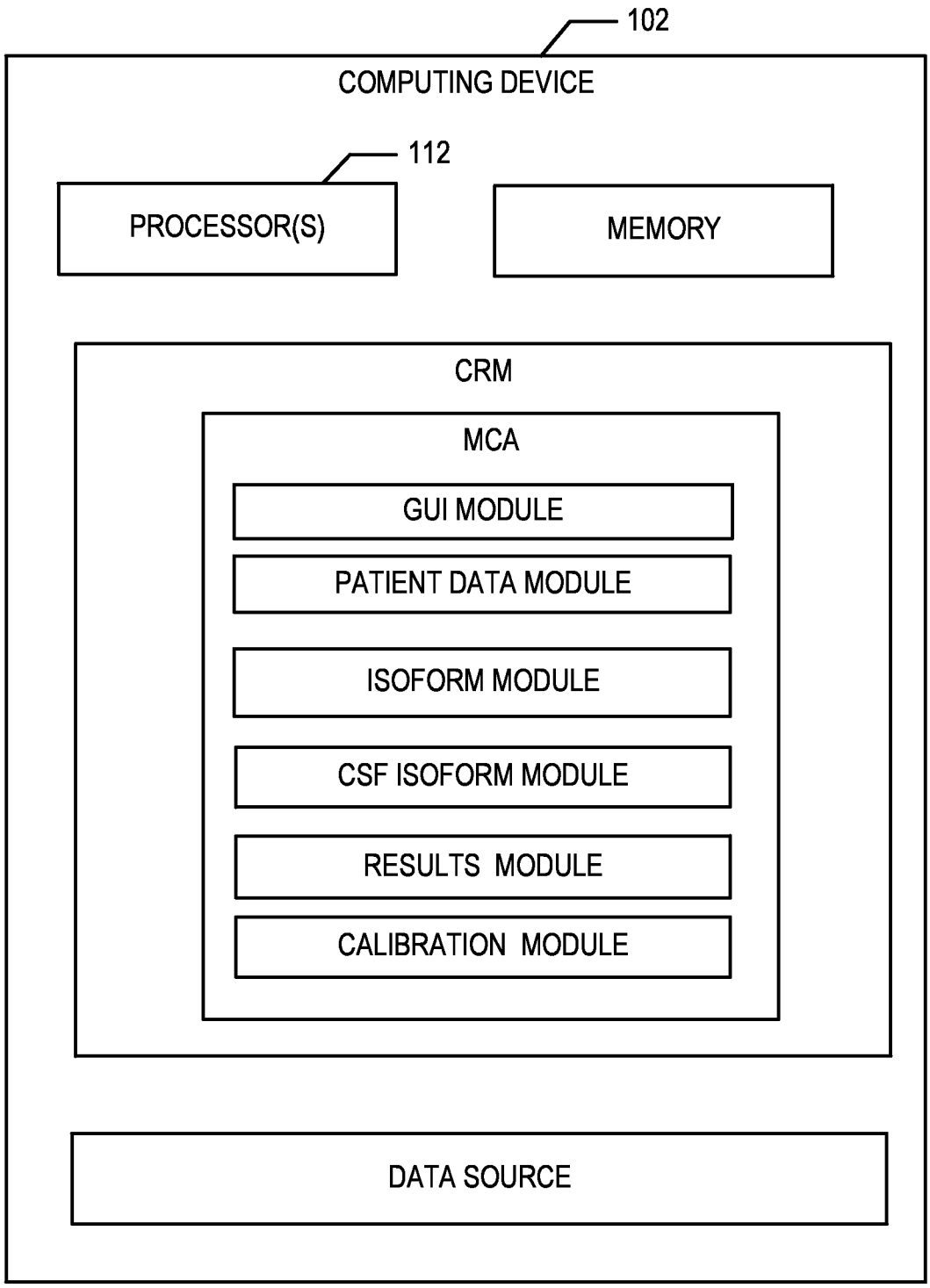
102
COMPUTING DEVICE
112
PROCESSOR(S)
MEMORY
CRM
MCA
GUI MODULE
PATIENT DATA MODULE
ISOFORM MODULE
CSF ISOFORM MODULE
RESULTS MODULE
CALIBRATION MODULE
DATA SOURCE

FIG. 10

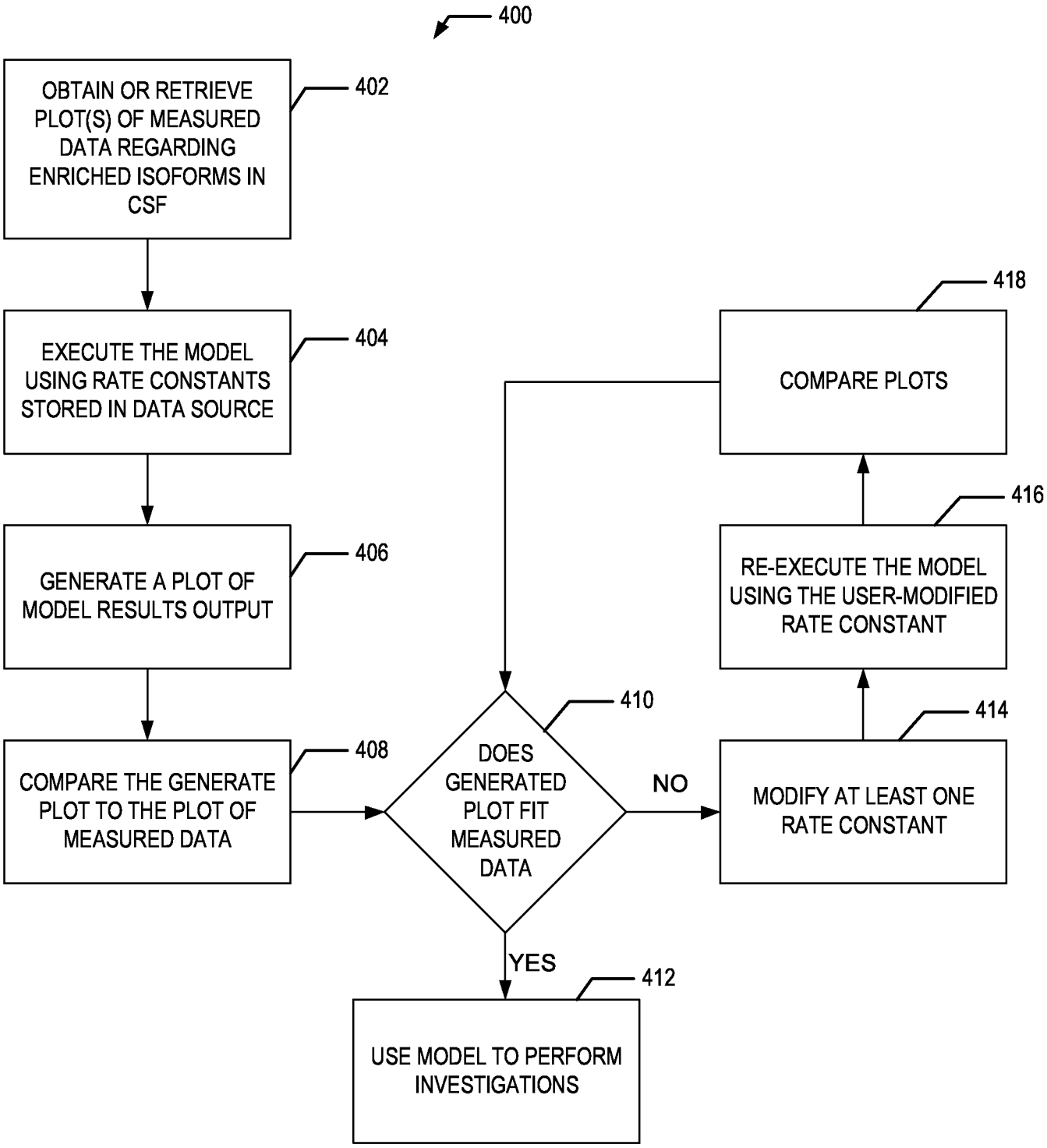
400
OBTAIN OR RETRIEVE PLOT(S) OF MEASURED DATA REGARDING ENRICHED ISOFORMS IN CSF
402
EXECUTE THE MODEL USING RATE CONSTANTS STORED IN DATA SOURCE
404
GENERATE A PLOT OF MODEL RESULTS OUTPUT
406
COMPARE THE GENERATE PLOT TO THE PLOT OF MEASURED DATA
408
DOES GENERATED PLOT FIT MEASURED DATA
410
NO
YES
MODIFY AT LEAST ONE RATE CONSTANT
414
RE-EXECUTE THE MODEL USING THE USER-MODIFIED RATE CONSTANT
416
COMPARE PLOTS
418
USE MODEL TO PERFORM INVESTIGATIONS
412

FIG. 11

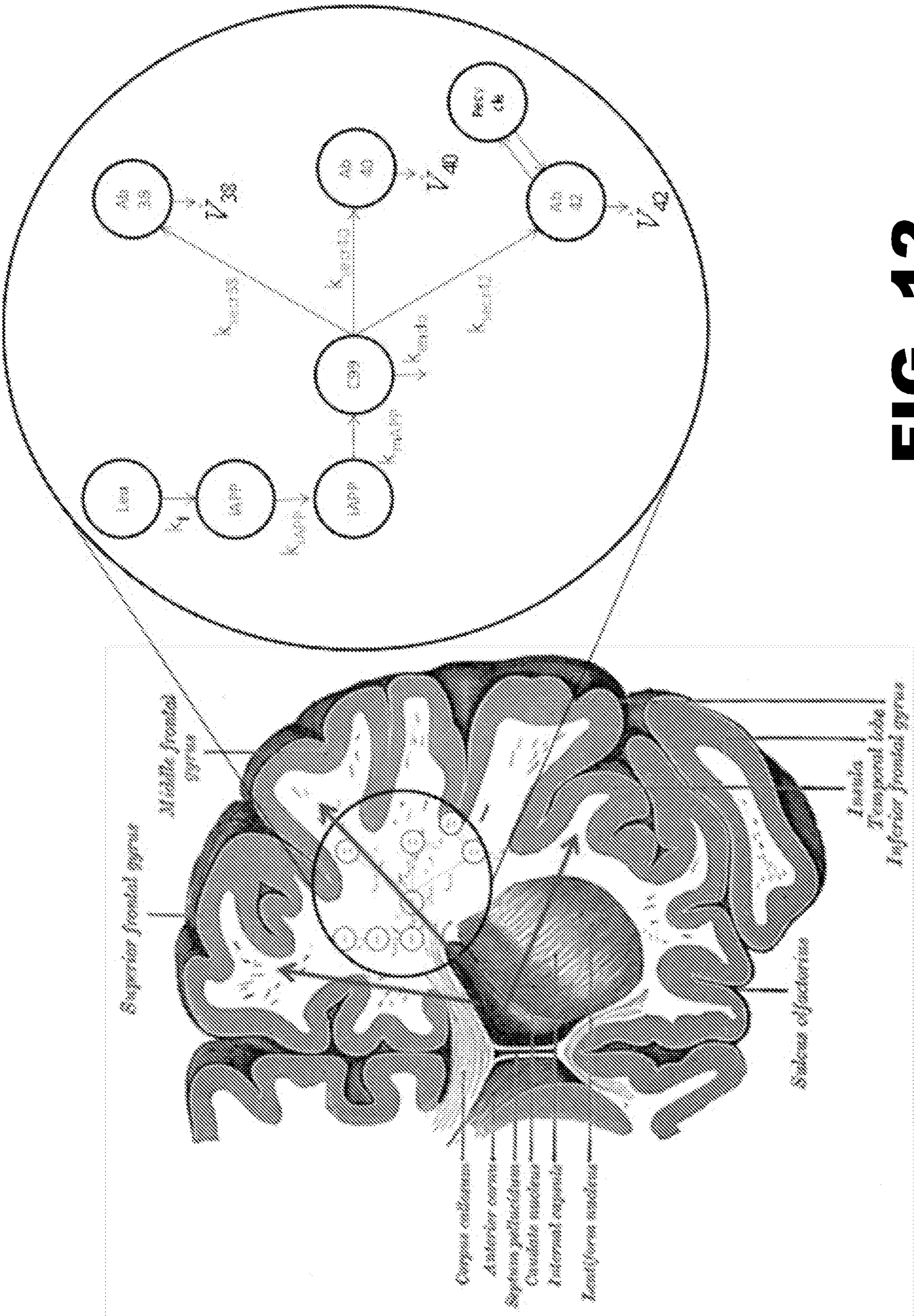
Superior frontal gyrus
Middle frontal gyrus
Insula
Temporal lobe
Inferior frontal gyrus
Sulcus olfactorius
Corpus callosum
Anterior cornu
Septum pellucidum
Caudate nucleus
Internal capsule
Lentiform nucleus

FIG. 12

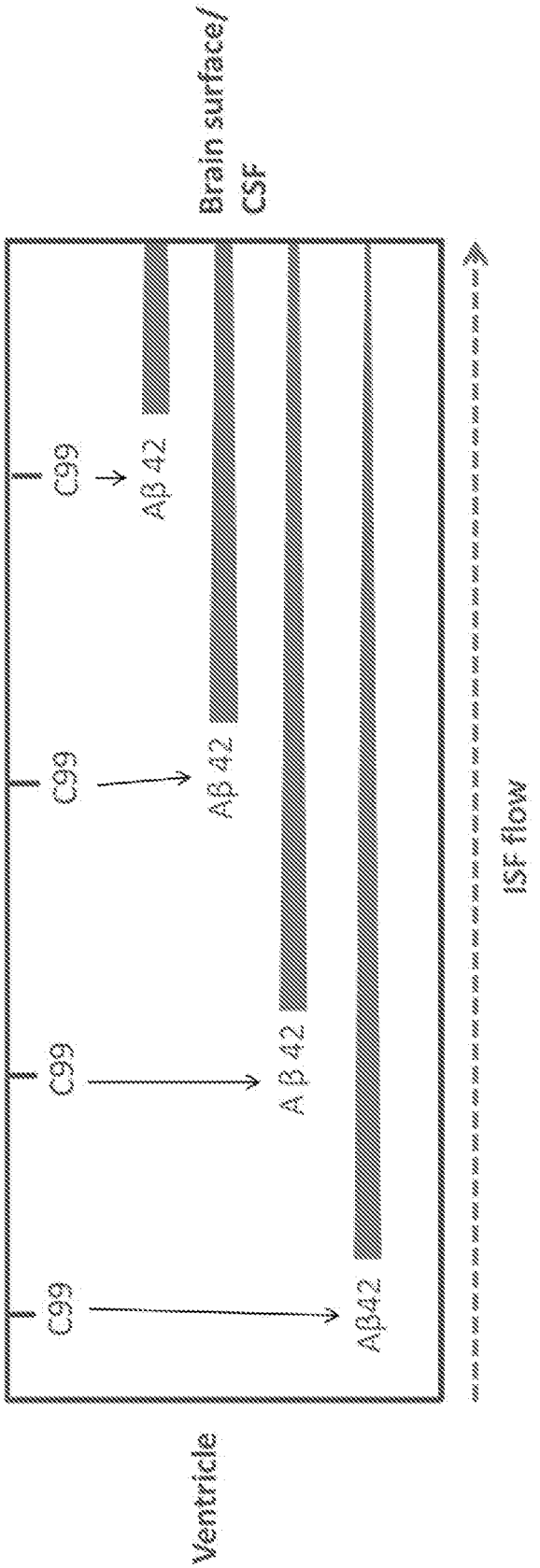
Brain surface/
CSF
C99
Aβ 42
C99
Aβ 42
C99
Aβ 42
C99
Aβ42
ISF flow
Ventricle

FIG. 13

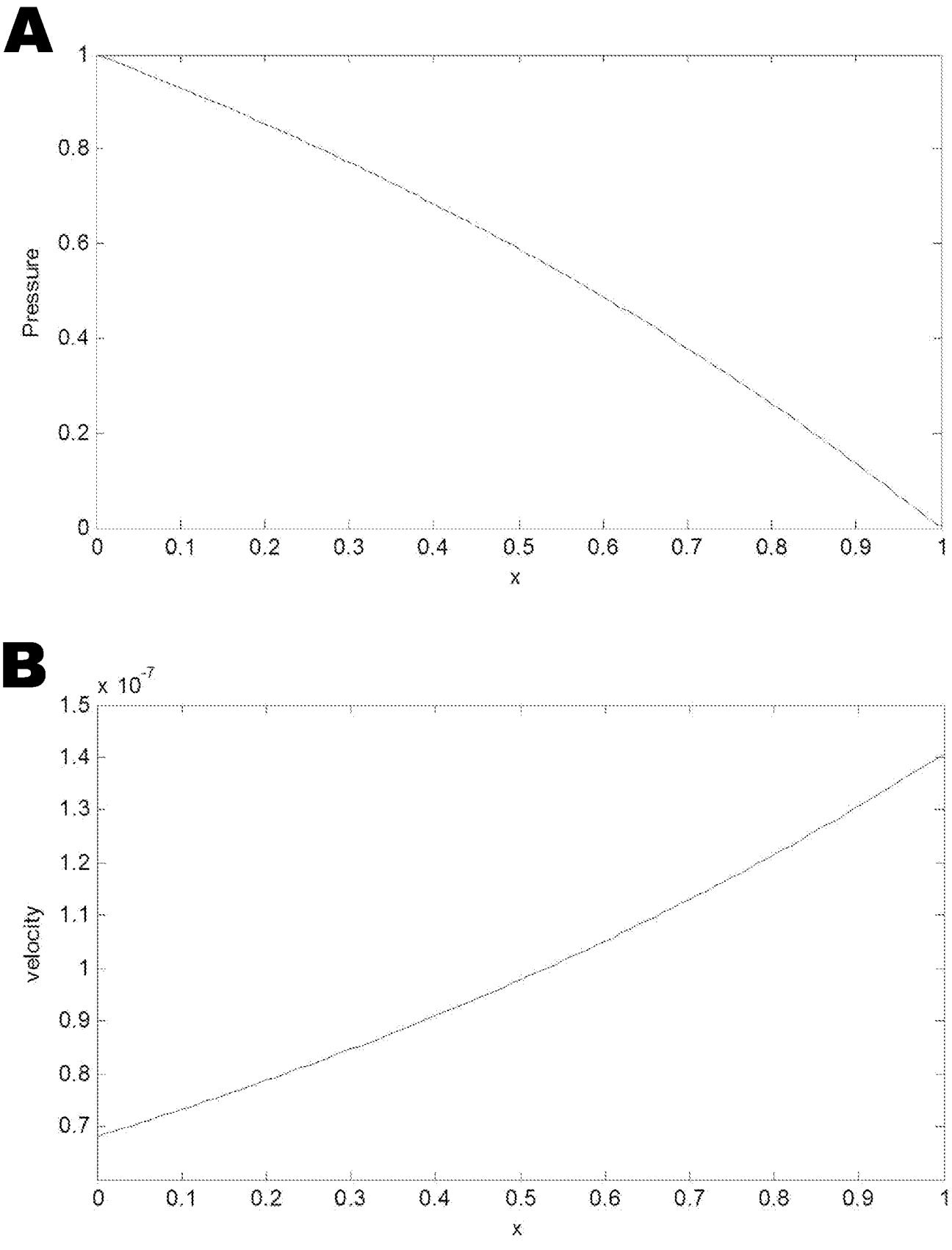

FIG. 14

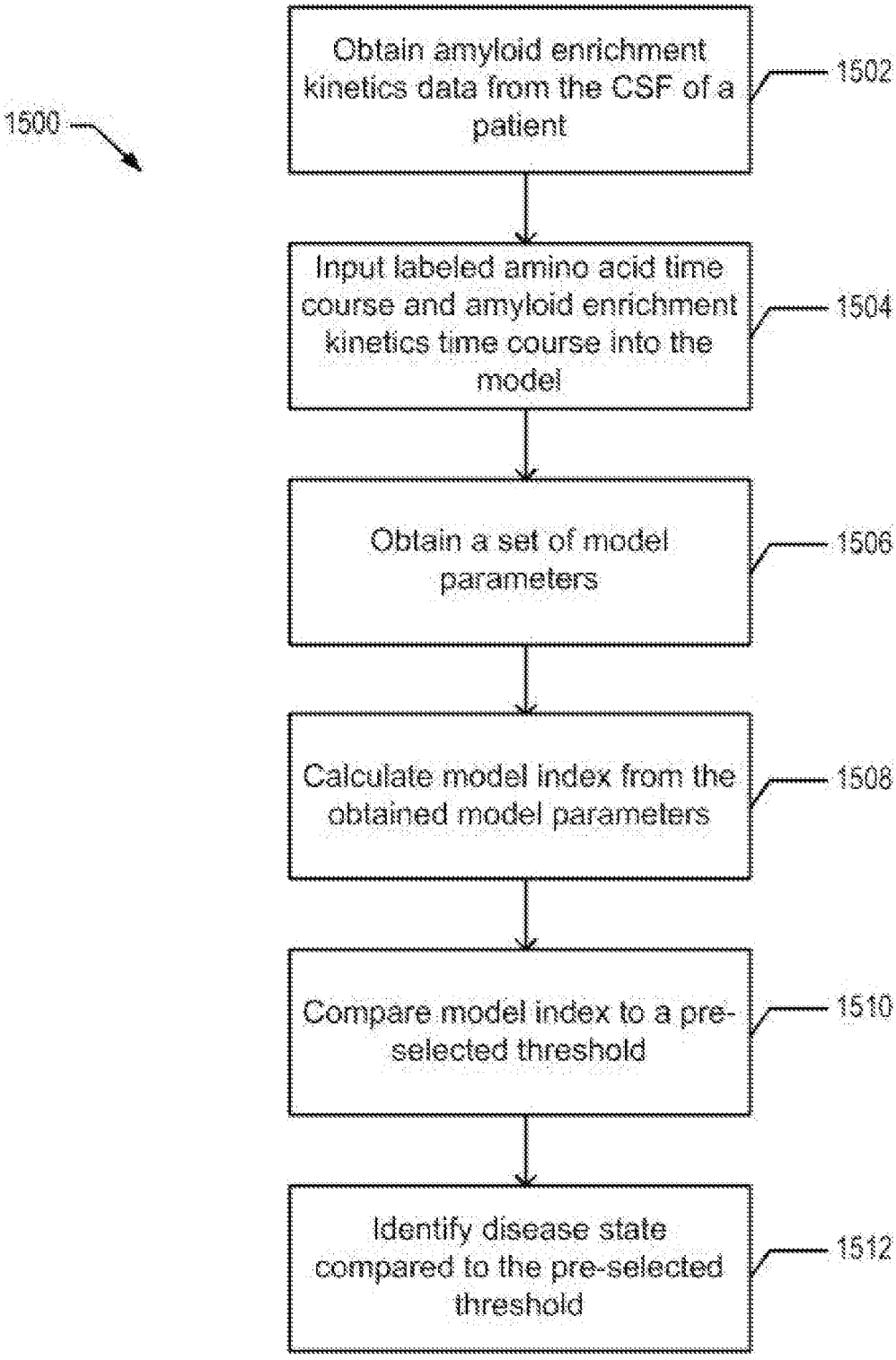
1500
Obtain amyloid enrichment kinetics data from the CSF of a patient
1502
Input labeled amino acid time course and amyloid enrichment kinetics time course into the model
1504
Obtain a set of model parameters
1506
Calculate model index from the obtained model parameters
1508
Compare model index to a pre-selected threshold
1510
Identify disease state compared to the pre-selected threshold
1512

FIG. 15

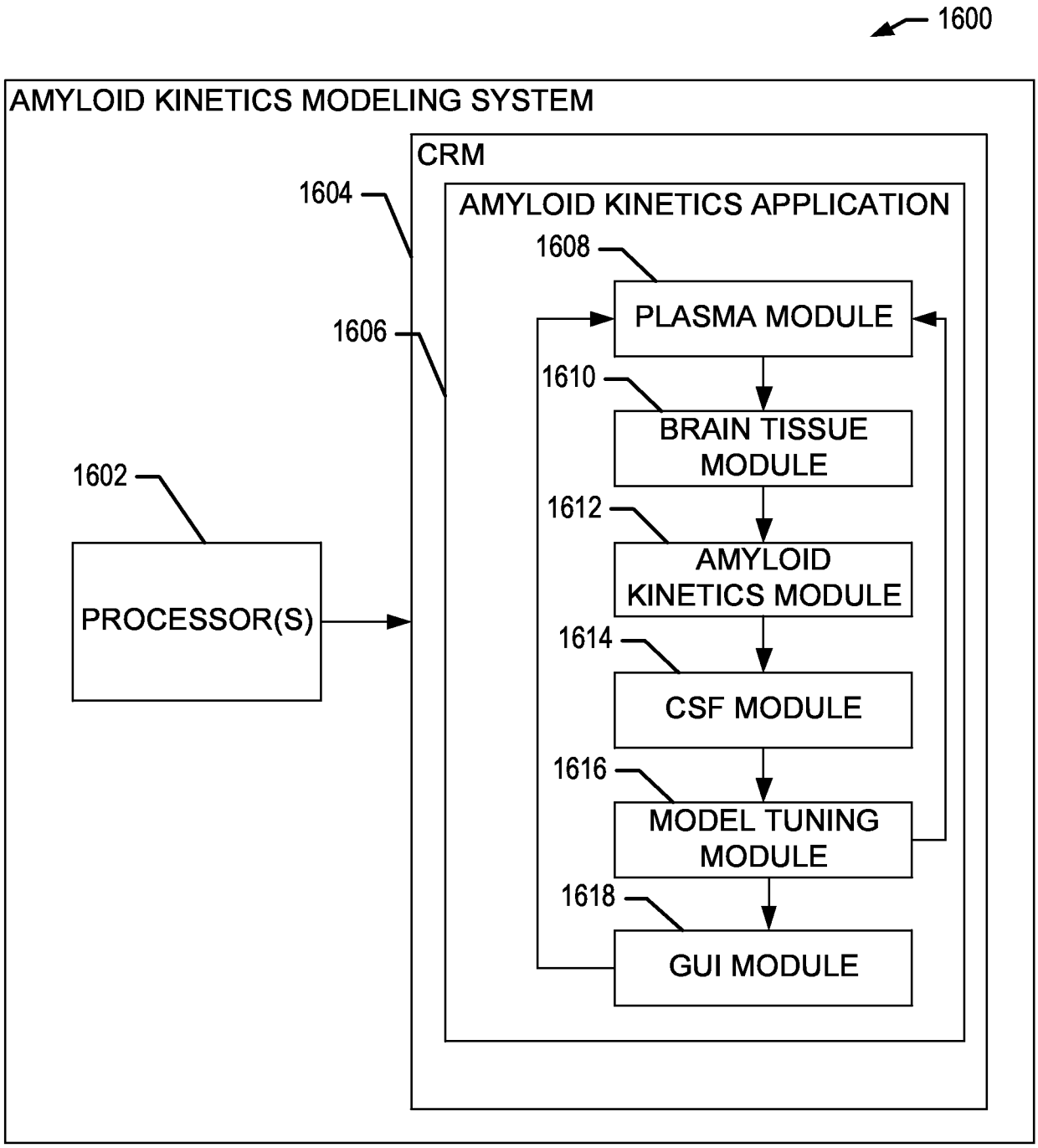
1600
AMYLOID KINETICS MODELING SYSTEM
CRM
1604
AMYLOID KINETICS APPLICATION
1608
PLASMA MODULE
1606
1610
BRAIN TISSUE MODULE
1602
1612
AMYLOID KINETICS MODULE
PROCESSOR(S)
1614
CSF MODULE
1616
MODEL TUNING MODULE
1618
GUI MODULE

FIG. 16

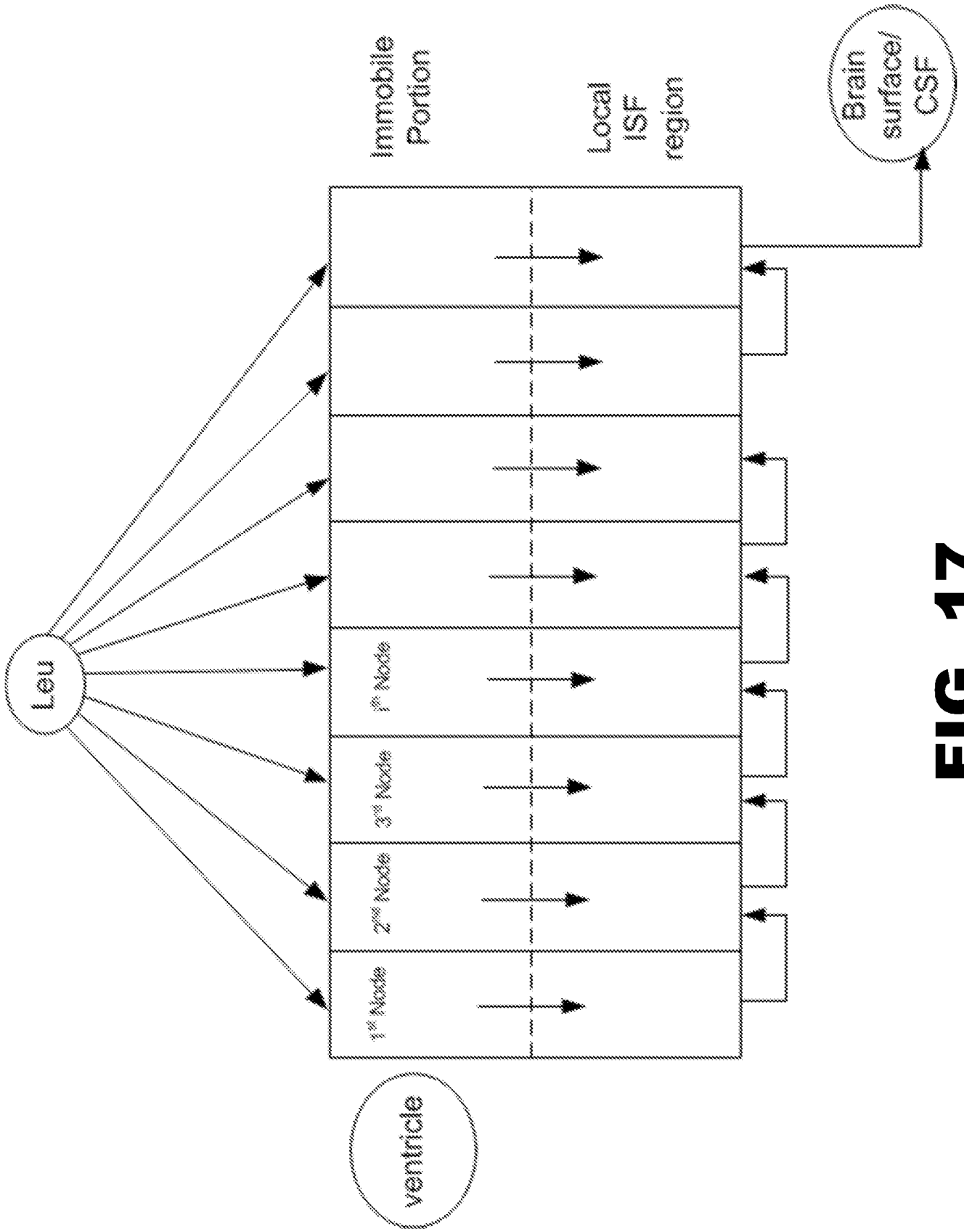
Leu
1st Node
2nd Node
3rd Node
nth Node
Immobile Portion
Local ISF region
Brain surface/ CSF
ventricle

FIG. 17

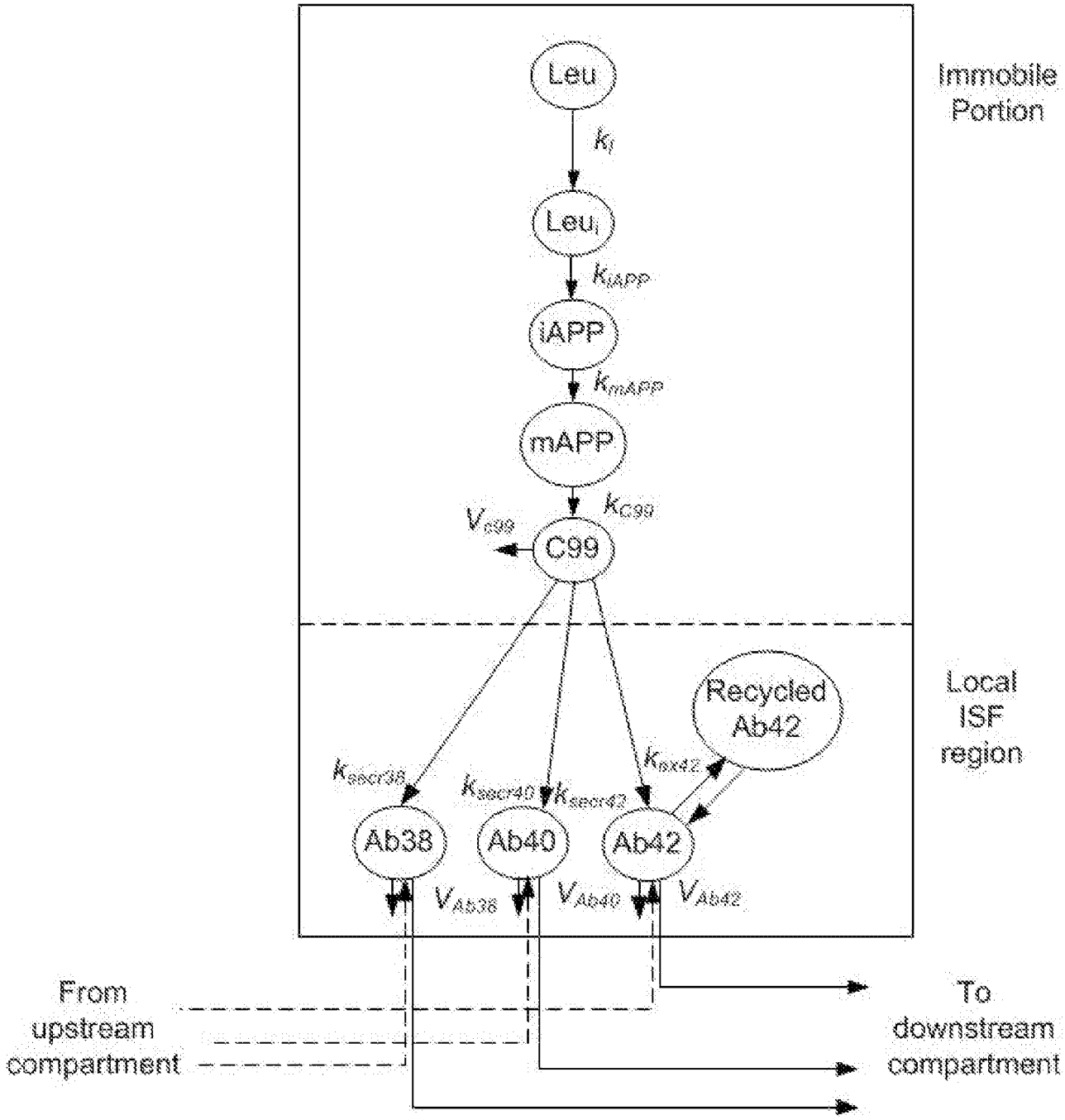
Leu
k_l
Leu$_l$
k_{iAPP}
iAPP
k_{mAPP}
mAPP
k_{C99}
V_{c99}
C99
Immobile Portion
Local ISF region
Recycled Ab42
k_{secr38}
k_{secr40}
k_{secr42}
k_{ex42}
Ab38
Ab40
Ab42
V_{Ab38}
V_{Ab40}
V_{Ab42}
From upstream compartment
To downstream compartment

FIG. 18

A

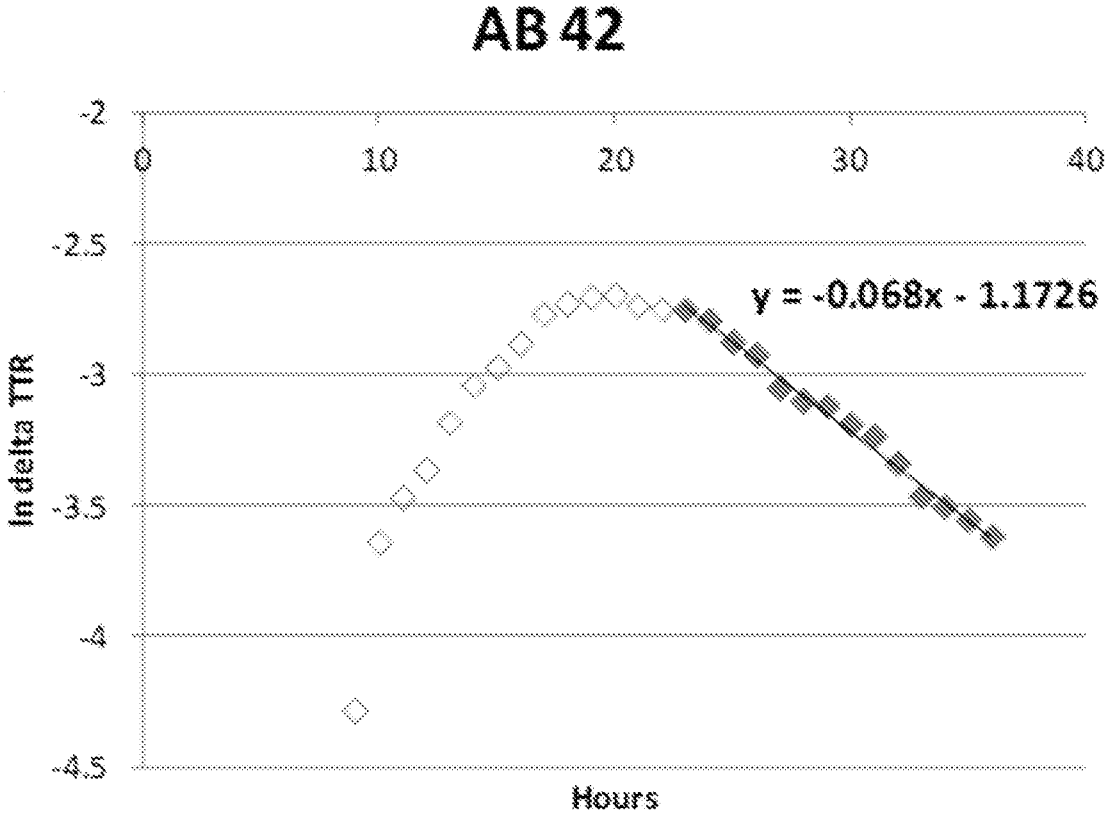
AB 42
-2
0
10
20
30
40
-2.5
-3
-3.5
-4
-4.5
y = -0.068x - 1.1726
ln delta TTR
Hours

B

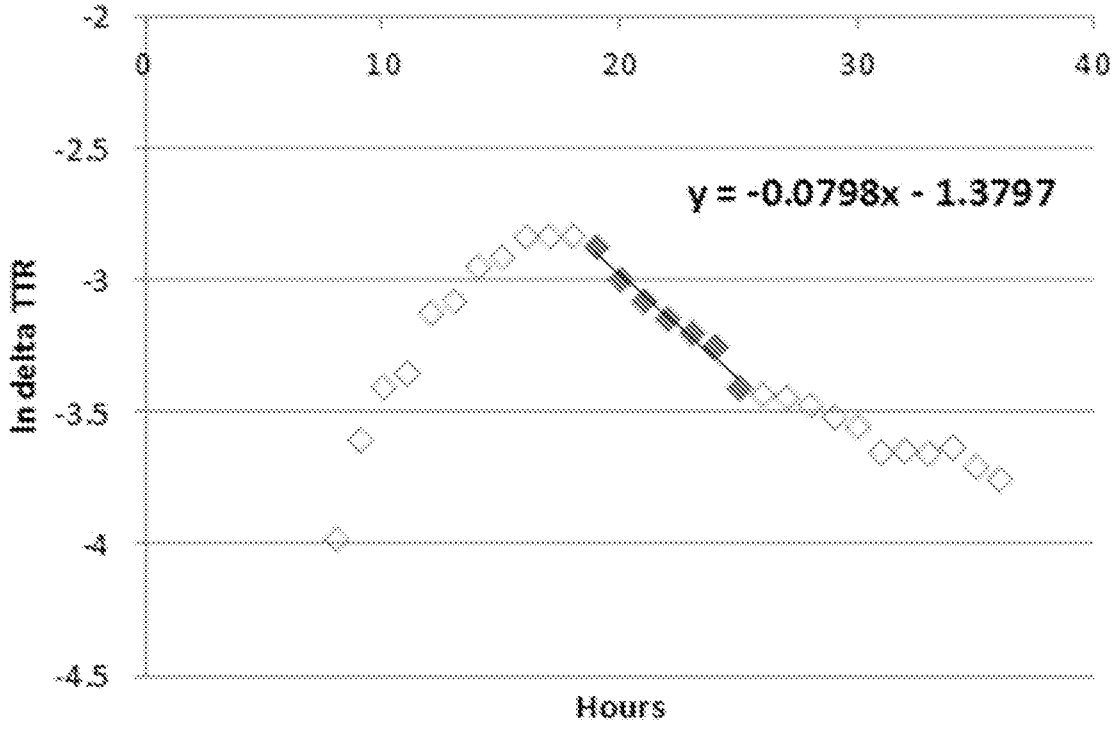
-2
0
10
20
30
40
-2.5
-3
-3.5
-4
-4.5
y = -0.0798x - 1.3797
ln delta TTR
Hours

FIG. 19

A

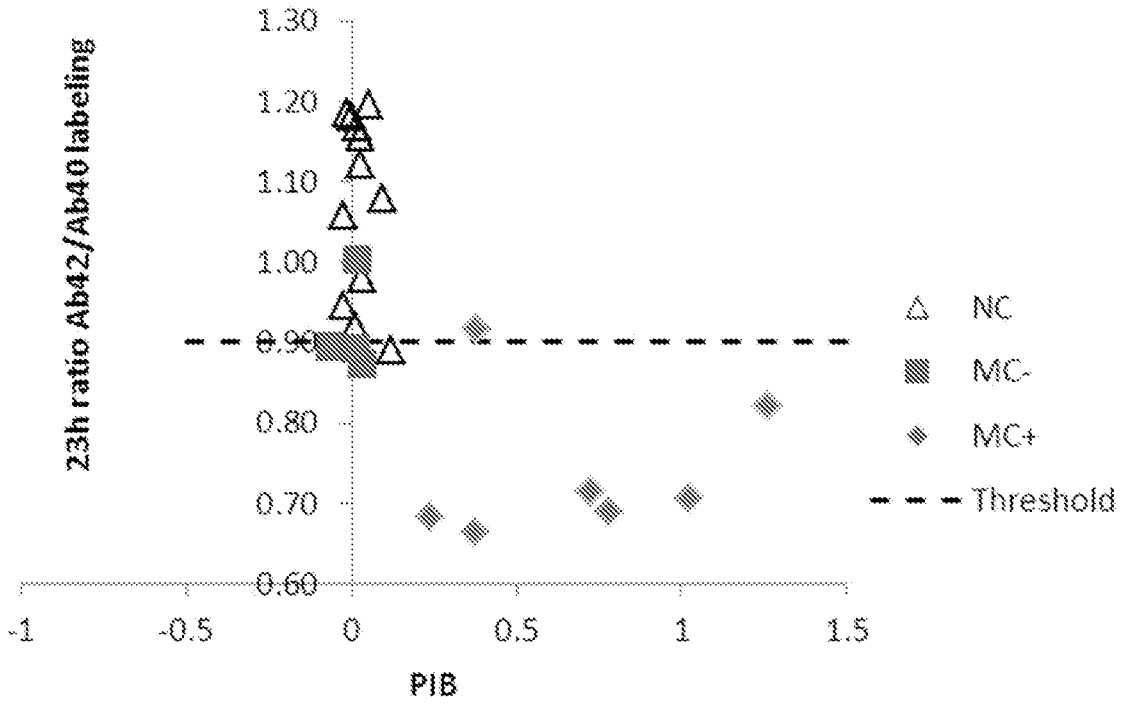
1.30
1.20
1.10
1.00
0.90
0.80
0.70
0.60
23h ratio Ab42/Ab40 labeling
-1
-0.5
0
0.5
1
1.5
PIB
NC
MC-
MC+
Threshold

B

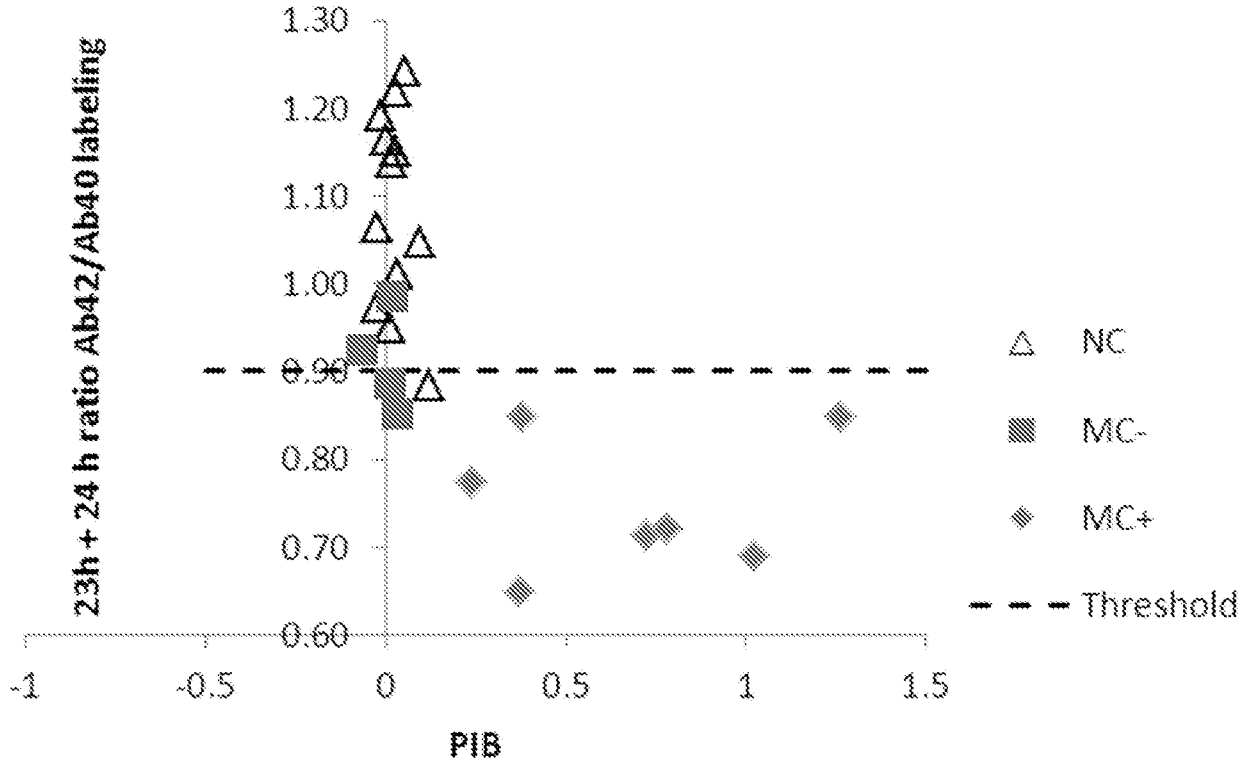
1.30
1.20
1.10
1.00
0.90
0.80
0.70
0.60
23h + 24 h ratio Ab42/Ab40 labeling
-1
-0.5
0
0.5
1
1.5
PIB
NC
MC-
MC+
Threshold

FIG. 20

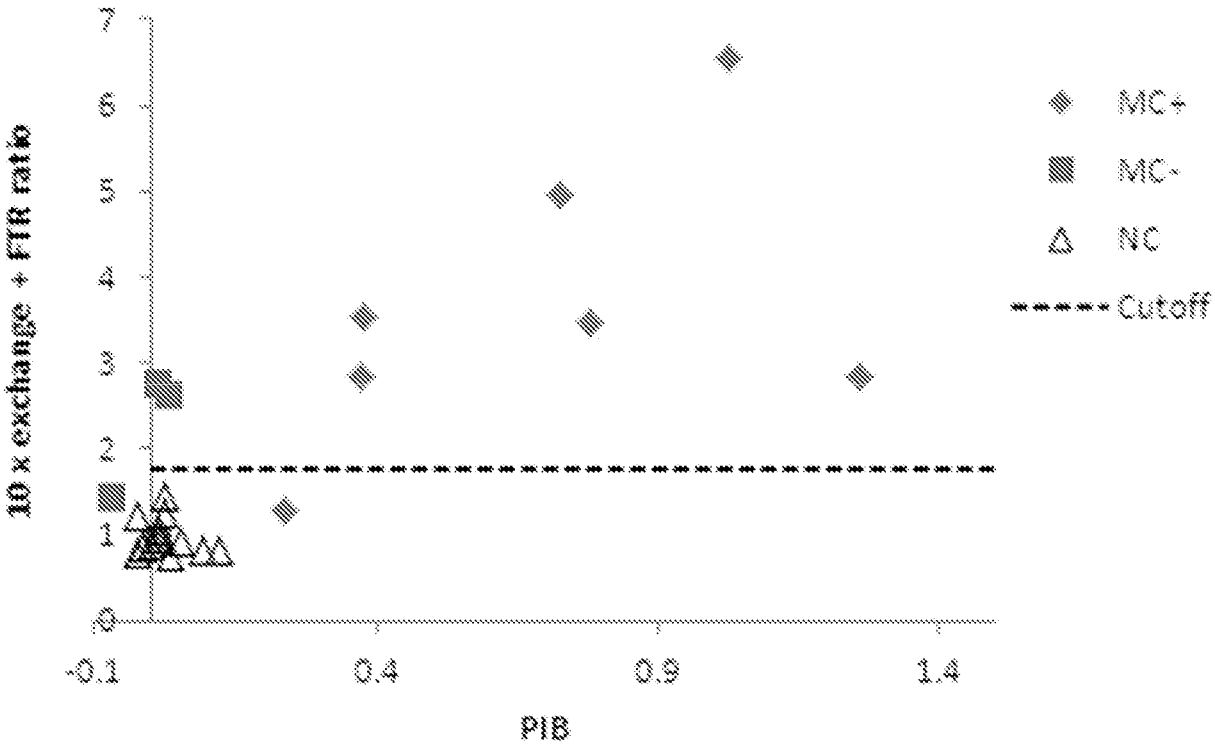
10 x exchange + FTR ratio
7
6
5
4
3
2
1
0
-0.1
0.4
0.9
1.4
PIB
MC+
MC-
NC
Cutoff

FIG. 20C

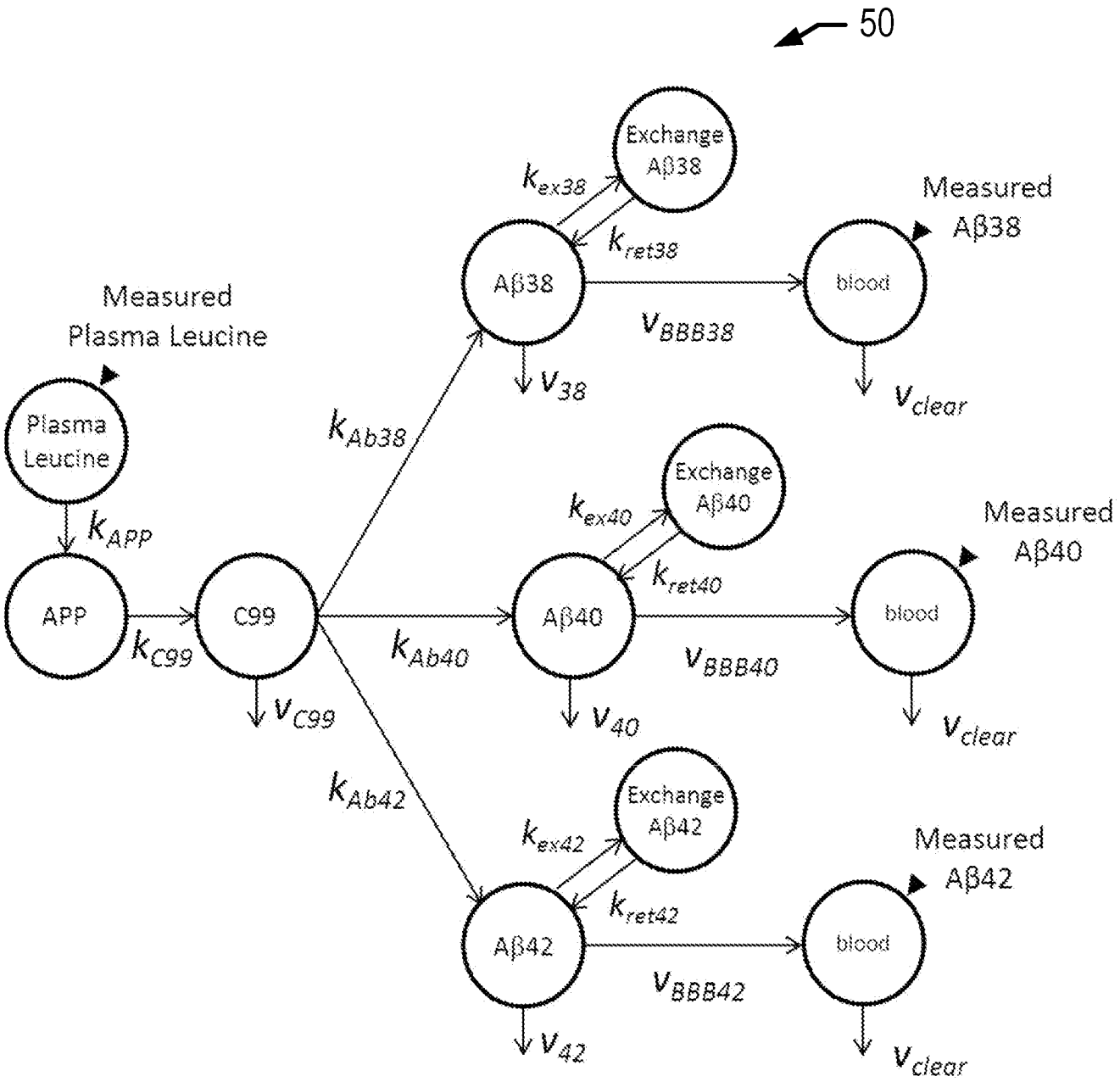
50
Exchange Aβ38
k_{ex38}
k_{ret38}
Aβ38
blood
Measured Aβ38
v_{BBB38}
v_{38}
v_{clear}
Measured Plasma Leucine
Plasma Leucine
k_{Ab38}
k_{APP}
Exchange Aβ40
k_{ex40}
k_{ret40}
Measured Aβ40
APP
C99
k_{C99}
k_{Ab40}
Aβ40
blood
v_{BBB40}
v_{C99}
v_{40}
v_{clear}
k_{Ab42}
Exchange Aβ42
k_{ex42}
k_{ret42}
Measured Aβ42
Aβ42
blood
v_{BBB42}
v_{42}
v_{clear}

FIG. 21

INTERNATIONAL SEARCH REPORT

International application No.
PCT/US2013/071042

A. CLASSIFICATION OF SUBJECT MATTER

G01N 33/68(2006.01)i, G01N 33/53(2006.01)i, G01N 33/48(2006.01)i

According to International Patent Classification (IPC) or to both national classification and IPC

B. FIELDS SEARCHED

Minimum documentation searched (classification system followed by classification symbols)
G01N 33/68; G01N 30/72; GOIN 33/566; C12Q 1/37; G01N 30/06; G01N 33/53; GOIN 33/48

Documentation searched other than minimum documentation to the extent that such documents are included in the fields searched
Korean utility models and applications for utility models
Japanese utility models and applications for utility models

Electronic data base consulted during the international search (name of data base and, where practicable, search terms used)
eKOMPASS(KIPO internal) & Keywords: amyloid beta, enrichment kinetics, calibration, APP, C99, plasma, BBB, CSF, compartmental model

C. DOCUMENTS CONSIDERED TO BE RELEVANT

Category *	Citation of document, with indication, where appropriate, of the relevant passages	Relevant to claim No.
A	US 2011-0294138 Al (BATEMAN et al.) 01 December 2011 See abst ract ; paragraphs [0021H0055] , [0079H0089] and claims 1-4 , 9-10 , 12-14 .	18-32 ,43-59
A	wo 2010-065878 Al (C2N DIAGNOSTICS) 10 June 2010 See the whole document .	18-32 ,43-59
A	MAWUENYEGA et al., `Decreased clearance of CNS β-amyloid in Alzheimer`s disease " Science , Vol.330 , No.6012, p.1774 (2010) See the whole document .	18-32 ,43-59
A	BATEMAN et al., "Human amyloid-β synthes is and clearance rates as measure d in cerebrosp inal fluid in vivo " Nature Medicine , Vol.12 , No.7, pp.856-861 (2006) See the whole document .	18-32 ,43-59
A	BATEMAN et al., "A γ-secret ase inhibitor decreases amyloid-β product ion in the cent ral nervous syst em" Annals of Neuro logy, Vol.66 , No.l , pp.48-54 (2009) See the whole document .	18-32 ,43-59

☒ Further documents are listed in the continuation of Box C. ☒ See patent family annex.

* Special categories of cited documents:
"A" document defining the general state of the art which is not considered to be of particular relevance
"E" earlier application or patent but published on or after the international filing date
"L" document which may throw doubts on priority claim(s) or which is cited to establish the publication date of another citation or other special reason (as specified)
"O" document referring to an oral disclosure, use, exhibition or other means
"P" document published prior to the international filing date but later than the priority date claimed
"T" later document published after the international filing date or priority date and not in conflict with the application but cited to understand the principle or theory underlying the invention
"X" document of particular relevance; the claimed invention cannot be considered novel or cannot be considered to involve an inventive step when the document is taken alone
"Y" document of particular relevance; the claimed invention cannot be considered to involve an inventive step when the document is combined with one or more other such documents, such combination being obvious to a person skilled in the art
"&" document member of the same patent family

Date of the actual completion of the international search	Date of mailing of the international search report
10 February 2014 (10.02.2014)	**11 February 2014 (11.02.2014)**

Name and mailing address of the ISA/KR
Korean Intellectual Property Office
189 Cheongsa-ro, Seo-gu, Daej eon Metropolitan City, 302-701, Republic of Korea
Facsimile No. +82-42-472-7140

Authorized officer
KΓM, Seung Beom
Telephone No. +82-42 -481-3371

INTERNATIONAL SEARCH REPORT

International application No.
PCT/US2013/071042

C (Continuation). DOCUMENTS CONSIDERED TO BE RELEVANT

Category*	Citation of document, with indication, where appropriate, of the relevant passages	Relevant to claim No.
PX	POTTER et al., `Increased in vivo amyloid-£42 production, exchange, and irreversible loss in presenilin mutations carriers` Science Translational Medicine, Vol.5, Issue 189, Article No.l89ra77 (internal pages 1-10) (12 June 2013) See the whole document.	18-32,43-59

INTERNATIONAL SEARCH REPORT

International application No.
PCT/US2013/071042

Box No. I Nucleotide and/or amino acid sequence(s) (Continuation of itemlc of the first sheet)

1. With regard to any nucleotide and/or amino acid sequence disclosed in the international application, the international search was carried out on the basis of :

a. a sequence listing filed or furnished

☐ on paper

☒ in electronic form

b. time of filing or furnishing

☒ contained in the international application as filed

☐ filed together with the international application in electronic form

☐ furnished subsequently to this Authority for the purposes of search

2. ☐ In addition, in the case that more than one version or copy of a sequence listing has been filed or furnished, the required statements that the information in the subsequent or additional copies is identical to that in the application as filed or does not go beyond the application as filed, as appropriate, were furnished.

3. Additional comments:

INTERNATIONAL SEARCH REPORT

International application No.
PCT/US2013/071042

Box No. II Observations where certain claims were found unsearchable (Continuation of item 2 of first sheet)

This international search report has not been established in respect of certain claims under Article 17(2)(a) for the following reasons:

1. ☒ Claims Nos.: 1-17,33-42
because they relate to subject matter not required to be searched by this Authority, namely:
Claims 1-17 and 33-42 pertain to diagnostic methods practiced on the human body, and thus relate to a subject matter which this International Searching Authority is not required, under Article 17(2)(a)(i) of the PCT and Rule 39.1(iv) of the Regulations under the PCT, to search.

2. ☐ Claims Nos.:
because they relate to parts of the international application that do not comply with the prescribed requirements to such an extent that no meaningful international search can be carried out, specifically:

3. ☐ Claims Nos.:
because they are dependent claims and are not drafted in accordance with the second and third sentences of Rule 6.4(a).

Box No. Ill Observations where unity of invention is lacking (Continuation of item 3 of first sheet)

This International Searching Authority found multiple inventions in this international application, as follows:

1. ☐ As all required addtional search fees were timely paid by the applicant, this international search report covers all searchable claims.

2. ☐ As all searchable claims could be searched without effort justifying an additional fees, this Authority did not invite payment of any additional fees.

3. ☐ As only some of the required additional search fees were timely paid by the applicant, this international search report covers only those claims for which fees were paid, specifically claims Nos.:

4. ☐ No required additional search fees were timely paid by the applicant. Consequently, this international search report is restricted to the invention first mentioned in the claims; it is covered by claims Nos.:

Remark on Protest

☐ The additional search fees were accompanied by the applicant's protest and, where applicable, the payment of a protest fee.

☐ The additional search fees were accompanied by the applicant's protest but the applicable protest fee was not paid within the time limit specified in the invitation.

☐ No protest accompanied the payment of additional search fees.

INTERNATIONAL SEARCH REPORT

Information on patent family members

International application No.
PCT/US2013/071042

Patent document cited in search report	Publication date	Patent family member(s)	Publication date
US 2011-0294138 Al	01/12/2011	AU 2009-314110 Al	20/05/2010
		CA 2743282 Al	20/05/2010
		EP 2376905 Al	19/10/2011
		JP 2012-508886 A	12/04/2012
		WO 2010-056815 Al	20/05/2010
WO 2010-065878 Al	10/06/2010	CA 2745839 Al	10/06/2010
		EP 2373988 Al	12/10/2011
		JP 2012-511154 A	17/05/2012
		US 2012-0015371 Al	19/01/2012

专利名称(译)	使用淀粉样蛋白-β富集动力学分析诊断淀粉样蛋白病理的方法		
公开(公告)号	EP2923209A4	公开(公告)日	2016-04-27
申请号	EP2013856598	申请日	2013-11-20
[标]申请(专利权)人(译)	圣路易斯华盛顿大学		
申请(专利权)人(译)	华盛顿大学		
当前申请(专利权)人(译)	华盛顿大学		
[标]发明人	BATEMAN RANDALL PATTERSON BRUCE W ELBERT DONALD L		
发明人	BATEMAN, RANDALL PATTERSON, BRUCE W. ELBERT, DONALD L.		
IPC分类号	G01N33/68 G01N33/53 G01N33/48		
CPC分类号	G16H50/50 A61B5/4088 G01N33/6896 G01N2333/4701 G01N2800/2821		
优先权	61/728692 2012-11-20 US		
其他公开文献	EP2923209A1		
外部链接	Espacenet		

摘要(译)

一种使用至少一种淀粉样蛋白的富集动力学测量来诊断患者中枢神经系统中的淀粉样病变的方法。提供同种型。此外，还有一个预测至少一种淀粉样蛋白的富集动力学的模型。提供了同种型，校准模型的方法，以及使用该模型诊断患者中枢神经系统中的淀粉样病变的方法。